Technical Transactions

Czasopismo Techniczne

Issue 6
Volume 2018 (115)

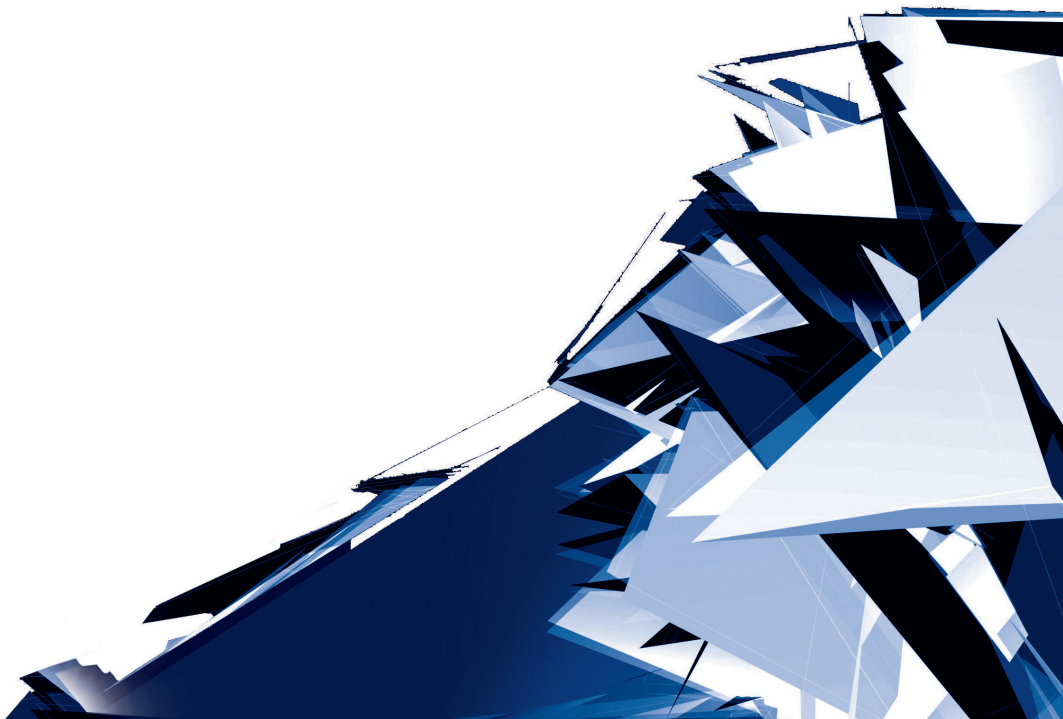

ISSN 0011-4561

Basic version of each Technical Transactions magazine is its online version
Pierwotną wersją każdego zeszytu Czasopisma Technicznego jest jego wersja online

Contents

MECHANICS

TECHNICAL TRANSACTIONS 6/2018
ARCHITECTURE AND URBAN PLANNING
DOI: 10.4467/2353737XCT.18.083.8688
SUBMISSION OF THE FINAL VERSION: 11/06/2018

Krystian Banet (kbanet@pk.edu.pl)
Faculty of Civil Engineering, Cracow University of Technology
Ewelina Stypułkowska
Faculty of Environmental Engineering, Cracow University of Technology

Adapting cracow's Stare Debniki area to the mobility needs of sight-impaired people

Adaptacja obszaru Starych Dębnik w Krakowie do potrzeb mobilności osób niewidomych

Abstract

An ageing society and the predicted increase in the visual impairment of older people requires attention to be paid to the accessibility and social inclusivity of urban spaces. This paper reviews spatial barriers with particular emphasis on the limited mobility of people with visual dysfunction. Furthermore, by the example of the Stare Dębniki area in Cracow, the paper includes improvement opportunities related to the accessibility of urban spaces. The detailed Let's make noise project was developed at the 'Przepis na miasto' workshop.

Keywords: blind, pedestrians, sustainable mobility

Streszczenie

Starzejące się społeczeństwo i przewidywany wzrost niepełnosprawności osób starszych wymaga zwrócenia uwagi na kwestie dostępności i społecznej integracji przestrzeni miejskich. W niniejszym artykule dokonano przeglądu barier przestrzennych ze szczególnym uwzględnieniem ograniczonej mobilności osób z dysfunkcją wzrokową. Ponadto, przedstawiono możliwości poprawy dostępności przestrzeni miejskiej na przykładzie obszaru Starych Dębnik w Krakowie. Szczegółowy wariant prezentujący Zróbmy hałas opracowany został w ramach warsztatów „Przepis na miasto"..

Słowa kluczowe: niewidomi, piesi, zrównoważona mobilność

1. Background: the mobility needs of sight-impaired people

Whether blind or sighted, our quality of life is strongly dependent on our abilities to make informed spatial decisions through the processing and synthesis of spatial information about our surroundings [5]. Despite medical progress, many still experience total or partial loss of vision. Regardless of the standard of their vision, blind people have the same mobility needs as sighted people. They have to go to work, school, or just for a walk. Sight-impaired people often travel to unfamiliar places for work, education, recreation or medical attention, and this is more problematic than travel to familiar places.

Blind people have problems leaving premises that are not equipped with elevators. If they surmount these odds, they have other problems on sidewalks and roads. Unfortunately, road and sidewalk infrastructures are not well suited to the needs of sight-impaired people. Visually impaired people either move around independently or with the aid of a sighted person who acts as a guide. Those who move around independently do so either alone with the use of their residual sight, or with the use of a mobility aid. The most common mobility aid used by pedestrians with poor sight to facilitate their independent mobility is a long white cane which is used to scan the ground in front of the person. Alternatively, a visually impaired person may have a guide dog to assist them with their mobility [4]. In Poland, infrastructure designers have started think more seriously about blind people in last 10–15 years. Previously, blind people were forced to overcome many difficulties when moving through cities. The UN Convention on the Rights of Persons with Disabilities states that the physical environment, means of transport, information and communication systems, as well as other devices and services must be made widely accessible in urban and rural areas through the recognition and elimination of accessibility barriers [9].

Sight-impaired people have a civil right to access information provided to other pedestrians [1] Regrettably, blind people still do not have the same level of accessibility to, for example, public transport and pedestrian crossings. For them, easy tasks are not effortless. Visually impaired pedestrians need to perform a number of tasks to cross safely and independently at signaled intersections. This task is more difficult in unfamiliar places. Firstly, they must recognize the boundary line between the pavement and the street to know they have come to an intersection. Curbs are used as a cue for blind people that they have come to an intersection. The next task for blind people is to determine the junction's geometry, e.g. the width of the street, the angle of the junction, and the presence of splitter islands. A lot of information about this comes from vehicular sounds, but crossing might be impossible when there is even only a little traffic. Blind pedestrians then have to determine the nature of traffic controls, such as the order, onset, and duration of the traffic and pedestrian phases. This can be achieved by listening to the traffic flow. Before crossing, blind pedestrians try to establish a heading precisely towards the opposite side [1]. After preparing to cross, blind people have to know when the pedestrian phase starts. Traditionally, pedestrians who are blind have been taught that the walk interval begins with the onset of traffic on the street perpendicular to their direction of travel. This strategy is effective at most junctions with fixed timed signals, concurrent pedestrian phases and no right-on-red [1]. In other cases this strategy might be

wrong. As this example shows, it is complicated for blind pedestrians to cross the road without any help. At a lot of junctions, curb ramps have become more prevalent, yet the geometry of junctions has become more complex and traffic has become quieter, both of which make it more difficult for the blind.

Not only is crossing the road an effort for blind people. Walking along bumpy and narrow sidewalks and using public transport or public utility buildings also presents a challenge. The UN Convention on the Rights of Persons with Disabilities does not indicate specific implementation standards for the above activities beyond public utility buildings and signs in Braille. Poland does not have unified rules of designing infrastructure for visually impaired people [8]. For years, the Polish Association of the Blind has attempted to address the needs of people with eyesight restrictions, their access to cultural goods, and their free and safe movement. In general, this association handles education related to blind and visually impaired people [9]. Increasing accessibility to public spaces for blind people can be achieved using rules of universal design. Products, the environment, programs and services should be designed in such a way as to be useful to as many people as possible, without the need for adaptation or specialized design.

2. Careful design of public spaces for blind people

City planning oriented to the needs of people with disabilities has become popular in recent years. When designing spaces, most urban planners remember to consider those with physical disabilities. Nevertheless, in many situations other conveniences are required for sight-impaired people that might also be helpful for other groups, e.g. the elderly. The most awkward aspects of being blind are limitations in spatial orientation, limited ability to move independently, and the necessity of other people's help [2]. Universal design and space adaptation helps not only to improve orientation in space, but can also improve the social life and work conditions of sight-impaired people. Especially in urban areas, people who are blind have problems with a sense of distance and depth, which is particularly important when overcoming differences in height, e.g. stairs, or when entering an area with a different degree of brightness. Blind people also have problems with distinguishing the sidewalk from the road, moving across large sidewalks and pedestrian areas, finding proper buildings, and moving in a straight line or interpreting traffic. The last two issues are especially dangerous when crossing roads [9]. In her research, Laskowska identified five places and situations which are dangerous for sight-impaired people: sidewalks, public transport stops and vehicles [3], streets, bus and railway stations and public utility buildings [6]. Even without curbs and parked cars, pavements are bumpy. Pedestrian crossings do not use one consistent system of sounds. Public transport stops and stations are not equipped with public address systems. Blind people cannot find the place to get in buses or trains. In addition, many public utility buildings do not have marked ways to elevators or main thoroughfares. Infrastructure for people who are blind must be designed such that blind people receive early warnings about what is going on around them. Sight-impaired people learn to navigate routes via characteristic

points. Orientation and wayfinding information should be provided by the use of high visibility and, where appropriate, tactile signing [4]. Hence the idea of tactile paths was born. These paths start and end in particular places like the entrance to a building or an elevator. The most important factor is that the space should be designed in a consistent, logical way [9]. Layouts of all pedestrian areas should be simple, logical and consistent as this enables people to memorize environments that they use regularly and predict and interpret environments they are encountering for the first time [4].

In this paper, the authors decided to focus on universal design aspects related to street designing (excluding informational sound schemes). The most common solution is tactile paving, which consists of a marked passage free of obstacles (90 cm width is recommended) whose objective is to guide sight-impaired people to particular places like pedestrian crossings or stairs [9]. When moving around the pedestrian environment, visually impaired people actively seek and make use of tactile information underfoot, particularly detectable contrasts in surface texture [4]. Tactile paving is a detectable warning system of indicators on the ground that is used to assist visually impaired pedestrians, whether or not they use a long cane [10]. The use of blister paving as a warning device at controlled and uncontrolled pedestrian crossing points is now well established. The installation of tactile paving surfaces should be considered as part of a wider package of measures to assist visually impaired people [4]. Tactile paving comprises two elements: guidance path (guide belt) and attention fields (blister surface, Fig. 1.). The blister surface should be wider than the guide belt and be installed on forks of tactile paths and in front of final points.

A blister surface is similar to tactile paving, with dropped curbs at pedestrian crossings (Fig. 2.). The tactile blister surface should be installed in the absence of an upstand at both controlled and uncontrolled crossing points where the footway has been dropped flush with the carriageway or where the carriageway has been raised to the level of the footway [4].

Another solution for sight-impaired people is a corduroy surface. The purpose of a corduroy surface is to warn visually impaired people of the presence of specific hazards, including steps, level crossings, or the approach to on-street rapid light transit platforms. They are also used where a footway joins a shared route [4].

Infrastructure designers should also remember about proper platform edge warning surfaces on public transport stops (Fig. 4.). The purpose of this surface is to warn sight-impaired people of the edge of all on-street tram or bus platforms.

To help people locate amenities, for example a ticket machine or post office, an information surface is recommended. This is helpful to blind people who are regular users of a particular area and will become familiar with the type of amenity indicated [4].

Urban designers should also remember to use proper contrast. From ophthalmologic tests it is clear that yellow is the best color for partially sighted humans and it should therefore be used to create contrast [9]. Street furniture (benches, baskets, flowerbeds) should be made of durable materials and devoid of sharp edges. All elements and their edges should be marked with a color that contrasts with the surroundings. Tactile typhlographic plans and schemes with information in Braille should supplement friendly infrastructure with consistent signs, contrasting colors and helpful sounds.

Fig. 1. Tactile paving (source: [10])

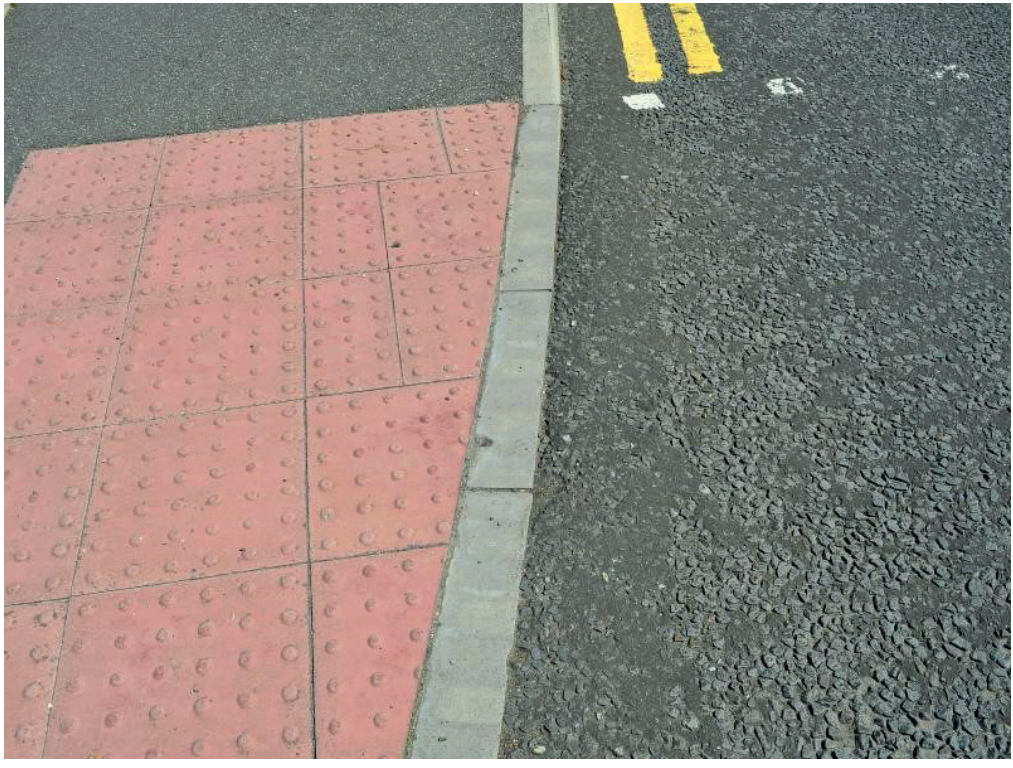

Fig. 2. Blister surface and dropped curb at a pedestrian crossing (source: www.DirectEnquiries.com, accessed 09.03.2018)

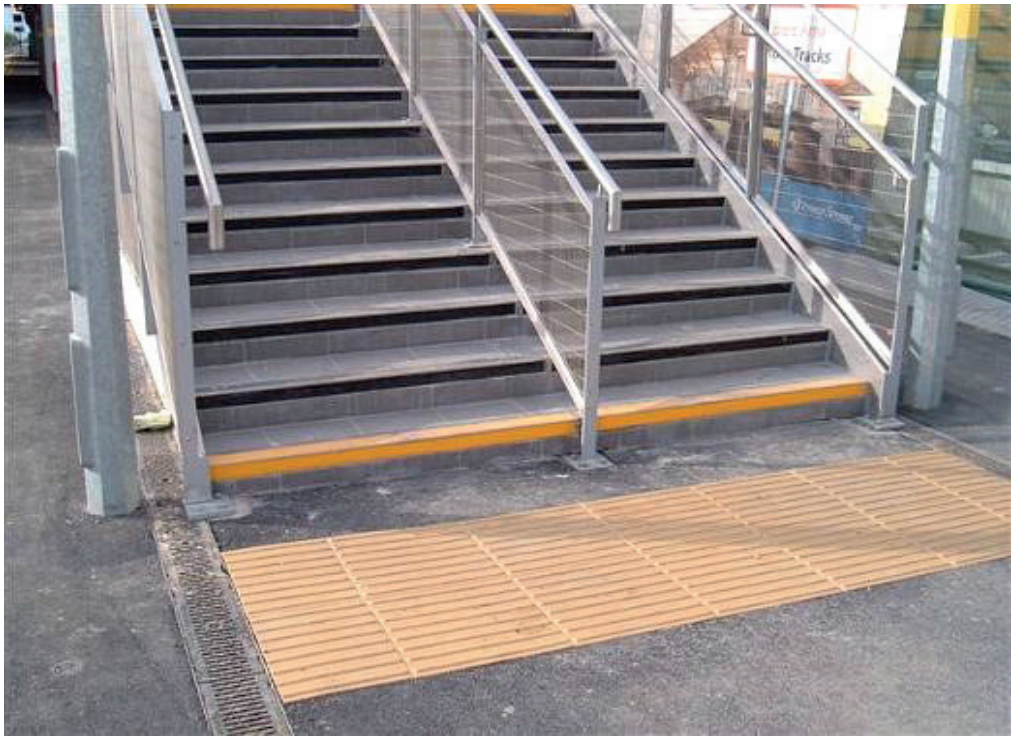

Fig. 3. Corduroy surface (source: www.tactilesurface.co.uk, accessed 10.03.2018)

Fig. 4. Platform edge warning surface on a tram stop
(source: www.marshalls.co.uk, accessed 10.03.2018)

3. Stare Dębniki – current conditions

Cracow is situated in the Lesser Poland region in south Poland on the Vistula River. Cracow's population is 766,700 people [11]. The city was founded in 1257, based on a location act which introduced city rights modelled on the Magdeburg law. From the founding of the city to the 20th century, Cracow grew. In 1910, nine surrounding suburban communities, including Dębniki, were incorporated into a single administrative unit: Cracow [7, 12].

Dębniki is one of eighteen districts of Cracow, located in the southwest part of the city. The district's area is 46.19 square kilometers. Stare Dębiniki is the northern part of Dębniki district and is delimited by Generała Bohdana Zielińskiego street, Monte Cassino street and Vistula River (between Zwierzyniecki and Grunwaldzki bridges). The primary land use of Stare Dębniki is residential housing (a mix of single and multi-family housing). Characteristic points of Stare Dębniki are Rynek Dębnicki, Saint Stanisław Kostka Church and Dębnicki park. Rynek Dębnicki (Fig. 5.) is the main square of Stare Dębniki and has the shape of an irregular quadrilateral. There are several schools in Stare Dębniki: the Primary School with Integration Units No. 30[1], the Secondary School of Integrating No. 3[2] and the Special School and Educational Center for Blind and Visually Impaired Children[3]. The latter was established in 1948. It is an important center of education, counseling and rehabilitation of a wide age range of children and youth with sight dysfunction.

Fig. 5. Rynek Dębnicki – main square of Stare Dębniki.
Photo by: Ewelina Stypułkowska (2018)

1 Szkoła Podstawowa z Oddziałami Integracyjnymi nr 30 – transl. note.
2 Zespół Szkół Ogólnokształcących Integracyjnych nr 3 – transl. note.
3 Specjalny Ośrodek Szkolno-Wychowawczy dla Dzieci Niewidomych i Słabowidzących – transl. note.

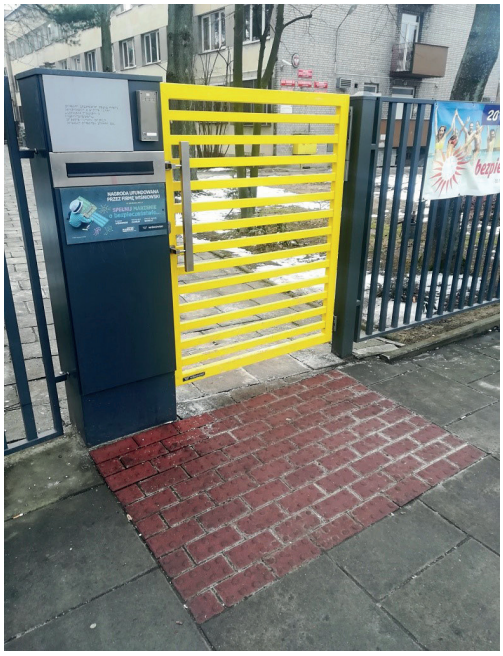

Fig. 6. School entrance gate.
Photo by: Ewelina Stypułkowska (2018)

Fig. 7. Rynek Dębnicki square – pedestrian crossing and bus stop.
Photo by Ewelina Stypułkowska (2018)

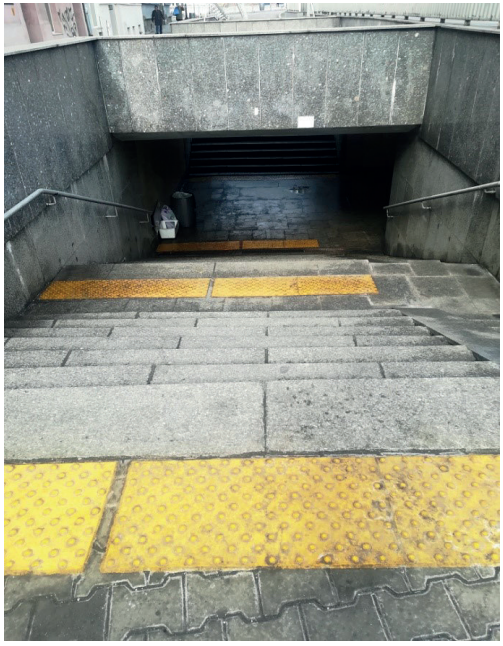

Fig. 8. Marii Konopnickiej street – underground passage.
Photo by Ewelina Stypułkowska (2018)

Fig. 9. Konopnickiej bus stop – platform edge warning surface.
Photo by Ewelina Stypułkowska (2018)

The authors analyzed the main walking route between the Special School and Educational Center for Blind and Visually Impaired Children and Konopnickiej bus stop, the nearest public transport stop with a high frequency of transport. During the inventory, attention was paid to places and situations which are dangerous for sight-impaired people. As mentioned in the second chapter, these are sidewalks, public transport stops and vehicles, streets, bus and railway stations, and public utility buildings [6]. The route leads about 400 m along Tyniecka street, Rynek Dębnicki and Antoniego Józefa Madalińskiego street to Konopnickiej bus stop. The school is equipped with a special entrance gate. It is adapted to sight-impaired people's mobility needs by its yellow color, description in Braille and blister surface (Fig. 6.). Furthermore, the school exit is marked by information and warning signs, so drivers must be careful.

The pavement along Tyniecka street is in good technical condition. A pedestrian crossing with traffic lights is located about 60 m from the exit gate. It is equipped with a blister surface, dropped curbs, and a pedestrian crossing control panel with transition plan and sound signal. The analyzed path does not require this pedestrian crossing to be crossed. The next pedestrian crossing is located on Rynek Dębnicki square (Fig. 7.). It is not equipped with traffic lights; it features dropped curbs and a rough cobble pavement. Rynek Dębniki is the most difficult area to pass. The entire Rynek Dębniki surface is a rough cobble pavement. There are many obstructions for sight-impaired people, such as cycle racks, concrete plant pots, and different levels (raised curbs). Rynek Dębnicki bus stop is not equipped with any information for impaired sight people; it is an information barrier [3]. Along Antoniego Józefa Madalińskiego street (about 210 m) there are two pedestrian crossings without traffic lights that are equipped with blister surfaces and dropped curbs. The pavement along Antoniego Józefa Madalińskiego street is in very good technical condition.

Konopnickiej bus stop is located on Marii Konopnickiej street, which is a four-lane road. Buses going to the center of Cracow leave from the other side of the street. The only way to get to the other street side is via an underground passage (Fig. 8.) The underground passage entrances are well marked: yellow blister surfaces with dropped curbs located on each level of the stairs. The underground level is poorly lit and is not equipped with any tactile pathing; especially notable is the absence of a guidance path. The platforms of Konopnickiej bus stop are equipped with blister surfaces at the platform edges (Fig. 9.). There is no information for impaired sight people; it is an information barrier [3].

4. Stare Dębniki change concept – *Przepis na miasto* workshop

In May 2017, a team from the Faculty of Civil Engineering of Cracow University of Technology[4] organized the "Przepis na miasto"[5] multidisciplinary workshop. A group of students from Cracow University of Technology, Cracow University of Economics, Wrocław

[4] WIL PK – Polish abbreviation, transl. note.

[5] The workshop took place between 18–20.05.2017. Krystian Banet and Ewelina Stypułkowska were organizing committee chairmen. The workshop was organized by KNSK Student Scientific Association of Transporartion Systems (Koło Naukowe Systemów Komunikacyjnych – transl. note).

University of Science and Technology, the University of Economics in Katowice, Adam Mickiewicz University in Poznań and European Students of Industrial Engineering and Management participated in the workshop. The end product of the workshop was six charts and mockups of fragments of Cracow's Stare Dębniki and Salwator districts. The fact that the work had a multidisciplinary character was crucial: the students represented branches of engineering associated with transport, spatial management, and urban and architectural design across two levels of higher education (Bachelor, Master). Students' work was supported by a panel of experts: Andrzej Szarata, Tomasz Kulpa, Marek Bauer, Mariusz Dudek, Aleksandra Faron, Katarzyna Nosal, Kinga Racoń-Leja, Agnieszka Szumilas, and Ada Wolny. The overall goals of the workshop were to connect the two banks of the Vistula river, to analyze urban transport system integration, and to propose changes in the selected public spaces.

The project which adapts Stare Dębniki area to the mobility needs of sight-impaired people is the *Let's make noise*[6] conceptual design (Figs. 10, 11). In this solution, the authors focused on Rynek Dębnicki square, the most difficult area to overcome by sight-impaired people. The concept assumed the revitalization of the public space. In this proposal, the removal of road lanes around Rynek Dębnicki square was intended to improve pedestrian safety. A reduction in private traffic would permit a friendly public space to be created. The authors proposed widening the sidewalks, introducing trees near buildings, changing the surfaces of pavements according to the needs of sight-impaired people, and improving free-standing small shops and street lighting. The concept assumed the revitalization of the municipal greenery and the introduction of a green pergola on the western side of Rynek Dębniki square. The greenery would protect space users from the sun. The authors proposed residential and non-residential land use, and small facilities on the ground floors of surrounding buildings. In the central part of Rynek Dębnicki

Fig. 10. The *Let's make noise* – design concept developed as a part of the *Przepis na miasto* workshop. Prepared by Jakub Salach, Małgorzata Stec, Maciej Pilny, Justyna Mazur, Natalia Kobza

[6] Authors: Jakub Salach (CUT), Małgorzata Stec (CUT), Maciej Pilny (WUT), Justyna Mazur (CUT), Natalia Kobza (ESIEM).

square, the authors designed an interactive board whose main aim is to teach and entertain using sounds such as clash, crackle, flutter, hiss, jingle, splash, twitter, and whistle. The *Let's make noise* conceptual design proposal would give a chance to integrate sight-impaired people with non-disabled people in a space in which people would be present at all hours.

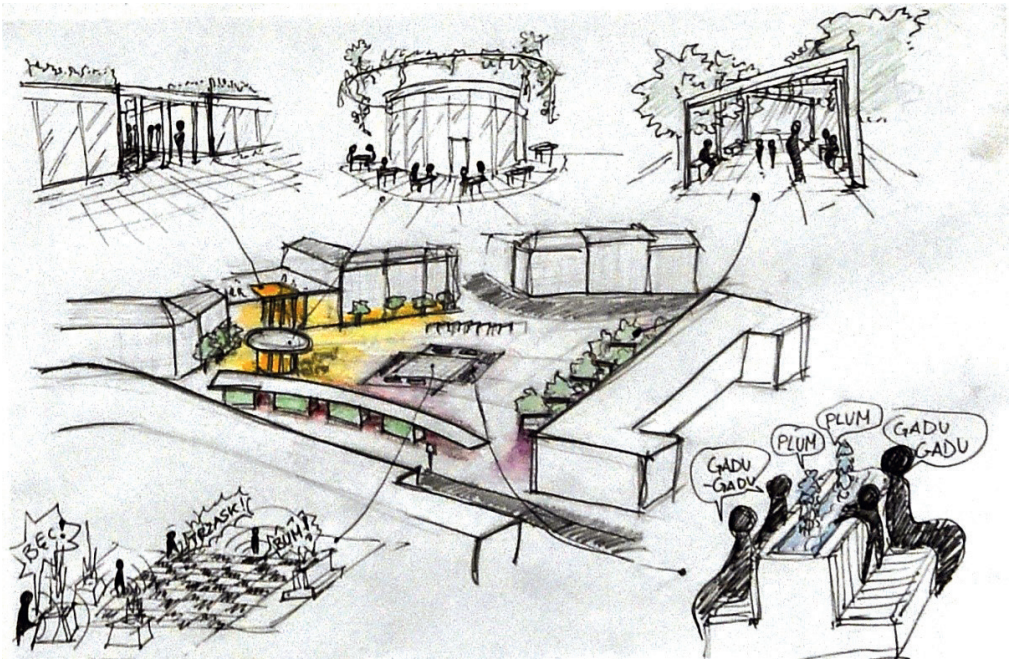

Fig. 11. The *Let's make noise* design concept developed as a part of the *Przepis na miasto* workshop. Prepared by Jakub Salach, Małgorzata Stec, Maciej Pilny, Justyna Mazur, Natalia Kobza

5. Conclusions

Sight-impaired people are a disadvantaged group in society because urban areas are not suited to their needs and expectations. Spatial designers should adapt urban spaces for people who are blind and create friendly and safe surroundings without spatial traps. This is especially important in areas which are frequently visited by blind people, e.g. the Stare Dębniki area in Cracow, where a school for blind children is located. One of the most popular solutions is the use of tactile paving, which is part of a detectable warning system of indicators on the ground that is used to assist visually impaired pedestrians. Another solution which is dedicated to sight-impaired people is corduroy surfaces. Infrastructure designers should also remember to create proper platform edge warning surfaces at public transport stops. In addition, an ageing society and the predicted increase in visual impairment of older people requires attention to be paid to the accessibility and social inclusivity of urban spaces.

References:

[1] Bentzen B. L., Barlow J. M., Franck L., *Addressing barriers to blind pedestrians at signalized intersections*, Institute of Transportation Engineers Journal, Natural Science Collection, 2000, 32-35.

[2] Bilewicz M., *Sytuacja życiowa osób niewidomych i słabowidzących – Kontekst teoretyczny,* [in:] *Bezpieczeństwo osób niewidomych i słabowidzących w ruchu drogowym. Wybrane aspekty praktyczne*, red.: Laskowska K., Filipkowski W., Glińska E., Wydawnictwo Uniwersytetu w Białymstoku, Białystok 2014.

[3] Dębiec M., *Dostępny transport kluczem do rehabilitacji społecznej i zawodowej osób niepełnosprawnych*, Tyfloświat, nr 4 (17) 2012, Fundacja Instytut Rozwoju Regionalnego.

[4] *Guidance on the use of Tactile Paving Surfaces*, Department of Transport, Government of United Kingdom [online], https://www.gov.uk/government/publications/guidance-on-the-use-of-tactile-paving-surfaces (access: 08.03.2018).

[5] Jacobson D. R., *Cognitive mapping without sight: four preliminary studies of spatial learning*, Journal of Environmental Psychology, Vol. 18/1998, School of Geosciences, Queen's University of Belfast, Belfast, Northern Ireland, U.K., 289-305.

[6] Laskowska K., *Katalog zagrożeń w ruchu osób niewidomych i słabowidzących,* [in:] *Bezpieczeństwo osób niewidomych i słabowidzących w ruchu drogowym. Wybrane aspekty praktyczne*, red.: Laskowska K., Filipkowski W., Glińska E., Wydawnictwo Uniwersytetu w Białymstoku, Białystok 2014.

[7] Małecki J., *W dobie autonomii galicyjskiej*, [in:] Dzieje Krakowa, praca zbiorowa pod red. J. Bieniarzównej, Vol. III, Wydawnictwo Literackie, Kraków 1979, 359-360.

[8] Poliński J., *Oznaczenia dotykowe dla osób niewidomych i słabowidzących część I – dotykowe elementy ostrzegawcze*, Problemy Kolejnictwa, vol. 157, 2012.

[9] *Projektowanie i adaptacja przestrzeni publicznej do potrzeb osób niewidomych i słabowidzących. Zalecenia i przepisy,* Instytut Tyflologiczny, Polskiego Związku Niewidomych, Warszawa 2016.

[10] *Tactile Paving Patterns,* http://www.bj56.org/tactile-paving-patterns.html (access: 09.03.2018).

[11] Statystyczne Vademecum Samorzadowca, Urząd Statystyczny w Krakowie, 2017, http://krakow.stat.gov.pl/statystyczne-vademecum-samorzadowca/ (access:11.03.2018).

[12] Wood Nathaniel D., *Becoming Metropolitan: Urban Selfhood and the Making of Modern Cracow,* DeKalb: Northern Illinois University Press 2010, 272.

If you want to quote this article, its proper bibliographic entry is as follow: Krystian Banet, Ewelina Stypułkowska, *Adapting cracow's stare debniki area to the mobility needs of sight-impaired people*, Technical Transactions, Vol. 6/2018, pp. 5-16.

TECHNICAL TRANSACTIONS 6/2018
ARCHITECTURE AND URBAN PLANNING
DOI: 10.4467/2353737XCT.18.084.8689
SUBMISSION OF THE FINAL VERSION: 12/06/2018

Damian Poklewski-Koziełł (damian.poklewski-koziell@pk.edu.pl)
Institute of Urban Design, Faculty of Architecture, Cracow University of Technology

In search of a healthy balance on the example of the New District of Seestadt Aspern in Vienna

W poszukiwaniu zdrowej równowagi na przykładzie nowej dzielnicy Seestadt Aspern w Wiedniu

Abstract

The aim of the article is to present one of the largest city expansion projects in Europe; it is currently being carried out on the north-eastern edge of Vienna and is known by the name Seestadt Aspern. Its design by the Swedish design office Tovatt Architects and Planners AB, which was selected through a competition in 2005, is characterized by an extraordinary wealth and variation of paved and green public spaces, as well as water bodies of varying accessibility which have been designed in such a manner as to create a system of safe and traffic-free walkable pathways and urban squares. The article will present a classification of the varied typology of the aforementioned spaces both in reference to urban plans, as well as to already built fragments of the city.

Keywords: Mixed-use development, sustainable mobility, walkability

Streszczenie

Celem artykułu jest przedstawienie jednego z największych projektów rozbudowy miasta w Europie, jaki jest obecnie realizowany na północno-wschodnich obrzeżach Wiednia, znanego pod nazwą Seestadt Aspern. Ten wyłoniony w 2005 roku w konkursie projekt, autorstwa szwedzkiego biura Tovatt Architects and Planners AB, charakteryzuje niezwykłe bogactwo i różnorodność przestrzeni publicznych utwardzonych, zielonych oraz akwenów wodnych o zróżnicowanej dostępności, które ukształtowano w taki sposób, by tworzyły system bezpiecznych, wolnych od ruchu kołowego ciągów spacerowych i placów miejskich. W artykule uszeregowano zróżnicowaną typologię wyżej wymienionych przestrzeni zarówno w odniesieniu do planów urbanistycznych, jak i do już zrealizowanych fragmentów miasta.

Słowa kluczowe: zabudowa o funkcjach mieszanych, zrównoważona mobilność, dostępność piesza

1. Introduction

The Seestadt district is located in the north-eastern part of Vienna. A number of important historical events are associated with this area. At the start of the nineteenth century it was a battlefield that saw the Austrian and Napoleonic armies clash twice[1]. The early years of the twentieth century, in turn, saw the construction of an airport located precisely within the borders of the area under discussion[2].

Seestadt's surroundings are extraordinarily attractive areas in terms of their natural environment. The area is located a small distance away to the south of the Donau Auen National Park, which is a sort of green belt connecting the conurbations of Vienna and Bratislava [18]. The area also borders the expansive farmland of the Marchfeld plain and a forest named after the politician and local government representative Norbert Scheed, which is located to the north[3].

The Seestadt district is one of Vienna's 13 strategic projects. Due to the expansion of the European Union's borders in 2004 to include new Central and Eastern European countries, Austria's geopolitical placement changed from that of a peripheral area to a central one. This provided a strong development impulse directed at building resilient socio-economic ties within the region, primarily with Slovakia, and especially with Bratislava, which is located only a one-hour drive away.

2. The competition

The district is being built on the basis of a two-stage tender procedure that took place in 2005. From among the submitted applications, a group of 10 companies was selected and invited to present their conceptual designs. The tender procedure was preceded by broad public consultations which saw the appointment of three persons to represent the voices of the residents of the surrounding districts. These were persons who were familiar with the area and had ties with it. The representatives, called "local experts", participated in further preparatory work at almost every stage of the design's evaluation. Their points of view were also taken into consideration during the preparation of tender specifications. They additionally played the

[1] At the Battle of Aspern, also known as the Battle of Essling, which occurred on 21–22 of May 1809, Napoleon's army was defeated. The second battle took place on 5–6 July 1809. It went down in history as the battle of Wagram and ended in a victory for Napoleon's forces. See KAMPFMITTEL BERICHT in materials available for download for bidders [17].

[2] In 1912 it was the largest and most advanced civilian airport in Europe and was also famous for its regular air shows that attracted almost 50 000 spectators. Over the years, however, its character changed from a civilian facility to a military one several times. During the Second World War it was a target of Allied bombing. The remains of the bombings from that period were still being found and neutralized as late as 2009–2013 [17].

[3] Due to a lack of green areas in the north-eastern part of Vienna, the area of the Norbert Scheed Wald forest has been assigned for development into a natural park. In the future it will constitute the city's green lungs - mixed-use areas of recreation and education about the natural environment, which will combine ecology, landscape protection, agricultural land, rest and recreation, as well as mobility and climate protection. Due to the proximity of the metropolitan railway line it has the chance to become a popular place of rest for Vienna's residents [19].

role of members of the competition jury, which made the decision concerning the selection of the most attractive vision of the site's development [20].

The tender procedure was finalized in 2005. The winning conceptual design was developed by the Swedish design studio Tovatt Architects and Planners, which participated as a consortium with the German construction company N + Objekt management GmbH. Tovatt Architects and Planners is a company that was founded by Ralph Erskine's long-time co-worker and later business partner, Johannes Tovatt[4].

The winning design proposal was praised for its flexibility, understood as the capacity for adaptation to changing socio-economic needs, which had to be taken into account due to the project's completion time being spread over several decades. However, flexibility should not mean evolution in an unknown direction. The winning design proposal provided a guarantee of the preservation of key assumptions that ensured the unique character of the project. It also made it possible to maintain high quality public spaces and ensured access to them regardless of the current completion phase [20].

3. Fundamental design assumptions

The conceptual design of the Aspern district in many aspects mirrors the model assumptions of walkable cities [25]. The structure of the buildings is characterized by small distances between blocks, making it possible to easily move between them. Building density was also a particular focus here, although the adopted indicators raise the most doubt. The mixed-use character of the complex means most of the basic services will be located a short walking distance away. The goal was to design a compact urban organism with short internal connections that is well connected to the city centre by public transport[5]. It is designed to contribute to changes in transport-related behaviour in such a way that walking, cycling and public transport will account for 80% of all trips.

3.1. Compositional and functional layout

We can identify three strong urban elements within the compositional layout. Open green areas were designed along the eastern and western border of the estate – an element of Vienna's so-called green belt – constituting not only a buffer zone for the surrounding low-density buildings, but primarily a spatial element that integrates the designed layout with the existing, environmentally and recreationally attractive areas[6]. In the future, these areas will be linked

[4] Johannes Tovatt started working for Ralph Erskine before he started studying at the Faculty of Architecture of the Royal Technical Institute in Stockholm. In 2000, Ralph offered him partnership at the company. The company was then renamed so as to honour the names of both partners. After Erskine's death, according to his wish, only Johannes' name has remained in the company name [21].

[5] In a broader context with the remaining part of the country and Europe, but primarily with Bratislava

[6] These areas are described in the introduction to this article.

into a continuous, linear system of greenery. One element that foreshadows this is the safe intersection of green areas with the planned A23 motorway in the northern part of Seestadt.

Remaining within the discipline of landscape architecture, the second defining element is the Park, which is placed in the central part of the layout and has an expansive water reservoir and accompanying greenery. Central Park[7] fulfils the role of the main recreational space, but it is also a hub for the remaining public spaces – both green and paved (Fig. 1). The construction of a lake in this area was possible thanks to the high level of groundwater[8] that was released by the large-scale excavation work.

The third compositional element that provides a unique character is the car transportation layout, which features an internal ring road. It fulfils the role of a local road, constituting the core of the vehicular transport infrastructure. The ring road has the shape of a bent ellipse. Local roads from every direction will lead inside it, binding the entire layout with the surrounding built environment, which mainly features residential forms of use. The district being designed will thus successfully provide commercial services to the residents of these areas[9].

Seestadt is being designed as a mixed-use residential development which implements the idea of the coexistence of places of residence and employment. Over 2 million square metres of floor area that will be assigned for various functions will be built on the 240 ha site. Half of the floor area will be dedicated to office, commercial and retail functions, as well as culture. Around 38% of the floor area has been reserved for residential forms of use. The remaining 11%, in a proportion of 60/40, has been assigned to industry and broadly understood social infrastructure. This specific mix of functions is meant to make Aspern a truly living urban organism. The goal is to limit needs in terms of travel and to create streets that teem with life.

3.2. Building density

Building densities have been correlated with the designed functional layout and with the strategy of compositionally accentuating important places through height. The highest net density indicators (exceeding 5.1 m^2t/m^2s) appear in the vicinity of the main squares that are located near public transport nodes. Higher indicators have additionally been planned near the urban blocks along the main streets, as well as along the eastern belt, as an element of a visual barrier around industrial areas.

As one gets closer to the external borders of the layout, the buildings become less dense. The urban blocks gain intimacy and greater contact with greenery. The lowest building density values (0.1 to 1.0 m^2t/m^2s) have been reserved for areas assigned for education and for the aforementioned industrial areas[10]. For areas outlined in accordance with demarcation lines,

---

7 The park's proper name, as used in the summarizing text of the Site Development Plan

8 The groundwater level is located at a depth of around 2 metres below ground level.

9 We then better understand the needs in terms of public consultations already performed at the pre-design stage.

10 The design does not delimit the size of the individual industrial buildings. They will be dependent on the needs of individual tenants. However, it is known that these will be large structures of low height, which is why their placement has been assigned at the greatest possible distance from places of residence and recreation.

the mean value of the net building density indicator is around 2.2 m^2t/m^2s, with the gross value for the entire area being around 0.92 m^2t/m^2s. This indicator takes into consideration all of the planned functions. Keeping in mind the fact that only 38% of the floor area has been assigned for apartments, the population density indicator – one of the key elements in determining the capacity to create living urban organisms – will be at a relatively low level of around 84 persons per ha[11].

3.3. Building height structure

The height of buildings was treated by the designers as a significant urban planning tool. Apart from the role of building densification described above, building height is treated as an essential element in shaping the composition of the complex. It is used to create accents, highlighting places that are functionally important within the city's skyline, such as public squares or circulation nodes. Providing an urban rhythm, they clearly improve orientation within the city [16]. The tall buildings in the north will play the role of a gateway into the city.

3.4. Paved public spaces

Paved public spaces constitute around 4.3% of the surface of the site. They are composed of squares, a commercial street, boulevards and sports and recreation areas. The rich palette of spaces dedicated to pedestrians also includes the streets within the internal urban blocks that were ignored by the authors when calculating the site surface balance. The wealth of planning tools such as one-way traffic, a specific configuration of buildings creating cameral squares and the placement of entrances to underground parking facilities right after the exit from the local road make these places friendly to pedestrians as well[12]. They broaden the already rich typology of public spaces. One argument for this is also the fact that they were designed with immense attention to detail and street furniture. Numerous benches, trees, parking spaces for bicycles, surfaces that are attractive and diverse in terms of colour and texture, as well as the lack of architectural barriers cause us to feel that the needs of pedestrians have been prioritized over motorized traffic without hindering it.

3.5. Green areas and water bodies

Green areas constitute around 26% of the surface of the site. When we exclude the eastern and western green corridor, this value falls to 9.3%.

Industrial areas will constitute a sort of an isolation barrier from the railway line, which leads directly to the Opel car factory, which is located to the south.

[11] Far below the 250 apartments per hectare which were recommended by, for instance, J. Jacobs (ca. 750 persons/ha) [10, p. 223].

[12] Driving a vehicle inside the quarter is prevented by vehicle barriers in the form of posts. This ensures that transit traffic goes around the quarters. Cars are seen sporadically and usually belong to visitors (Fig. 2).

Greenery is the dominant form of space dedicated to people. It constitutes 85% of all public spaces in this area[13]. We can list 5 different types according to size, role within the corridor layout[14], social role, and degree of accessibility. Green areas are also characterized by a clearly defined hierarchical structure. This includes not only private spaces (e.g. small farming fields, semi-private spaces) as a part of the development of internal courtyards (Fig. 4), but also public spaces, which are the dominant form.

The largest area is occupied by type 1, which forms the eastern and western green belt –the main element that integrates with the surrounding attractive nature areas. The second type is the central park, which is the reference point for the next two types of linear layouts of greenery. These are made up of parks which play the role of the main pedestrian and bicycle traffic corridors and the role of side corridors that feature a more cameral character. The fifth type of park space is the neighbourhood parks that are distributed all around the area – the so-called Grätzlpark[15].

3.6. Road layout

The core of the circulation system is the ring road, a type of internal bypass which will be linked to the planned A23 motorway as well as the surrounding roads (Fig. 5). The architects proposed a rich typology of streets, adapted to the capacity and scale of the surroundings. The widths measured between boundary lines range from 12 m to 32 m. The roads inside the urban blocks were designed as one-way roads. Most of the parking spaces were arranged in relatively shallow underground parking facilities located close to the exit from the access road. The garages have flat, green roofs.

3.7. Transport systems

Access to various forms of transport is a characteristic quality of the layout. In order to provide circulation services, a metropolitan railway line – extended explicitly for this purpose and placed above ground level so as not to create a physical barrier – has been provided. In addition, the design assumes the use of a metropolitan bus and a tram line. It will run along the main commercial street, with a terminus near the northern metropolitan railway station. Essential local, national and international railway connections have been provided here. The rich modal offer is supported by the promotion of environmentally friendly individual mobility. First of all, the district has been equipped with points for the rental and charging of municipal bicycles (including cargo bicycles which make it possible to transport, for instance,

[13] 70% excluding the eastern and western green corridor from the balance. Paved public spaces constitute 15% (balance including the green corridors) and 30%, respectively.

[14] This constitutes a network of pedestrian and bicycle connections which is an alternative to motorized vehicular traffic.

[15] The word Grätzl is an old word used in Vienna to describe a small neighbourhood unit, but not a district, as it is too large. Grätzl is more like a quarter or an urban block in one's place of residence, where people know each other well [22].

heavier groceries). The promotion of sustainable mobility would not have taken place had it not been for the previously discussed network of green corridors which provide a safe and quick form of travel.

4. The Aspern district today – the implementation of conceptual design assumptions

Almost 10 years have passed since construction started. The completed fragment is expansive enough to ascertain the compliance of the finished element with its conceptual assumptions. After arriving in Aspern, we can state that despite its considerable distance from the centre of Vienna, the extended metropolitan railway line provides a quick connection that does not exceed 30 minutes of travel time. Our attention is attracted not only by the exact compliance with the design of the metropolitan railway route outline, but also the compliance of the spatial form – a railway line raised above ground level. The central point of the layout is an expansive park with a lake, which – similarly to the design – was created from groundwater which was released by the large-scale excavation work. Apart from the central park we can observe three other park areas located precisely where they were placed in the conceptual design. These include Hannah-Arendt-Park (Fig. 6), Yella-Hertzka-Park, as well as the Madame d'Ora communal gardens. Similarly to the streets, they are named after famous women. There will also be another linear park, whose conceptual design was selected through an architectural competition that came to a conclusion towards the end of 2017 [23]. Its location has been slightly altered in comparison to the original assumptions. Today it is meant to primarily occupy the areas underneath and directly adjacent to the metropolitan railway route. The conceptual design was acknowledged for its ability to integrate the infrastructure of the metropolitan railway route with the architecture of the landscape. Of note is also the continuation of the idea of a neighbourhood park featured in the initial plans, as well as of the character of the local green corridor.

The Hermine-Dasovsky-Platz paved public square (Fig. 3) has been built inside one of the urban blocks in accordance with the conceptual design.

The layout of the ring road, along which commercial services have been placed on ground floors, can already be seen within the structure of the buildings. There is a minimum of traffic within the internal urban blocks. In this area the city can appear as if it were abandoned.

Due to its considerable size, the construction of the estate had to be divided into stages spread over a period of time. The last of them is to be completed towards the end of the 2030s. However, each of the stages constitutes a functional whole. Already at this early stage the residents have access to all the necessary elements in terms of transport, commercial services and retail, as well as green areas and schools. Construction work is currently ongoing on the urban block called Lakeside Park Quarter [24], which was assigned in the conceptual design for the construction of a research campus. Nine different construction projects are being carried out by different construction companies based on different conceptual architectural designs. For the most part, the dominant type of buildings are urban hybrids combining within

them residential forms of use, retail, and offices in line with the live and work idea. Typical residential buildings have, however, been designed with commercial ground floors which also feature day care facilities, in addition to providing access to the greenery of the internal urban block. The aforementioned functions are being rounded out by the buildings of the dormitory and a multi-story parking facility. Work on another quarter, called Am Seebogen Quarter, is to start towards the end of 2018, continuing the aforementioned principles concerning the built environment.

5. Conclusion

The Seestadt district should be considered one of the most interesting urban projects currently being carried out in Europe. Its further development should be observed with particular attention that is directed at evaluating the effectiveness of the adopted urban model in the creation of an urban organism that teems with life, as well as in changing the actual transport behaviour of residents as a result of the skilful promotion of alternative forms of travel to individual car transport. Doubts concerning the above can only be raised by the relatively low population density, which is a result of assigning most of the areas for non-residential forms of use, including large-scale industry.

References

[1] Bojanowski K., Lewicki P., Moya Gonzàlez L., Palej A., Spaziante A., Wicher W., *Elementy analizy urbanistycznej*, Program Tempus JEN-3533 - Publ. PK, Kraków 1998.

[2] Bonenberg W., *Ulica jako element krajobrazu miasta*, [in:] *Odnowa Krajobrazu Miejskiego – Pomysły-Programy-Projekty*, ULAR, Politechnika Śląska, Gliwice 2005.

[3] Dover V., Massengale J., *Street Design: The Secret to Great Cities and Towns*, Wiley, New Jersey 2014.

[4] Frumkin H., Frank L., Jackson R., *Urban Sprawl and Public Health: Designing, Planning, and Building for Healthy Communities*, Island Press , Washington 2004.

[5] Gehl J., *Life Between Buildings: Using Public Space*, Island Press, Washington 2011.

[6] Gehl J., *Cities for People*, Island Press, Washington 2010.

[7] Glaeser E., *Triumph of the city,* Pan Macmillan, London 2011 (Kindle edition).

[8] Gyurkovich J. (ed.), *Miasto w mieście/City within the City*, Czasopismo Techniczne Architektura, z. 2-A/2004.

[9] Gyurkovich M., *22@Barcelona – miasto cywilizacji wiedzy,* [in:] *Współczesne problemy w architekturze i urbanistyce*, Gyurkovich J. (ed.), vol. 2, Kraków 2012, p. 25-56.

[10] Jacobs J., *Śmierć i życie wielkich miast Ameryki*, Fundacja Centrum Architektury, Warszawa 2014.

[11] Jacobs J., *The economy of Cities*, Vintage Books, New York 1970 (Kindle edition).

[12] Kantarek A.A., *O orientacji w przestrzeni miast,* Wydawnictwo Politechniki Krakowskiej, Kraków 2013.
[13] Kukiel M., *Wojny napoleońskie,* Publ. Kurpisz, 2007.
[14] Langdon Philip, *Within walking distance. Creating livable communities for all,* Island Press, Washington 2017.
[15] Leśniewski S., *Wagram 1809,* Wydaw. Bellona, 2003.
[16] Lynch K., *Obraz Miasta,* Archivolta Michał Stępień, Kraków 2011.
[17] https://www.aspern-seestadt.at/city-news/h7a (access: 2018.04.23).
[18] https://www.donauauen.at, (access: 15.04.2018).
[19] https://www.wien.gv.at/umwelt/wald/erholung/wienerwald/norbert-scheed-wald.html, (access: 15.04.2018).
[20] https://www.wien.gv.at/stadtentwicklung/shop/broschueren/pdf/flugfeldaspern-kurzfassung-englisch.pdf, (access: 15.04.2018).
[21] http://www.tovatt.com, (access: 17.04.2018).
[22] https://www.reiseschneiderei.com/graetzl, (access: 15.04.2018).
[23] https://www.aspern-seestadt.at/city-news/park_am_seebogen_ausstellung_und_werkstattgespraech, (access: 15.04.2018).
[24] https://www.aspern-seestadt.at/en/business_hub/quarters__development/lakeside_park_quarter, (access: 15.04.2018).
[25] Speck J., Walkable city: how downtown can save America, one step at a time, Farrar, Straus and Giroux, New York2012
[26] Zuziak Z.*, Forma metropolitarna i zrównoważona mobilność,* Czasopismo Techniczne, vol. 1-A/2010.
[27] Zuziak Z., *Strefa podmiejska w architekturze miasta. W stronę nowej architektoniki regionu miejskiego,* [in:] Lorens P. (ed.), *Problem suburbanizacji,* Urbanista, Warszawa 2005, p. 17-32

Fig. 1. View to the south on the Central Park and the metropolitan railway line. Image source: original work

Fig. 2. View on one of the streets inside the residential urban blocks. Image source: original work

Fig. 3. Hermine-Dasovsky-Platz. View to the north-east. Image source: original work

Fig. 4. View of the semi-private greenery of the residential courtyards. Image source: original work

Fig. 5. View of the ring road. Image source: original work

Fig. 6. Hannah-Arendt-Park. View of the education campus. Image source: original work

TECHNICAL TRANSACTIONS 6/2018
ARCHITECTURE AND URBAN PLANNING
DOI: 10.4467/2353737XCT.18.081.8563
SUBMISSION OF THE FINAL VERSION: 11/06/2018

Liudmyla Ruban (knuba.landscape@gmail.com)
Faculty of Architecture, KNUCA - Kiev National University of Construction and Architecture

Principles of architectural and landscape design of water areas

Zasady projektu architektury i krajobrazu obszarów wodnych

Abstract

Nowadays, the paradigm of coexistence with the planet's aquatic environment is changing due to the impact of many factors, among which climate change plays a principal role. The importance and necessity of finding new rules for the coexistence of water and humans on the planet is a reality of our time. The Paper justifies the necessity of considering Water areas as an object of urban planning and landscape design. There are three main ideas that uncover the meaning of the subject according to the principles of designing Water areas: considering them as habitat environments, investigation of changes in the lives of the current generation in accordance with the necessity to adapt to climate change, studying a nation's memory in a historical retrospective and in the process of searching for historical national identity. The study considers water depending on its physical state.

Keywords: architectural and landscape design, water areas, habitat, environment, adaptation to climate change, historical memory of nation, physical state of water: solid, liquid, gas

Streszczenie

W dzisiejszych czasach paradygmat współistnienia planety ze środowiskiem wodnym zmienia się z powodu wpływu wielu czynników, wśród których główną rolę odgrywa zmiana klimatu. Znaczenie i konieczność znalezienia nowych zasad współistnienia wody i ludzi na planecie jest rzeczywistością naszych czasów. Artykuł uzasadnia konieczność uznania obszarów wodnych za obiekt planowania miejskiego i projektowania krajobrazu. Istnieją trzy główne idee, które odkrywają znaczenie tematu zgodnie z zasadami projektowania obszarów wodnych: uznanie ich za środowiska siedliskowe, badanie zmian w życiu obecnego pokolenia zgodnie z koniecznością dostosowania się do zmian klimatu, badanie pamięci narodu w retrospektywie historycznej oraz w procesie poszukiwania historycznej tożsamości narodowej. Badanie uwzględnia wodę w zależności od jej stanu fizycznego.

Słowa kluczowe: projektowanie architektoniczne i krajobrazowe, obszary wodne, siedlisko, środowisko, adaptacja

1. Introduction

Earth is a blue planet, the surface of which is distributed between water and land. 71% of the planet is covered with water. In the past most attention in landscape and architectural practice was paid to coastal and riparian areas,-while water was usually used for economic or decorative reasons. Nowadays the paradigm of coexistence with water has changed due to many factors, among which climate change plays a principal role. While the industrial revolution has determined our civilization's development in recent centuries, the only way to evolve successfully now is to embrace the ongoing green revolution. It is quite difficult to disagree with the general statement of Dr. Hart Porsch of Balam Investments, LLC, that "the future state of Green is Blue" [1].

2. The aim of the research

The aim of this research is to reveal the main trends and principles of the design of water areas in an architecture and landscape context and to determine social aspects of their influence on further development.

3. Description of water areas and their design in an architectural and landscape context

3.1. 'Water areas' – a new term and the main principles of architectural and landscape design

The importance and necessity of finding new rules for the coexistence of water and humans on the planet due to the climate change is a current reality.

So, it is necessary to consider 'Water Areas' as an object of urban planning and landscape design [2]. Let us evaluate all the pros and cons from a professional point of view and try to clarify why water areas have potential in architectural and landscape usage, how long they have been used by humans, and their prospects for the wellbeing of people on the planet. '*Water areas*'[1] is a new term introduced by the Author in the theory of urban development and landscape architecture.

In fact, humans have long used water areas extensively for their own needs. Let us analyze how.

The term 'Water areas' implies areas under natural bodies of water such as oceans, seas, lakes or rivers. Water areas include the water surface, the water column and the underwater shore. They are potential areas for future human settlement. This leads to the introduction of a new urban construction concept for the development of aquatic spaces of the planet and the

[1] The term 'Water Areas' was approbated in the works of the scientific and technical conferences «Energy-Integration-2017», «Underwater Technologies-2017» at KNUBA, UA; International Multidisciplinary Scientific Conferences on Social Science and Arts SGEM 2016, Bulgaria.

territorial waters of countries. Thus, the geographic system of land and water in its projection on spatial planning is the zone of their mutual inter-influence, which must be designed at a qualitatively new level [2]. The peculiarities of their design take into account the natural processes of water ecosystems, etc. [3].

Like all urban planning and landscape design objects, water areas also need principles of architectural and landscape design. We may consider some of the following main principles: the principle of complementarity of water and land coastal territories; the principle of transference; the principle of balanced cooperation; the principle of a technologically diverse architectural-design approach to the utilization of water in landscape architecture, etc. For example, the principle of transference assumes the transfer of elements of water areas to coastal areas and vice versa to achieve and enrich a variety of architectural and landscape solutions.

3.2. The architecture and landscape context of water areas

What are the principles of the spatial composition of water areas? From a landscape and architectural point of view, what does it mean to live in direct contact with water, near water, on water or under water? We discuss three main ideas that uncover the meaning of the subject.

Irreversible climate change and innovations in social development at the beginning of 21st century are related to changes in the paradigm of coexistence with the planet's aquatic environment. In the Author's opinion, the importance of water areas is primarily related to considering water territories as habitat environments. Secondly, the urban planning politics of land and water areas should be changed in accordance with the necessity of adapting to climate change. Lastly, changes in the paradigm of coexistence with the planet's aquatic environment

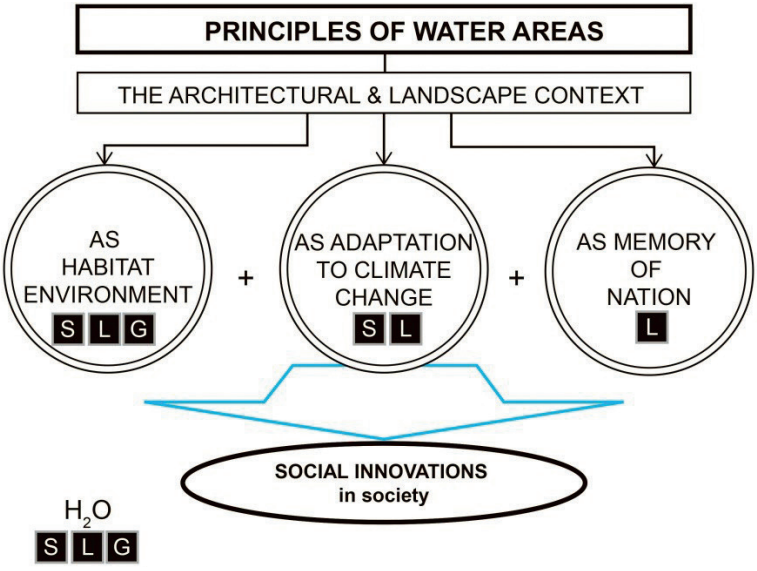

Fig. 1. Diagram of Designing Water Areas (by Liudmyla Ruban). Physical state of water: S – solid, L – liquid, G – gas

influence attitudes towards natural water bodies from a historical perspective and raise the issue of uncovering its meaning in historical and national development. Therefore, historical national memory is tied to determination of the role of water bodies in the development of civilizations: they can be either big rivers or seas. This influences contemporary approaches to the planning of memorial places [4]. All these aspects lead to social innovations in society and enhanced living conditions. The diagram below shows the main trends and design principles of water areas, Fig. 1.

Water is the only substance on our planet which can naturally be present in all three possible physical states. The general concepts of architectural-landscape usage of water components depend on the physical state of water and are outlined by the Author in articles [5–8]. Additionally, the Author has previously investigated the application of water components in solid and liquid states at various scales [9–11]. So, the existence of water as a liquid, solid and gas can help us to investigate the architecture and landscape principles of composing water areas in a more embracing way.

3.3. Architecture and landscape design of water areas as habitat environments

Liquid State: on water

In this part, we examine water as a habitat in its three possible physical states: liquid, solid and gas. The main focus is on marine ecosystems and their possible future development in the 21st century as these currently seem the most popular. The possible planning of underwater and above-water settlements and analysis of international projects over the past five years can provide us with a general idea of the direction in which the architectural-landscape practice of water areas is developing [10]. The conducted analysis of international experience in the design and planning of new cities in aquatic environments highlights new approaches in modern engineering and technology solutions, revealing the potential of marine ecosystems for future development and housing.

Futuristic living suddenly seems to be approaching quite rapidly. For five years, California-based company The Seasteading Institute has been conducting research into the potential for permanent innovative communities that float on the sea. DeltaSync and their associates completed their concept in December 2013. The company signed a deal with the French Polynesian government to begin construction in the Pacific in 2018. The first floating city with significant political autonomy may be established by 2020 [12]. However, people living on the surface of water is not something extraordinary to our planet. For example, the Uros people created an artificial floating island in the Lake Titicaca, in Peru, South America. This is a traditional form of living on the water of a lake. The Uros build their homes and boats from reeds called totora. Each artificial island can support about 10 houses.

Liquid State: under water

Other contemporary evidence of the active usage of water areas can be found in numerous examples of existing underwater dwellings or tenements for people. The diversity of public underwater buildings at the beginning of the 21st century can be separated into the following

categories: hotels with underwater accommodation; hotels with underwater restaurants; individual floating rooms or small houses. Hotels with underwater accommodation have been built all over the world in the USA, Maldives, Emirates, Singapore, etc. The first underwater hotel, Jules' Undersea Lodge, appeared in 1986 in Key Largo, Florida. The newest is Resorts World Sentosa, Singapore. Underwater restaurants in hotels can be found in the Maldives, Emirates etc. Floating rooms or small independent houses have existed in Sweden since 2000 (in a lake near Stockholm; in Lake Mälaren in Västerås), and in Tanzania since 2006 (Manta Resort on Pemba Island in Zanzibar). In fact, underwater usage is the newest trend in Green Blue underwater infrastructure. There are several fantastic examples, e.g. Green Ocean Farming (Cangas, Galicia, Spain), which uses the entire water column and ropes on which thousands of mussels grow to commercial size. This is green ocean farming. No pesticides, feed or antibiotics are needed, and these mussels are recognized as among the best in the world. Small-scale ocean farms which practice multi-trophic aquaculture like this one can provide sustainable food and biofuel, clean up the environment, and facilitate the reversal of climate change.

Solid state

Our research also considers accommodation in permafrost where water is in its solid form as ice and snow. The Arctic is a dynamic, heterogeneous and contested territory today. Catalyzed by climate change and increasing pressure from globalization and natural resource demands, the region is entering a new and unprecedented era in which greater environmental, political, economic and social fluxes are both challenging and redefining its future. Areas of permafrost, for example Nunavut, a rapidly transforming region and one of the newest independent territories in Canada since 1990, has a strong demand for urban planning projects. Among the most interesting projects for snow and ice environments, it is worth also mentioning some others: the new Halley Research Station, Brunt Ice Shelf, Antarctica, 2005–2012; the Transformable Antarctic Research Facility Project, 2014; the concept Alpine Capsule by Ross Lovegrove, 2010; and the Large-Scale Hydroponic-Farming «Arctic Harvester» near Greenland, 2013.

The beginning of the 21st century saw steady development of the ice architecture sector, as evidenced by the appearance of new buildings and facilities. Strong competition in tourism leads to new exotic ice objects, not only ice hotels, but elements of spa centers, churches, chapels, museums of ice sculptures, etc. The range of ice architecture is constantly expanding and seems limitless. Usually, ice hotels are temporary buildings made of snow, sculpted blocks of ice, and in some cases steel framing. Most ice hotels are reconstructed every winter and depend on constant sub-zero temperatures during construction and operation. In addition, ice interiors in hotel suites have become quite popular.

Gaseous State

Gas, the third and the most intriguing state of water, is now in the focus of research. The last 10 years of the creative mind of one dreamer show that Cloud Cities can exist not only in the imagination: "The Cloud Cities series by Tomás Saraceno shows a world without scale

or definable reference points. A seemingly endless landscape covered with a very thin layer of water erases the ground plane, placing the subject matter in the middle of an ostensibly null space" [13]. Man can successfully use water vapor, as shown by the example of the Blue Lagoon Spa Center in Iceland. The Center is located in a lava field in Grindavík on the Reykjanes Peninsula in southwestern Iceland and is used by visitors for total healthy relaxation. The Blur Building, a media pavilion for Swiss EXPO on Lake Neuchatel in Yverdon-les-Bains, Switzerland, is an artificial cloud on the surface of a lake, designed in 2002 by Diller, Scofidio and Renfro [14, p.80].

3.4. Architecture and landscape design of water areas as a contribution to adaptation to climate change

The role of water landscapes in adaptation to climate change is highly significant. The paradigm of modern coexistence with natural water bodies, according to the author, is characterized by not only seeing natural water bodies as a source of threat which demands permanent protection, but also from the standpoint of understanding the natural processes of aquatic ecosystems and the need for adaptation to climate change. Attitudes need to change in this regard. To open the design of water areas in this direction, environmental art-installations can help a lot in understanding the urgency of the climate adaptation process.

Liquid State

One symbolic work from the turn of the 21st century was a climatic installation project called 'Green River' created by Olafur Eliasson in various countries around the world [15]. This way of using water areas in art installations attracted global attention to the contemporary problem of environmental pollution and how to fix it.

Solid state

Environmental issues affect every human being on our planet. Contemporary environmental art installation works have targeted environmental protection, attracting attention to water pollution, protection of glaciers, and other problems related to climate change. This can be illustrated by numerous art works which utilized water in its solid state as ice. A good example is the Iceberg Murals by Sean Yoro (aka "Hula") which were painted in Iceland in 2015. This new series of artworks is entitled 'A'o'Ana or a Warning about climate change'. "On the shoreline, Hula has painted the image of an arm reaching onto an icy mass. Within a few weeks, the murals will be forever gone" [16]. Other examples are ice installations in European cities: 'Ice Watch' by Olafur Eliasson, which allows people to listen to and feel the ice [17]. Artists also want to attract mass attention with the assistance of sculpture. The sculptures by sculptor Nele Azevedo showed the natural process of climate change in a very lucid and clear manner. In 2008 in Italy and in 2012 in Chile Azevedo put more than 1,200 little ice figures to sit and relax on the steps of famous buildings. These human silhouettes, called Monumento Minimo, only stayed a few hours before "melting into the crowd" [18].

3.5. Architecture and landscape design of water areas as historical national memory.

Liquid State

The architectural and landscape design of water areas is also concerned with creating a social urban environment in which inter-generational cultural and historical memories are included. Regarding the author's paradigm of coexistence with aquatic surroundings, the attitude to landscape water bodies has changed in recent years: from taking them into account as just an object of nature, to regarding them as an integral part of the spiritual heritage of a nation. There are many historical science works dedicated to the study of the meaning of different water bodies such as a seas or great rivers in the historical process of humanity [19]. The focus of composing water areas as human memory is related, in our opinion, to the architectural-landscape setting of memorial places [4]. Along with the general idea and design, the natural condition of a site and particular elements of landscaping play an important role in planning the composition of memorials

One of the most expressive landscapes is a sea shore with its natural rocks, waves and tides. A meaningful and unusual example of a combination of a sculpture alongside the natural features of a sea shore is demonstrated by the Monument to the Partisan Woman at the Biennale Gardens in Venice. This monument is devoted to the memory of the partisan movement, and the women who contributed to the fall of fascism in Italy. The monument makes a very strong impression when the limp figure of a woman lying on the ground is covered by the waves. "Great art as a reminder of the horror of humanity. The monument was designed by Carlo Scarpa, and it's a great design. Never meant to float – and the female form is submerged at high tide. Maybe that submergence and disappearance says something about the fate of women in war" [20].

The riparian areas along rivers can also be used in relation to the memory of a nation, but in a different way. The main principles (the complementarity of water and coastal areas; transference; balanced cooperation) can be illustrated by examples of 20th century Ukrainian architectural and landscape practice. It worth mentioning that not only great rivers but also small streams can play a significant role in architectural and landscape design of historical sites. The Dnipro River and its tributaries in Kiev play a significant role in the general planning of the city; its role can be revealed by the architectural and landscape features of the planning solutions. A unique landscape characteristic of Kiev is the contrast of the high right bank and the low left bank along with the breadth of Dnipro river bed and its natural islands. The architectural-landscape design of the slopes of the high right bank of Dnipro River in Kiev consists of a number of historical parks, objects of sacral architecture and historical monuments. Among them are the famous Kievo-Pecherskaya Lavra and the Memorial Complex of World War II with the Monument of the Motherland. One notable planning solution of the Memorial complex is the imitation of Dnipro River with the assistance of an artificial reflecting pond and a group of monumental sculptures, all of which combine with Dnipro River in the background of the panoramic view. In such a way, the principle of transference is used in the general planning of coastal areas.

A similar landscape situation – a river bed with the contrast of its banks – can be found in another place in Kiev, but due to various urban reasons and conditions it is rarely seen at all. This is Lybid River, which was once a high water but is now a degraded watercourse completely swallowed up by the city. The Baikovo Memorial Cemetery was built on the slopes of the eponymous mountain on the riparian areas of Lybid River in 1834. Next to it the architectural Park of Memory (1967–1982) complex was built in the mid-20th century [21, 22]. This complex provides a unique planning example of a place of historical memory in the city (Fig. 2 a and b). "The plastic forms of Memorial Park are filled with ideas. The dominant idea is motion – the eternal, unstoppable motion of Life. It is also an invitation to everyone to think about themselves, about an implication, about a time. The materialized metaphors are water, mirror, reflection, transition, and entrance portal (it cannot be used as an exit)" [21, p. 355], Fig. 2. Being based on the principle of transference, the theme of water was developed by the author-sculptors in several ways: in the fluidity and smoothness of the created terraces as well as in a pool that reflects the monumental relief of the Memorial Wall, with a total length of 213 m, Fig. 3a. The artistic relief up to 14 meters in height became an integral part of the powerful system of the retaining wall of the slope. The third method of using the plastic features of water was to create an artificial reservoir with a system of vertical jets that create a vertical water wall delineating the various functional zones of the complex. The project was implemented in 10 years and was opened to the public in 1978. To great public regret, a decision was made to cover the unique relief with a concrete sarcophagus in 1982 and a unique artistic object was therefore lost. Now, instead of water in the reservoirs, bushes and young trees grow, and there is only a concrete retaining wall, Figs. 2c, 3b, c and the historical Lybid River again "disappeared".

4. Results

The qualitative change of the paradigm of modern coexistence with natural water bodies nowadays leads to changes in the architecture and landscape design of water areas. The principles of composing water areas are also manifested in the complex interactions of historical processes, national characteristics, global problems and the readiness of mankind for these challenges. The disclosure of the architectural and landscape meaning of water areas once again allows us to realize the role of architecture in changing national mentality and the necessity of such changes in historical, national, and environmental terms. The question of prosperity in the future – the happy future of mankind – is directly connected to the present.

The future existence of mankind on the planet, its direct dependence on the quality of drinking water, as well as the critical state of the planet's aquatic ecosystems and irreversible climate change determine changes in attitudes towards water areas and raise questions about the complimentary coexistence of human beings and the aquatic environment.

In the paper, the author illustrates the great importance of understanding contemporary problems such as the fragility of aquatic ecosystems. It is necessary to change the mentality of humankind in order to support and implement corresponding decisions. According to the author, revealing principle issues in this way should influence the development of new

innovative approaches to architecture and landscape design of land and water areas on the principles of complementarity and balanced cooperation, which will qualitatively improve the environment in the future.

5. Summary

The main conclusions are:

1) Water areas are a new object of architectural and landscape design;
2) The research examines the principles of architectural and landscape design of water areas: the principle of complementarity of water and land coastal territories; the principle of transference; the principle of balanced cooperation; the principle of a technologically diverse architectural-design approach to the utilization of water in landscape architecture, etc.
3) The main trends of the design of water areas are revealed from three positions: as habitat environments, as the need to adapt to climate change, and as the memory of a nation.
4) The different states of water (solid, liquid and gas) are considered in the research.
5) The architectural and landscape context in composing water areas once again allows us to realize the principal role of architecture in changing the mentality of humankind and the opportunities it provides in creating qualitatively new habitats by the development of a specific design approach

References

[1] http://www.balamescape.com/ *The Balam Escape, A Sustainable Edutainment Community of the 21st Century* (access:28.02.2018).

[2] Ruban L., *The System of Coastal and Water Areas in The Modern Theory and Practice of Urban Planning and Landscape Architecture*; Sci.-Tech. Collection: Urban Development and Regional Development, Kiev, KNUCA, 2017. Issue 65, P. 475-483 (in Ukrainian).

[3] Ruban L., *Natural-Hydrological Protection for waterfront territories: "Blue-Green" Initiative*, Conference Proceedings of International Multidisciplinary Scientific Conferences on Social Science and Arts SGEM 2016 "History of Arts, Contemporary Arts, Performing & Visual Arts, Architecture and Design", Book 4, STEF92 Technology Ltd., Sofia 2016, pp. 443-450.

[4] Ruban L., *The architecture and landscape organization of memorials to prominent people: study of water features*, The Journal of Urban Design and Architecture, vol. XLIV, 2016, pp. 195-202.

[5] Ruban L., *Modern Trends in the Usage of Water in Contemporary Architectural-Landscape Practice*, The new Ideas of New Century – 2014: The Fourteenth International Scientific Conference Proceedings: in 3 vol. Pacific Ocean State University, Khabarovsk, Pacific Ocean State University, 2014, Volume 3, pp. 160-166 (in Russian).

[6] Ruban L., *Three States of Water: How Technology Makes Water a Construction Material,* Technical Transactions, vol. 8-A/2014, pp. 27-37.
[7] Ruban L., Kuc S., *Water as the Factor of Techno-creation*, Proceedings of a 2nd Annual International Conference of Architecture and Civil Engineering (ACE-2014), Global Science and Technology Forum (GSTF), Singapore 2014, pp. 50-54.
[8] Ruban L., Kuc S., *Contemporary Water Landscapes. Trends, Issues and Techno-creation,* GSTF Journal of Engineering Technology (JET), vol. 3, No. 1, July, 2014, p. 96-105.
[9] Ruban L., *Decorative Features of the Phenomenon of "Water" for the Modern Architectural and Landscape Practice: Statics and Dynamics Forms*; Sci.-Tech. Collection: Modern Problems of Architecture and Urban Development. Kiev, KNUCA, 2017, Issue 49, pp. 343-352 (in Ukrainian).
[10] Ruban L., *Underwater Urban Studies: Modern Issues and Trends*, Sci.-Tech. Collection: Underwater Technology. Kiev, KNUCA, 2016. Issue 3, pp. 54-65.
[11] Ruban L., *Decorative Features of the Phenomenon of "Water" for the Modern Architectural and Landscape Practice: Study of Solid State*, Sci.-Product. Collection: Architectural Bulletin. Kiev, KNUCA, 2017, Issue 13. pp. 316-325 (in Ukrainian).
[12] https://www.seasteading.org/floating-city-project/ *The Floating Island Project: French Polynesia* (access:28.02.2018).
[13] http://tomassaraceno.com/projects/cloud-cities-flying-garden/ *Flying garden -Cloud cities* (access: 28.02.2018).
[14] Preton-Pinney G., *The Cloudspotter's Guide*, London: Hodder&Stoughton, 2006.
[15] http://olafureliasson.net/archive/artwork/WEK101541/green-river / *Green River by Olafur Eliasson* (access:28.02.2018).
[16] https://www.widewalls.ch/street-artist-hula-iceberg-mural/ *A Street Artist Paints on Melting Icebergs - Meet Sean Yoro aka Hula*, (access:28.02.2018).
[17] http://olafureliasson.net/archive/artwork/WEK109190/ice-watch / *Ice watch by Olafur Eliasson* , (access:28.02.2018).
[18] https://www.neleazevedo.com.br/minimum-monument / *Néle Azevedo, Minimum Monument,* (access:28.02.2018).
[19] Ruban L., *Architectural & Landscape Organization of Waterfront Territories: Historical – Cultural Potential*, Conference Proceedings of International Multidisciplinary Scientific Conferences on Social Science and Arts SGEM 2016 "History of Arts, Contemporary Arts, Performing & Visual Arts, Architecture and Design", Book 4, STEF92 Technology Ltd., Sofia 2016, pp. 229-236.
[20] https://muse.jhu.edu/article/364596/pdf / *Renata Codello, Joanna Dezio, Carlo Scarpa's Monument to the Partisan Woman*, (access:28.02.2018).
[21] Erofalov-Pilipchak B.L., *Architecture of Soviet Kiev*; Kiev, Publishing house A + C, 2010, 640 p. (in Russian).
[22] Erofalov B.L., *Architectural Atlas of Kiev*; Kiev, A+C, 2013, pp. 352 (in Russian and English).

If you want to quote this article, its proper bibliographic entry is as follow: Krzysztof Tomczyk, Marek Sieja, *Relationship between the absolute error and parameter values of voltage output accelerometer*, Technical Transactions, Vol. 6/2018, pp. 29-40.

a)

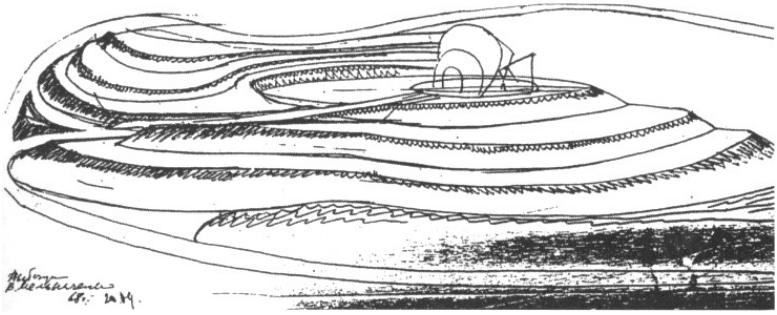

b)

c)

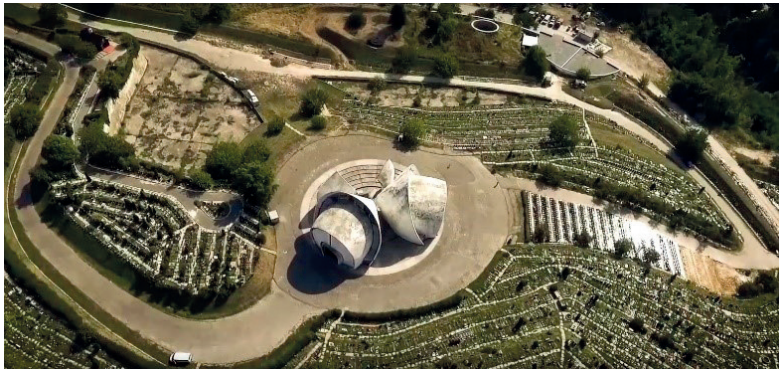

Fig. 2. Memory Park Crematorium on Baikova mountain on the riparian areas of Lybid River, Kiev, Ukraine, 1967–1982, by artist–monumentalists Ada Rybachuk, Vladimir Melnichenko: a) authors' sketch, 1968, [21]; b) general aerial view of the complex, 1978, [21]; c) general aerial view of the complex, 2017.

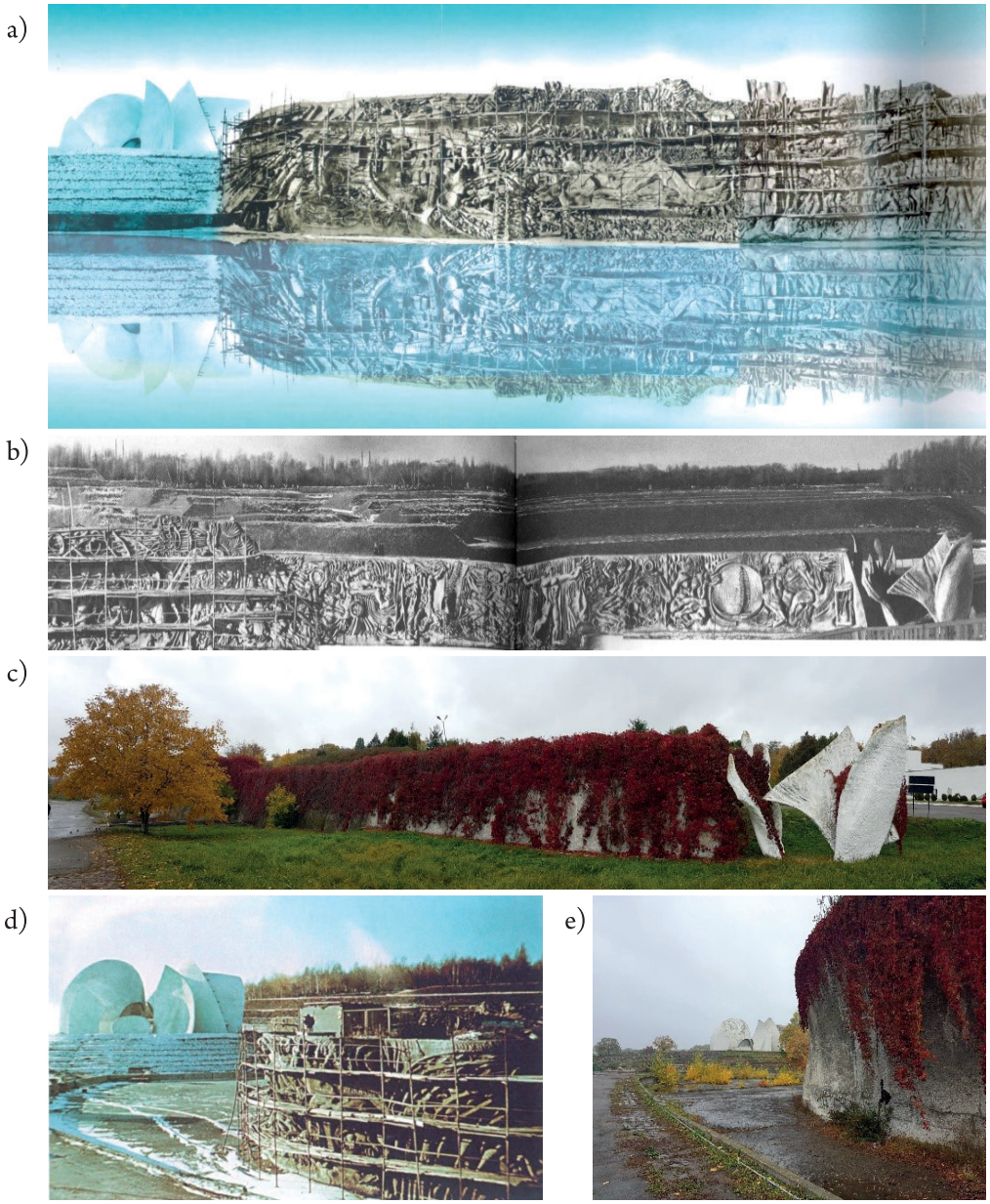

Fig. 3. A comparison of the Memorial Wall: construction in 1978 (a, b, d) and its state in 2017 (c, e). The 1978 photos (a, b, d) are from [21] and the photos of its current state (c, e) are by Ruban L.

TECHNICAL TRANSACTIONS 6/2018
CHEMISTRY
DOI: 10.4467/2353737XCT.18.085.8690
SUBMISSION OF THE FINAL VERSION: 11/05/2018

Karolina Kula
Agnieszka Łapczuk-Krygier (lapczuk@chemia.pk.edu.pl)
Institute of Organic Chemistry and Technology, Cracow University of Technology

Diazafluorene in 1,3-dipolar cycloaddiction reactions: short review

Diazafluoren w reakcjach 1,3-dipolarnej cykloaddycji: krótki przegląd

Abstract

This review is an attempt to systemise knowledge within the field of 1,3DC reactions of diazafluorene with different dipolarophiles. This paper is arranged according to the dipolarophile structure. We are hoping that this review can help organic chemists who deal with the preparation of five-membraned heterocycles.

Keywords: diazafluorene, 1,3-dipolar cycloaddition, 1,3-dipol

Streszczenie

Niniejszy przegląd stanowi próbę usystematyzowania stanu wiedzy w obszarze reakcji 1,3DC diazafluorenu z różnymi dipolarofilami. Materiał został uporządkowany na podstawie budowy dipolarofila. Mamy nadzieje, iż przegląd będzie pomocny chemikom organikom zajmującym się preparatyką związków heterocyklicznych.

Słowa kluczowe: diazafluoren, 1,3-dipolarna cykloaddycja, 1,3-dipol

1. Introduction

This publication is a review of literature concerning diazafluorene as a 1,3-dipole in 1,3-dipolar cycloaddition reactions, which enable creating heterocyclic compounds.

Pyrazolines are a diverse group of compounds, which demonstrate biological activity. These connections are often researched from a pharmacological perspective. They are characterised by an exceptional antibacterial [1, 2], antiviral [2, 3] as well as antifungal effect [2]. Apart from microbiological activity, pyrazolines stimulate the central nervous system (CNS), which in turn allows them to be used as means of treating illnesses, such as depression [4, 5] or epilepsy [5].

Moreover, the literature points towards using pyrazolines as painkillers [6, 7] or anti-inflammatory [2, 4, 6–9], antipyretics [5], antiulcer [6], antirheumatic [8] , antitubercular [5], anticancer [10] or hypotensive [5] drugs.

Pyrazolines are characterised by antioxidant activity [5]. These properties led scientists to research possibilities of using heterocyclic as antineoplastic drugs [3, 5].

Pyrazolines are also used in industry. They mostly serve as dyes [11–13]. They are used as insecticides and herbicides as well, however, to a lesser extent [11, 14].

The process of 1,3-dipolar cycloaddition (in brief 1,3DC) is the most universal method of creating five membered carbo- and heterocyclic compounds [13]. When using diazafluorene (as 1,3-dipole) as an addent, one can produce connections of a pyrazoline [11–26] skeleton within its structure. Those connections are valuable from a practical perspective [1–10]. In addition, cycloaddition with diazafluorene allows synthesis of spatially crowded groups of spiro-pyrazolines, an adduct otherwise hard to produce [27].

1,3DC reactions between diazafluorene and electrophilic dipolarophiles, which lead to heterocycles, were discovered at the beginning of the XX century. The eldest, and as such historically first record in literature of these reactions comes from 1916. German chemists *Staudinger* and *Galue* carried out a reaction between diazafluorene (1) and diphenylketene (2). As a result, they received 3-fluoren-4,40-diphenylpirazolin-5-on (3). The process is realised relatively mild conditions and has a yield of 15% [15].

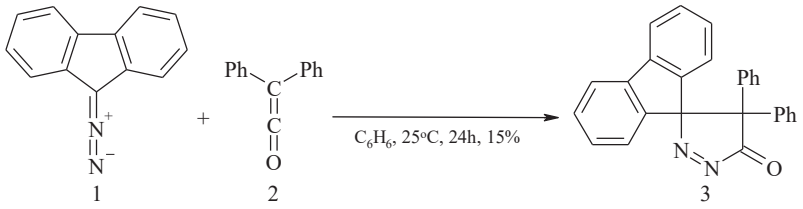

Fig. 1. Synthesis of 3-fluoren-4,4-diphenyl-Δ^1-pyrazoline-5-one (3)

2. Reactions of diazafluorene with dipolarophiles which has >C=C< an ethenyl core

Cycloaddition between diazafluorene (1) and dimethyl chlorofumarate (4) is an example of a reaction with dipolarophile with an ethenyl core. The process is realised a temperature of 25°C and benzene as a solvent, and has a 75% yield. Theoretically, it is possible for the >C=O bond from the dipolarophilic part of the compound to participate in this reaction. However, it remains intact as the reactivity of >C=C< part is relatively high. This is a typical phenomenon, which also occurs in other >C=C< and >C=O configurations [16, 18, 28].

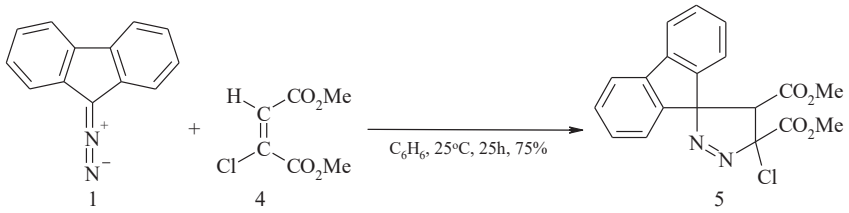

Fig. 2. Synthesis of 3-fluoren-4,5-dicarbonylmethoxy-5-chloro-Δ^1-pyrazoline (5)

Another example of a similar reaction is synthesis in which (3,3-dimethyl-2-phenyl-cyclopropenyl)-diphenylphosphin oxide (6) is present. In order for the process to occur, a temperature of 50°C and benzene as a solvent are required. The reaction is selective, similarly to the previous example, resulting in one of two possible regioisomeric adducts [16].

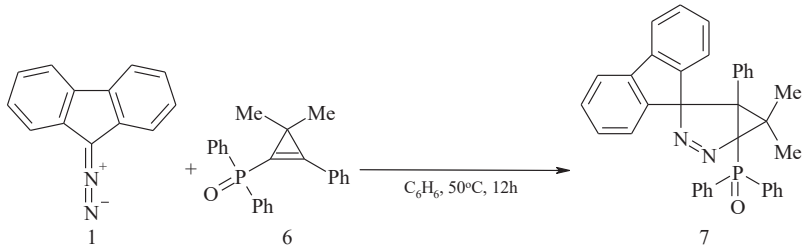

Fig. 3. Reaction between diazafluorene (1) and (3,3-dimethyl-2-phenylcyclopropenyl)-diphenylphosphin oxide (6)

Yet another similar cycloaddition with N-phenyl-maleimide (8) as dipolarophile can be observed in milder conditions, with a required temperature of 0°C [28].

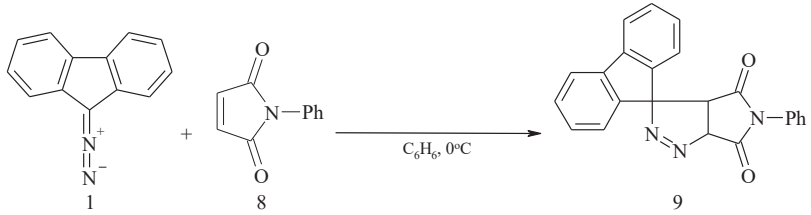

Fig. 4. Synthesis of 3-fluoren-4,5-dicarbonylmethoxy-5-chloro-Δ^1-pyrazoline (9)

Functionalised bicyclo[2.2.0]hex-5-enes, which are characterised by a sp^2-sp^2 strained system, also have been tested as dipolarophiles with >C=C<, for example, a reaction of diazafluorene (1) with 2,3-diazobicyclo[2.2.0]hex-5-ene-2,3-dicarboxylic acid dimethyl ester (10) The process is realised at a temperature of 25°C and diethyl ether as a solvent, and leads to a single product [18].

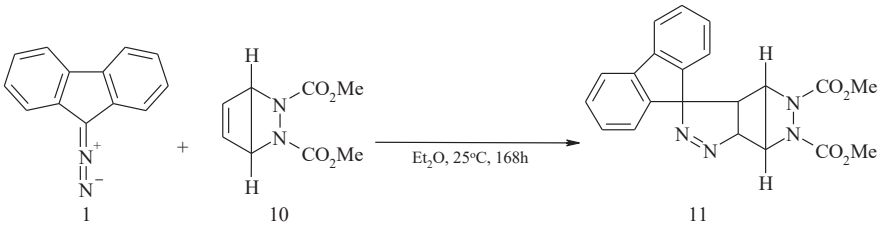

1 10 11

Fig. 5. Reaction between diazafluorene (1) and 2,3-diazobicyclo[2.2.0]hex-5-ene-2,3-dicarboxylic acid dimethyl ester (10)

According to the authors, processes with 5-oxabicyclo[2.2.0]hex-2-en-6-one (12), 2-isopropyl-2-aza-bicyclo[2.2.0]hex-5-en-3-one (15), as well as 2,3-diazobicyclo[2.2.0]hex-5-ene-2,3-dicarboxylic acid methyl ester (18), are carried out in a similar manner. They require a temperature between 0-40°C and diethyl ether as a solvent, forming two isometric end products. It is worth noting that by applying higher temperatures, the reaction's time can be shortened. However, temperatures which are too high can cause nitrogen to disappear from Δ^1-pyrazoline rings [18].

With regards to the reaction depicted below, the author states that a division of end product isomers is not possible [18].

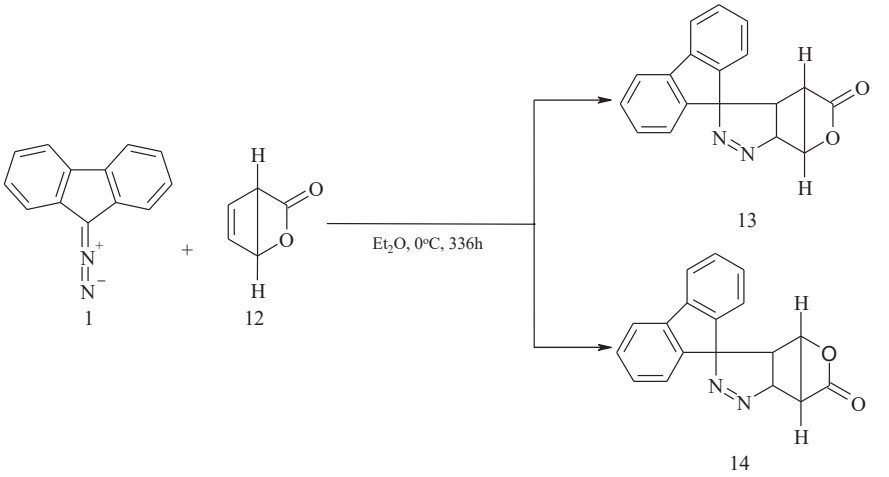

1 12 13 14

Fig. 6. Reaction between diazafluorene (1) and 5-oxabicyclo[2.2.0]hex-2-en-6-one (12)

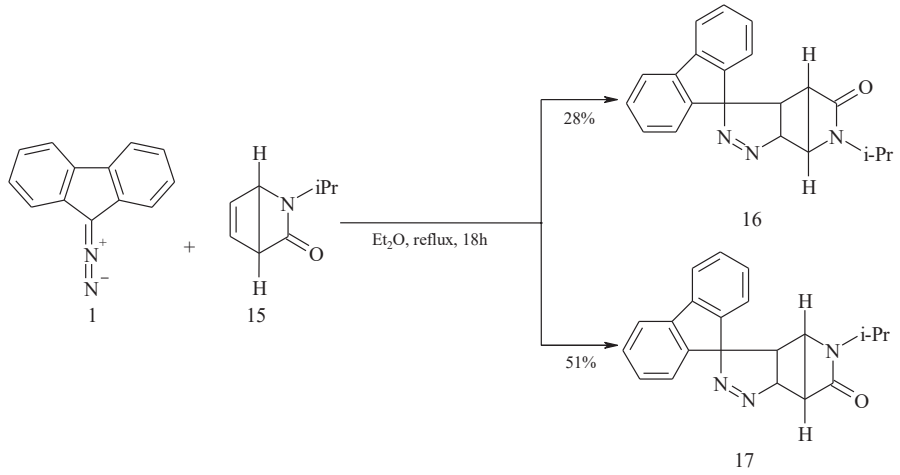

Fig. 7. Reaction between diazafluorene (1) and 2-isopropyl-2-aza-bicyclo[2.2.0]hex-5-en-3-one (15)

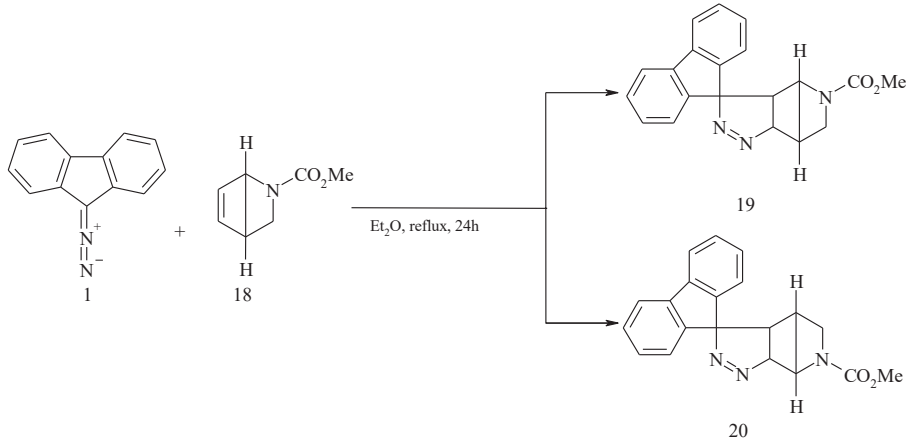

Fig. 8. Reaction between diazafluorene (1) and 2,3-diazobicyclo[2.2.0]hex-5-ene-2,3-dicarboxylic acid methyl ester (18)

Not all reactions between diazafluorene (1) and dipolarophile with an ethylene part result in a cyclic product. An example of an unexpected mechanism is a series of reactions with (E)-2-aryl-1-cyano-1-nitroethenes (21). They are realised at a temperature of 25°C and benzene as a solvent, and lead to derivatives of hydrazines. During the reaction, a particle of cyanonitrocarbene is eliminated, which in turn leads to an acyclic product [29].

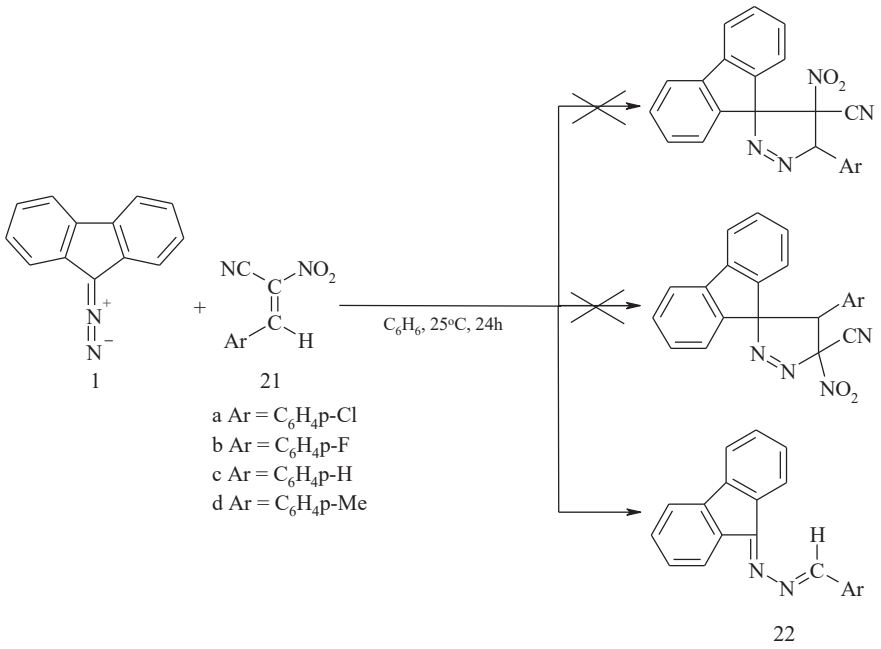

Fig. 9. Synthesis of 1-arylidene-2-(9H-fluoren-9-ylidene)-hydrazones (22a-d)

3. Reactions of diazafluorene with dipolarophiles which has –C≡C– an acetylene core

According to literature, the first synthesis of dipolarophiles with an acetylene core was carried out in 1943. It is a reaction between diazafluorene (1) and propynoic acid methyl ester (23), described by *Aphen*, with an end result of one of two possible regioisomeric products – analogue of pyrazole. The processes is realised at a temperature of 25°C and diethyl ether as a solvent [14].

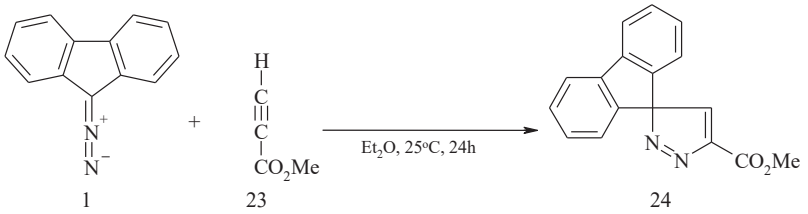

Fig. 10. Synthesis of 3,3-diphenylenepyrazolenine carbonic acid-(5)-methyl ester (24)

A reaction with dimethyl acetylenedicarboxylate (25) leads to synthesis of 3,3-diphenylene-pyrazolenine dicarbonic acid-(4,5)-dimethyl ester (26) under the same conditions [14].

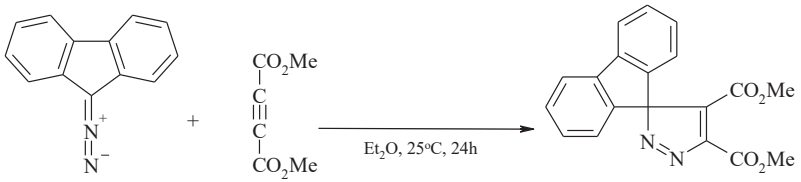

Fig. 11. Synthesis of 3,3-diphenylenepyrazolenine dicarbonic acid-(4,5)-dimethyl ester (26)

A synthesis with ditert-buthyl acetylenedicarboxylate (27) as dipolarophile is carried out in a similar manner. The processes is realised at a temperature of 25°C and benzene as a solvent [19].

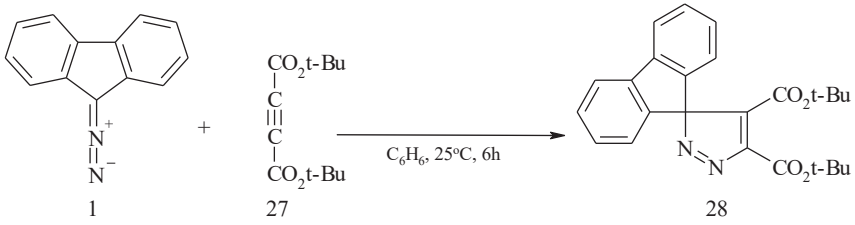

Fig. 12. Synthesis of 3,3-diphenylenepyrazolenine dicarbonic acid-(4,5)-ditert-buthyl ester (28)

Similarly, as a result of a reaction with phenylpropynoic acid methyl ester (29), one of two possible regioisomeric products can be created. The processes is realised at a temperature of 25°C and diethyl ether as a solvent [14].

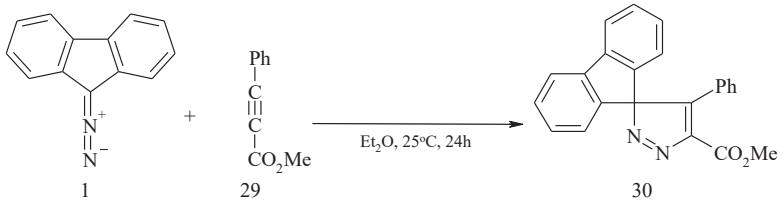

Fig. 13. Synthesis of 3,3-diphenylene-4-phenylpyrazolenine carbonic acid-(5)-methyl ester (30)

There is only one product of a reaction with FI-DIBO (31). Theoretically, cycloaddition at two parts of particles >C=C< and -C≡C- is possible. Moreover, the ethylene group is much more reactive than the acetylene core one. Nevertheless, the -C≡C- part is more exposed than >C=C<, and that determines the path of the reaction. The process is realised at a temperature of 20°C and dichlorometane as a solvent, and has a yield of 95% [12].

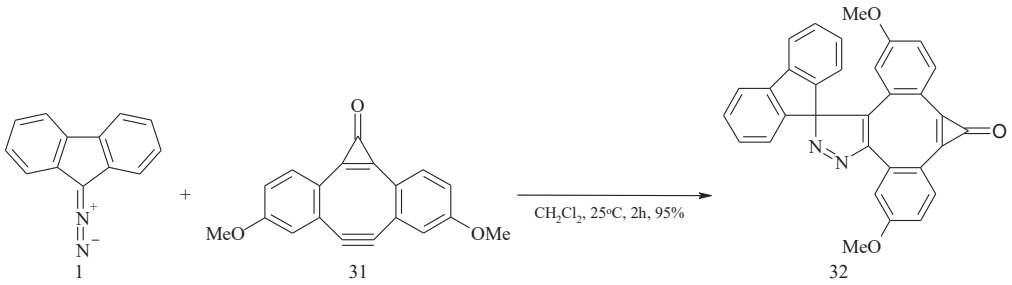

Fig. 14. Reaction between diazafluorene (1) and FI-DIBO (31)

During the process of cycloaddition with diazafluorene (1), syn-dibenzo-1,5-cyclooctadiene-3,7-diyne (33) two parts -C≡C-. As a result, a polycyclic adduct is created. The process is realised at a temperature of 25°C and benzene as a solvent, and has a yield of 46% [11].

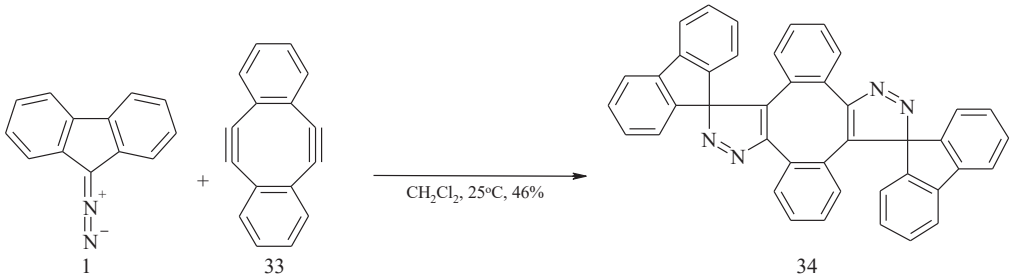

Fig. 15. Reaction between diazafluorene (1) and syn-dibenzo-1,5-cyclooctadiene-3,7-diyne (33)

1,3DC between diazafluorene (1) and 3-methyl-1,2-dehydrobenzene (35) leads to two isomers. The process is realised 1,4-dioxane as a solvent [12].

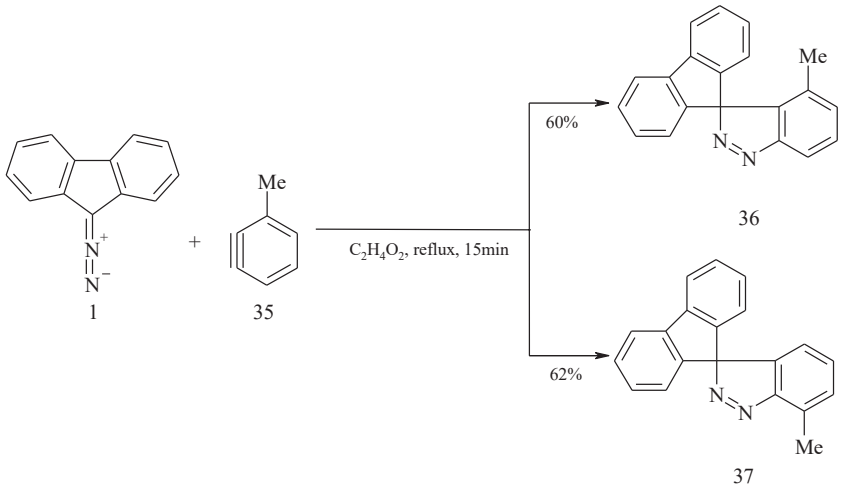

Fig. 16. Reaction between diazafluorene (1) and 3-methyl-1,2-dehydrobenzene (35)

A reaction between diazafluorene (1) and 1,2-dehydrobenzene (38), with a yield of 80%, is also known [13].

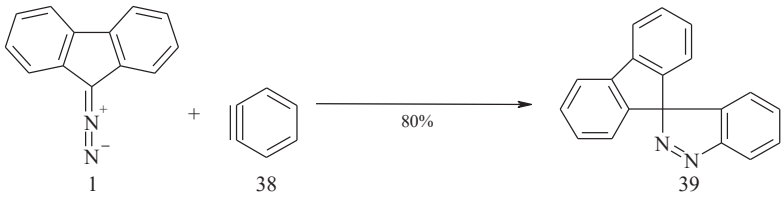

Fig. 17. Reaction between diazafluorene (1) and 1,2-dehydrobenzene (38)

The most recent literature describes diazafluorene reactions with a series of derivatives of phenylethynyl sulfones The processes are realised at a temperature of 20°C under protection from light, and has a yield of 71–77% [30].

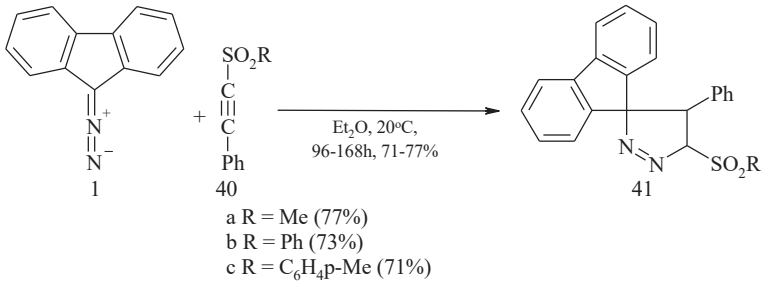

Fig. 18. Reaction between diazafluorene (1) and derivatives of phenylethynyl sulfones (40a-c)

4. Reactions of diazafluorene with dipolarophiles which has a heteroatomic core

According to literature, reactions of diazafluorene with dipolarophiles, which have a heteroatomic core, occur mostly on O=C< [20, 22] parts, creating oxadiazoline, -P=C< (phosphadiazoline) [23], and S=C< (thiadiazoline) [21, 25].

A reaction with 1,1,1,3,3-pentafluoro-2-propanone (42) is an example of 1,3DC diazafluorene (1) with dipolarophile with a carbonyl group. The process is realised at a temperature of 25°C and diethyl ether as a solvent [20].

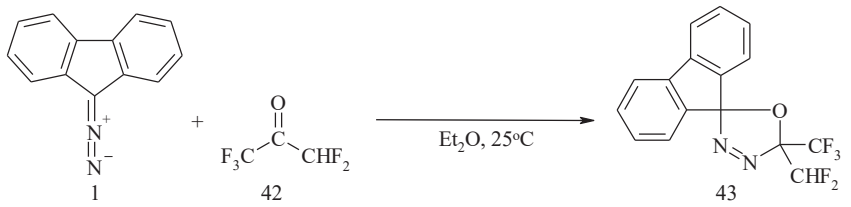

1 42 43

Fig. 19. Reaction between diazafluorene (1) and 1,1,1,3,3-pentafluoro-2-propanone (42)

Yet another example of a similar reaction is cycloaddition with acenaphthene quinine (44). The process is realised with benzene as a solvent as well as at a boiling temperature, and has a yield of 35% [22].

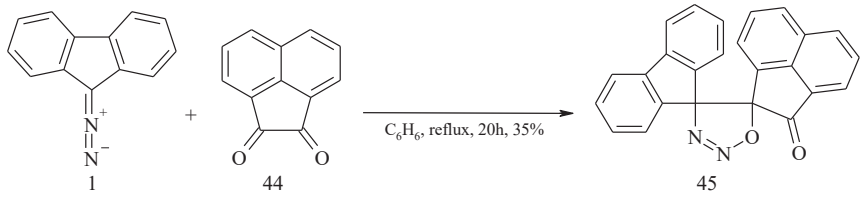

1 44 45

Fig. 20. Reaction between diazafluorene (1) and acenaphthene quinine (44)

A reaction with 2-acetyl-5-tert-butyl-1,2,3-diazaphosphole (46) is an example of 1,3DC diazafluorene (1) with dipolarophile which has a phosphadiazoline group -P=C<. The process is realised at a temperature of 20°C and cyclohexane as a solvent, and has a yield of 65% [23].

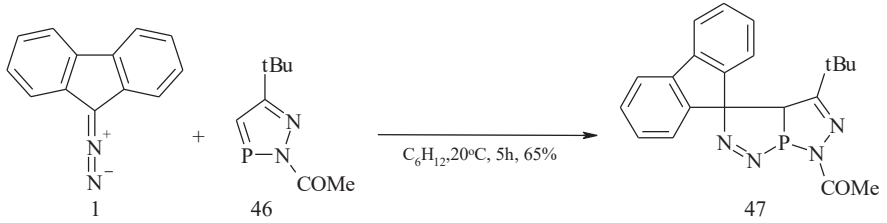

1 46 47

Fig. 21. Reaction between diazafluorene (1) and 2-acetyl-5-tert-butyl-1,2,3-diazaphosphole (46)

Similarly, reaction with 2-acetyl-5-methyl-1,2,3-diazaphosphole (48) leads to a cyclical product with a yield of 89%. The process is realised at a temperature of 20°C and hexane as a solvent (time 3h) [21].

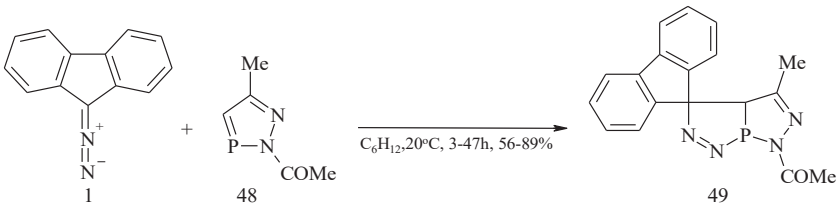

1 48 49

Fig. 22. Reaction between diazafluorene (1) and 2-acetyl-5-methyl-1,2,3-diazaphosphole (48)

Diazafluorene (1) also reacts with dipolarophile with thiadiazoline group S=C<. A reaction with methyl diethoxyphosphinecarbodithioate 1-oxide ester (50) creates 1,3,4-thiadiazoline. The process is realised at a temperature of -65°C and tetrahydrofuran as a solvent [21].

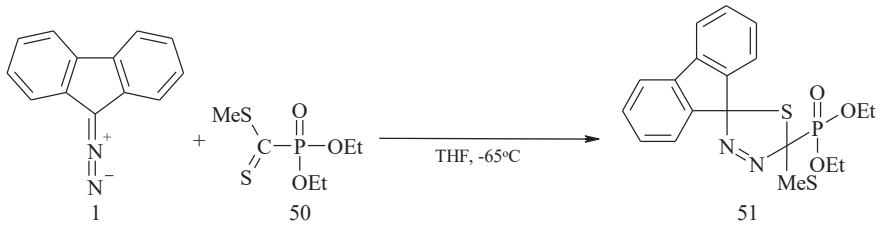

1 50 51

Fig. 23. Reaction between diazafluorene (1) and methyl diethoxyphosphinecarbodithioate 1-oxide ester (50)

A cycloaddition with adamantane-2-thione (52) is yet another example. The process is realised at a higher temperature and tetrahydrofuran as a solvent, and has a yield of 15% [25].

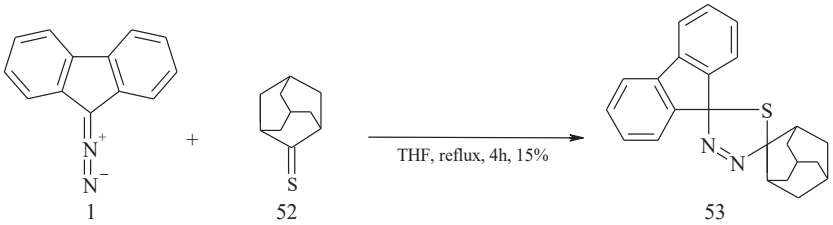

1 52 53

Fig. 24. Reaction between diazafluorene (1) and adamantane-2-thione (52)

5. Conclusions

The process of 1,3DC is the most universal method of creating five membered carbo- and heterocyclic compounds. When using diazafluorene (as 1,3-dipole) as an one of addent can produce connections of a Δ^1-pyrazoline skeleton within its structure. Those connections are valuable from a practical perspective. This review is an attempt to systemise the state of

knowledge in the field of 1,3DC reactions of diazafluorene with different dipolarophiles. This paper is arranged according to the dipolarophile structure, reviewed reactions with dipolarophiles, which has an ethenyl, an acetylene or heteroatomic core.

References

[1] Desai J. M., Shah V. H., *Synthesis and biological activity of cyanopyridine, isoxazole and pyrazoline derivatives having thymol moiety*, Indian J. Chem. 42B/2003, 382–385.

[2] Kini S., Gandhi A. M., *Novel 2-Pyrazoline Derivatives as Potential Antibacterial and Antifungal Agents*, Indian J. Pharm. Sci. 70,1/ 2008, 105–108.

[3] Havrylyuk D., Zimenkovsky B., Vasylenko O., Lesyk R., *Synthesis and Anticancer and Antiviral Activities of New 2-Pyrazoline-Substituted 4-Thiazolidinones*, J. Heterocycl. Chem. 50, S1/2013, E55–E62.

[4] Palaska E., Aytemir M., Uzbay I. T., Erol D., *Short communication Synthesis and antidepressant activities of some 3 , 5-diphenyl-2-pyrazolines*, Eur. J. Med. Chem. 36/2001, 539–543.

[5] Rahman M. A., Siddiqui A. A., *Pyrazoline Derivatives: A Worthy Insight into the Recent Advances and Potential Pharmacological Activities*, Int. J. Pharm. Sci. Drug Res. 2, 3/2010, 165–175.

[6] Amir M., Kumar S., *Synthesis and anti-inflammatory, analgesic, ulcerogenic and lipid peroxidation*, Indian J. Chem. 44/2005, 2532–2537.

[7] Berrocal-Romero J. M., Contijoch-Llobet M. M., Cuberes-Altisent M. R., Frigola-Constansa J., *Pyrazoline derivatives, their preparation and application as medicaments*, WO 99/62884, 2001.

[8] Nugent R. A., Murphy M., Schlachter S., Dunn C., Smith R. J., Staite N. D., Galinet L., Shields S. K., Aspar D. G., Richard K. A., Rohloff N. A., *Pyrazoline bisphosphonate ester as novel antiinflammatory and antiarthritic agents*, J. Med. Chem. 36, 1/1993, 134–139.

[9] Nugent R. A., Murphy M., Schlachter S. T., Dunn C. J., Smith R. J., Staite, L. A. Galinet N. D., Shields S. K., Aspar D. G., Richard K. A., Rohloff N. A., *Pyrazoline bisphosphonate esters as novel antiinflammatory and antiarthritic agents*, J. Med. Chem. 36, 1/1993, 134–139.

[10] Gomha S. M., Abdallah M. A., Al-Showiman S. S., Morad M. A., Mabkhot Y. N., *Synthesis of new pyridopyrimidinone-based thiadiazoles and pyrazolines as potential anti-breast cancer agents*, Biomed. Res. 28, 22/2017, 9903–9909.

[11] Durr V. H., Klauck G., Peters K., Von Schnering H. G., *Ein neues planares, antiaromatisches Dibenzo[8]annulen*, Angew. Chem. 95, 4/1983, 321.

[12] Friscourt F., Fahrni C. J., Boons G. J., *Fluorogenic Strain-Promoted Alkyne-Diazo Cycloadditions*, Chem. - A Eur. J. 21, 40/20150, 13996–14001.

[13] Burgert W., Große M., Rewicki D., *Gespannte alkyl-aromatische Systeme, 6. 7bH-Indeno[1,2,3-jk] fluorene und 2H-Cyclopenta[jk]fluorene aus Spiroindazolen und -pyrazolen; Regioselektivität einer intramolekularen Cyclisierungsreaktion*, Chem. Ber. 115, 1/1982, 309–323.

[14] van Alphen J., *Pyrazolines and their rearrangement to form pyrazoles. II. (Pyrazole and pyrazoline derivatives, IV)*, Recl. Trav. Chim. Pays-Bas, 43/1975, 51–59.

[15] Staudinger H., Gaule A., *Diphenylendiazomethan,* Berichte der Dtsch. Chem. Gesellschaft, 49, 2/1916, 1951–1960.
[16] Heydt H., Busch K., Regitz M., *Untersuchungen an Diazoverbindungen und Aziden, XXXVI. [3 + 2]-Cycloaddition von Diazoalkanen an 1-Cyclopropenyl-phosphinoxide; Isomerisierung der Cycloaddukte,* Liebigs Ann. der Chemie, 1980, 4/1980, 590–599.
[17] Naik A.B., Narwade M., *Studies in Influence of Dielectric Constants on Complex Equilibria Between Substituted Pyrazolines and Lanthanide Metal Ions Ph Metrically*, Am. J. Sci. Res. 3, 2/2008, 212–216.
[18] Hassenriick K., Hiichstetter H., Martin H., Steigel A., Wingen H., *Dipolar Cycloaddition Reactions with Heterocyclic Bicyclo[2.2.0] hexenes. A Contribution to the syn-anti Selectivity os cis-3,4-Disubstituted Cuclobutanes,* Chem. Ber. 120/1987, 203–212.
[19] Burgert W., Rewicki D., *Reaktionen von Spiro[fluoren-9,3'-[3H]pyrazolen] und Spiro[2-cyclopropen-1,9'-fluorenen] mit Nucleophilen*, Chem. Ber. 117, 7/1978, 2409–2421.
[20] Shimizu N., Bartlett P.D., Worth F., *Cycloaddition of Diazoalkanes to Penta- and Hexafluoroacetones. Isolation of A 3 -1,3,4-Oxadiazolines and Their Decomposition via Carbonyl Ylides,* J. Am. Chem. Soc. 100, 13/1978, 4260–4267.
[21] Mlostoń G., Urbaniak K., Linden A, Heimgartner H., *A new approach to 2,2-disubstituted 1-(methylsulfanyl)vinyl phosphonates via an intermediate thiocarbonyl ylide,* Tetrahedron 65, 39/2009, 8191–8198.
[22] El-Sawi E.A., Mostafa T.B., Radwan, H.A., *Phosphorylation of some new acenaphthenequinone derivatives*, Chem. Heterocycl. Compd. 45, 8/2009, 981–989.
[23] Guo X., Feng L., Wang Q., Li Z., Tao F., *1,3-Dipolar cycloadditions of 9-diazofluorenes and diphenyldiazomethane to 2-acyl-2 H -1,2,3-diazaphospholes,* J. Heterocycl. Chem., 43, 2/2006, 353–359.
[24] Arbuzov B.A., Dianova E.N., Sharipova S.M., *Reaction of 2-Phenyl(Acetyl)-5-Methyldiazaphosphole With Diazomethane and Diazofluorene,* Bull. Acad. Sci. USSR, Div. Chem. Sci. (English Transl.) 30, 5/1981, 873–876.
[25] Adam W., Encarnación L.A.A., *The synthesis of spiro[adamantane-[1,2]dioxetanes],* Chem. Ber. 115, 7/1982, 2592–2605.
[26] Jasiński R., *Reakcje 1,3-dipolarnej cykloaddycji: aspekty mechanistyczne i zastosowanie w syntezie organicznej,* Radomskie Towarzystwo Naukowe, Radom 2015.
[27] Jasiński R., *On the question of zwitterionic intermediates in 1,3-dipolar cycloadditions between hexafluoroacetone and sterically crowded diazocompounds,* J. Fluor. Chem. 176, 1/2015, 35–39.
[28] Mustafa A., Zayed S.M.A.D., Khattab S., *Reactions with Diazoalkanes. V. Action of Diazoalkanes and of Aryl Azides on N-Arylmaleimides,* J. Am. Chem. Soc. 78, 3/1956, 145–149.
[29] Jasiński R., Kula K., Kącka A., Mirosław B., *Unexpected course of reaction between (E)-2-aryl-1-cyano-1-nitroethenes and diazafluorene: why is there no 1,3-dipolar cycloaddition?,* Monatshefte fur Chemie, 148, 5/2017, 909–915.
[30] Vasin V.A., Masterova Y.Y., Razin V.V., Somov N.V., *Thermal, acid-catalyzed, and photolytic transformations of spirocyclic 3H-pyrazoles formed by reactions of methyl, phenyl, and p-tolyl phenylethynyl sulfones with 9-diazofluorene,* Russ. J. Org. Chem. 50, 9/2014, 1323–1334.

If you want to quote this article, its proper bibliographic entry is as follow: Karolina Kula, Agnieszka Łapczuk-Krygier, *Diazafluorene in 1,3-dipolar cycloaddiction reactions: short review*, Technical Transactions, Vol. 6/2018, pp. 41-54.

TECHNICAL TRANSACTIONS 6/2018
CIVIL ENGINEERING
DOI: 10.4467/2353737XCT.18.086.8691
SUBMISSION OF THE FINAL VERSION: 16/05/2018

Evgen Aleshinskiy
Transport Systems and Logistics Department, Ukrainian State University of Railway Transport

Vitalii Naumov (vnaumov@pk.edu.pl)
Faculty of Civil Engineering, Cracow University of Technology

Oksana Pestremenko-Skripka
Railway Stations and Junctions Department, Ukrainian State University of Railway Transport

The modelling of technological processes at border transfer stations in Ukraine

Modelowanie procesów technologicznych na przejściach granicznych na Ukrainie

Abstract

In the process of the transfer of railway wagons between countries, the main role in processing the flow of cargo is assigned to a border transfer station. Additional border operations – such as customs, environmental, veterinary, phytosanitary, and epidemiological control – have led to a significant increase in the number of detained railway wagons. As a result of these increases, delays in the deliveries of both import and export cargoes have also increased. Reducing the duration of the delivery of goods by rail could be achieved through reductions in the times taken to process trains at border transfer stations – risk management systems based on the principle of selective survey operations in international traffic processing provide such an opportunity..

Keywords: border transfer station, simulations, Petri nets, risk management system

Streszczenie

W procesie przemieszczania wagonów kolejowych pomiędzy krajami główna rola w przetwarzaniu przepływu towarów jest przypisana do stacji przejść granicznych. Dodatkowe operacje graniczne – takie jak kontrola celna, środowiskowa, weterynaryjna, fitosanitarna oraz epidemiologiczna – przyczyniają się do znacznego wzrostu liczby zatrzymanych wagonów kolejowych. W wyniku tych zatrzymań wzrastają również opóźnienia w dostawach zarówno towarów importowanych, jak i eksportowych. Skrócenie czasu dostawy towarów koleją można osiągnąć poprzez zmniejszenie czasu potrzebnego na obsługę pociągów na przejściach granicznych – stwarzają taką możliwość systemy zarządzania ryzykiem w międzynarodowym ruchu kolejowym bazujące się na zasadach selektywnych badań.

Słowa kluczowe: stacje przejść granicznych, symulacje, sieci Petriego, system zarządzania ryzykiem

1. Introduction

European integration processes in Ukraine should be based on the advanced principles of effective systems of governance. This requires a preliminary analysis of the compliance of these processes with national government policy and requires organisational and legal support. Due to the existing trends in global technological development, Ukraine should provide facilitating procedures for the passage of import and export cargoes through border transfer stations (BTS) with regard to rail freight. Therefore, Ukraine should soon adopt the appropriate European standards to which it has formally joined and which are captured in such major international acts as the International Convention on harmonization and simplification of customs procedures (Kyoto Convention) and the Resolution of the Customs Cooperation Council concerning the framework standards of safety and harmonization of the international trade. These contemporary principles implemented in the system of management and risk analysis could be used as effective tools for controlling the stability of Ukraine's foreign trade activities.

The continuous increase in foreign trade requires the continual improvement of international transport and the improvement of cross-border transfer stations. In rail transport, in which the operations of all the structural parts are interconnected, difficulties that may arise at certain BTS can seriously influence the overall efficiency of the railway network operation.

Despite the fact that since 2014 the volume of international traffic at railway transport of Ukraine has significantly reduced due to the Russian occupation of Crimea and military aggression in Donetsk and Luhansk regions, the unproductive downtime at the border stations has not decreased. Additionally, in 2018, the European Union plans to close the project on modernization and the construction of border checkpoints with Ukraine, which was launched in 2014. This project was aimed at helping to integrate the Ukrainian economy with neighbouring countries – Poland, Hungary, Slovakia, and Romania. In the opinion of the EU, the BTS modernisation project aimed at shortening the periods of border crossing and improving customs procedures, did not achieve its goals.

Currently, the turnaround time of trains at BTS is determined by the duration of paperwork, customs, and border inspection, which is usually several times longer than the time required to perform the technical and commercial operations. During the period from 2010 to 2017, a significant proportion (47.8%) of the total number of detained rail freight wagons make units that were detained by a carriage service sector, 24,3% – cars that were delayed by commercial service management (handling, cargo packaging breach, etc.), 13,3% – cars detained by the customs. These delays significantly affect the downtime and the number of detained rail freight wagons, and together with a shortage of rolling stock, this creates significant problems for both the Ukrainian Railroad Company (Ukrzaliznytsia) and cargo owners.

In order to speed up the functioning of checkpoints and reduce the downtime resulting from the delay of rail freight wagons, it is necessary to improve the operation of customs checkpoints, to adjust their parameters to common European standards of technology and to implement the use of electronic information and documents in the distribution of goods.

This paper aims to propose a tool for the simulation of the technological processes which occur at BTS and to use the simulation results for risk estimations while managing the railway transport system.

2. Literature review

At present, the main areas of the research focus on the optimisation of cargo delivery systems which uses computer simulations and various mathematical methods and models of the optimisation of international rail freight traffic.

One of the first BTS operation optimisation models was created by K. Mironenko in order to solve the problem of how to reduce the duration of stay at the wagon reloading stations. This model was a mathematical model of the reloading process that took into account the priority of freight wagons to the loading fronts, cargo handling complexity, and the static load of rail freight wagons [1].

As a new impulse to research the problems relating to international rail freight traffic, a system of international transport corridors was developed in 1991 and approved in 1994 [2]. In Ukraine, many studies were carried out after the introduction of the resolution on the Approval of the Concept of Creation and Operation of a National Network of Transport Corridors in Ukraine by the Cabinet of Ministers of Ukraine no. 821 from 08.04.1997 [3]. The main scientific and practical merit of solving the problem of the development of international transport corridors in Ukraine belongs to G. Kirpa [4, 5]. Recently, the relevance of studies for improving the BTS operational processes at Ukrainian border stations has also been underlined in publications [6] and [7].

The most relevant areas of study in the field of BTS operation include the analysis of transport system reliability, the development of the efficient (or even optimal) sequences of operations for implementing transportation processes including international rail transport technological schemes, the allocation of capacity for international railway transport [8-15]. Issues relating to the computer automation of border stations are discussed in [8]; furthermore, the authors of [9] have discussed problems regarding increasing the performance of intermodal railway freight terminals.

Current research suggests that excessive delay of rail freight wagons at border stations reduces the reliability of the international transport system and may lead to a reorientation of international transit cargo flows in order to bypass the territory of Ukraine. However, it should be noted that until 2007, the problem of optimising the border and customs operations to reduce downtime and increase the transfer capacity of border stations was not considered in studies of Ukrainian scientists. The problem has been studied in detail in thesis [12]; however, the operations of control services at border stations were not considered sufficiently. The task of improving the information subsystem of BTS has been addressed in thesis [13]; however, the possibility of introducing modern systems analysis and risk management tools for cargo handling procedures at BTS has not been taken into consideration.

The mentioned literature analysis leads to the conclusion that, as a result of the uncertain nature of technological processes at railway transport and unpredictable nature of demand for transport services, the problem of improving freight distribution systems under the terms of reducing the freight units' downtime must be solved with the use of risk management tools.

3. Simulation model of the process of servicing the wagons at Ukrainian BTS

To develop the simulation model, a structured and logical framework for cooperation between the operational lines at border stations has been formed. This can be represented as a diagram of the operations for processing trains which combines fifteen major elements, most of which are the technical customs operations (Fig. 1).

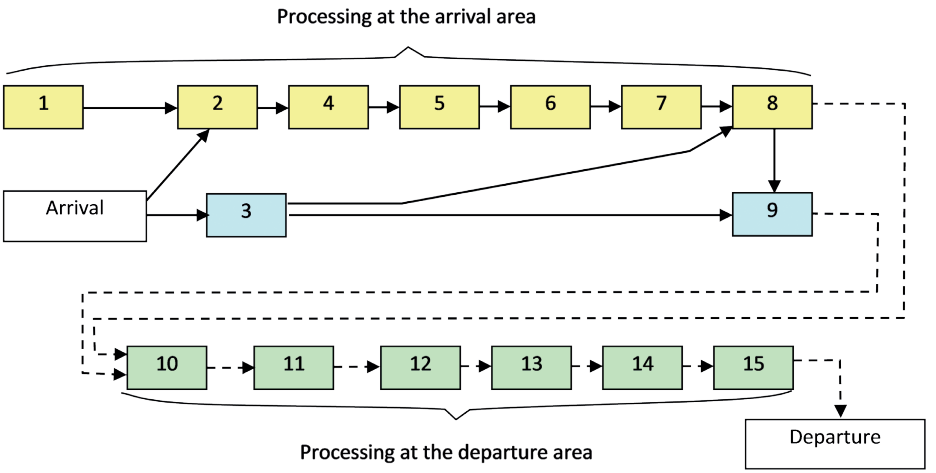

Fig. 1. Structural scheme of information processing at BTS

The numbered blocks on Fig. 1 present the generalised technical operations listed in Table 1.

The most restrictive operations at BTS are the operations that are related to customs control and documents processing. This leads to frequent delays of rail freight wagons at transfer stations. Therefore, it is necessary to list the main reasons why the freight wagons cannot simply pass a border station and are instead being delayed.

More than fifty reasons for delays have been found at Ukrainian border stations; the most frequent fourteen reasons (which make up more than 74% of the additional idle time) are listed in Table 2.

The listed delays in customs operations significantly increase the duration of freight wagon processing at the Ukrainian BTS. Sometimes, there are the cases that may even stop entry at the customs border and cause the refusal of freight wagons and cargo.

Table 1. List of the railway processing operations and respective information flows

Operation number	Operation content
1	receiving the data at the information system in the form of the train transfer declaration, discarding the train
2	delivery of train documents to technical office
3	technical and commercial check control of the train
4	checking the train documents according to the list of discarding
5	checking of data, providing updates
6	checking by veterinary service, phytosanitary and sanitary service, ecological and radiological testing, frontier services
7	testing the veracity of documents, testing the availability of appropriate customs payments
8	checking the train documents by customs services
9	processing operations relating to the train composition (sorting, formation of trains, shunting, coupling, uncoupling cars, loading and unloading or reloading, replacement of cars, etc.)
10	transfer of the cargo customs declaration by declarants and producing electronic copies
11	checking the declaration and its copies by customs experts
12	making adjustments in the information system concerning detached freight wagons in order to produce the train transferring declaration
13	checking the train documents by the cargo customs services
14	selecting the proper train transfer declaration and train documents
15	converting and delivering the train documents, sending the data to the next station

Table 2. The main reasons for freight wagon delays at BTS

Operation code	Reasons for delay of wagons
X1	customs inspection
X2	customs registration
X3	no information received from the customs administration
X4	technical and commercial failure of a freight wagon
X5	data mismatch in the transportation and technical bill and the cargo customs declaration
X6	delay caused by phytosanitary, veterinary, sanitary, and frontier services
X7	delay caused by ecological and radiological testing services
X8	improper execution of documents
X9	absence or closure of a dispatcher's code
X10	dividing the routes
X11	no information found in the central database
X12	no invoice received
X13	other reasons (for example, groundless non-acceptance of goods by a neighbouring state)
X14	delays according to additional orders (e.g. a temporary ban on the import-export operations)

For a detailed analysis of customs procedures, a simulation model of a border station has been developed. For this model, a system of parallel information processing facilities and a system of simultaneously operating facilities should be simulated. Petri nets models are some of the most advanced approaches that are currently available which enable the incorporation of such systems. Petri nets are widely used for simulations of railway transport systems. The most recent studies [16–19] use this tool for solving problems of forming the technological lines of the passenger trains, security and vulnerability analysis on time protocol of the railway network, etc. It also worth mentioning that Petri nets are one of the most appropriate simulation tools for studies using statistical modelling methods. This mathematical tool monitors the status of all the model elements in real time and provides values of all simulated statistical parameters used for the model description.

The developed generalised macro-level model of the line for the processing of rail freight wagons, documents and information flows at BTS is shown in Fig. 2. In this model, the major transitions are numbered according to the list of operations on arrival and departure (Fig. 1). Shaded positions (X1, X2, etc.) indicate the main causes of wagon delays at BTS at the relevant stages of processing.

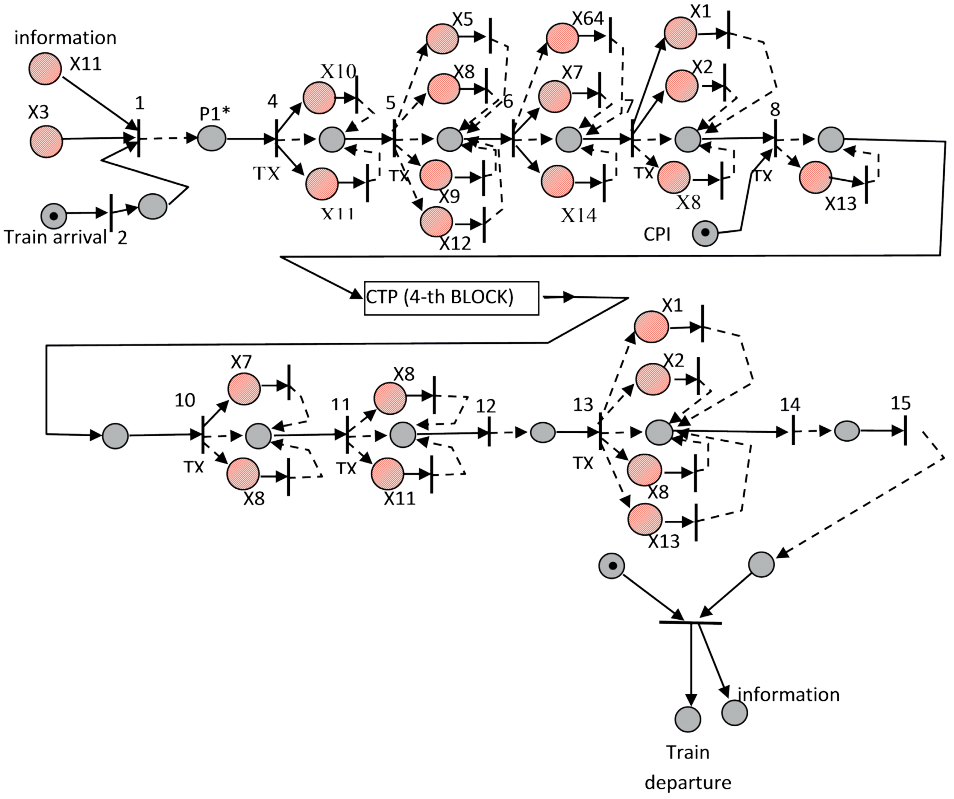

Fig. 2. Macro-level model of cargo handling processes relating to customs at BTS

The presented model operates in the following way. With the arrival of the train at the station (chip in the position P1), the availability of free tracks for receiving trains is checked (the position P3 has a capacity limit equal to the number of tracks). After the train is accepted, the locomotive is uncoupled and is sent to the depot. The technical point inspection (TPI) and commercial point inspection (CPI) then commence. However, these operations are performed in parallel, and several servicing teams may be able to process several trains simultaneously, thus removing the need for them to wait in line. Along with maintenance TPI and CPI operations, customs operations are also commenced. Unless there is any delay, the operations from 1 to 15 listed above are performed consistently. However, real-word observations demonstrate that the processing of arrival and departure operations of trains may be delayed at each stage (shaded position) – the probability of which is determined by transitions of TX-type. A list of the main causes of delay is presented in Table 2.

As shown in Fig. 2, the first delay may occur before the customs inspection. First of all, email customs administration may be lacking (X3) and there may be a lack of information in the database of the information system (X11). If email customs administration and information about wagons have been entered in the database (the presence of chips at positions X3 and X11), a review starts according to the provided data (operation 4), after delivering to a technical office PD (operation 2). At this stage, if the documents mismatch, freight wagon delays are possible due to breakdown of the route (X10). Additionally, there is the possibility of delays for other reasons (X13) – these are generally possible at any stage, but to simplify the model, a few possible scenarios (during arrival and departure operations) are considered. Possible delays (X10 and X13), are determined by statistical observations, the transition of TX-type could be set. These points apply to each of the fifteen stages of processing. It should be noted that Fig. 2 is a simplified representation and does not describe the whole technological process of the BTS operation, which consists of several blocks (in particular, operations X3, X9 and some others which may be performed in other blocks).

A functional simulation of the BTS operation may be conducted using the proposed model with regard to proposals on the processing technology optimisation. Comparison of the modelling results for the existing and proposed technologies may be carried out with the use of such criteria as the number of delayed freight wagons and the total duration of delays at the BTS. The best forecasting results which take into account unknown parameters could be achieved with the use of the fuzzy logic methods. Recent examples of the use of fuzzy methods for the optimisation of rail transport systems are presented in [20–22]. Simulations using Petri nets allow researchers to receive forecasting information on the operation of each of the BTS subsystems – a model built with the fuzzy logic tools provides further predictions and prevents the risks.

To assess risk and determine its effects, different rating systems can be used. In 2003, the World Customs Organisation developed a standardised risk assessment methodology [23]. In most cases, there is a common system of high, medium, and low risk – an alternative approach is the use of three types of corridors: green, yellow and red. Data relating to risk assessment must be applied taking into account the main factors influencing the implementation of

import and export operations in railway transport systems. The following key factors should be defined as the parameters affecting the passage of trains at BTS:

- country where from a consignment originates,
- type of cargo,
- type of train,
- invoice value of consignment,
- net weight of consignment.

In the frame of this study, on the basis of the conducted analysis of technological operations in the processing of goods within a full cycle of border operations, an algorithm of the execution of customs procedures at BTS which considers an operational risk has been developed. A flowchart of the procedure of customs control based on [24] is shown in Fig. 3.

The declarant or the owner of the goods submits a properly completed cargo customs declaration and shipping documents to the customs office. An electronic copy of the customs declaration is added to the customs database. Incoming information is analysed by the automated system in order to determine the level of risk that returns the final estimate. If no violations are found, the consignment is sent to the green zone and is passed without any delay. If the risk module of the information system shows that the potential risk is of low-level, the consignment enters the yellow zone, at an average level of risk – to the orange zone, and at a high level – to the red zone; these zones are characterised by a corresponding list of procedures.

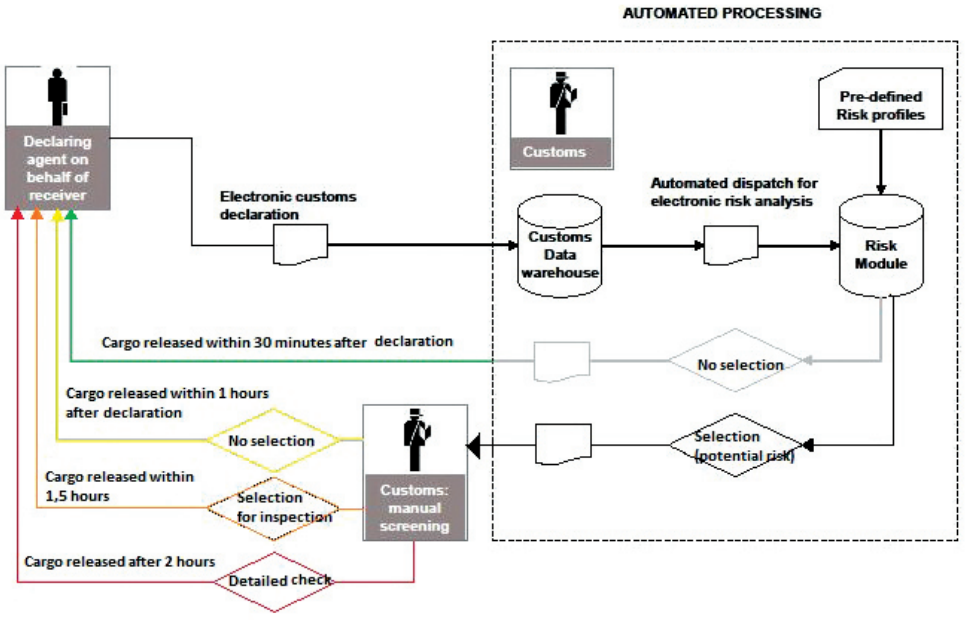

Fig. 3. Structure diagram of the customs control procedure based on the operation risk module

A correlation and regression analysis on the basis of the numerical results obtained from the described simulation model should be performed in order to determine the level of transport system reliability for the proposed risk management system. The use of these techniques allows us to assess the dependency of performance indicators and identify their mutual influence.

After analysing the impact of certain factors (cargo nomenclature, the country of origin and destination, the type of rolling stock, the invoice value of the goods, the net weight) on the delay values, a distribution of factors according to the conventional risk zones shown in Table 3 is performed.

Table 3. Conventional risk areas of the customs control process

Correlation coefficient	Displayed colour	Measures
1 ... 0,70	Red Zone	A high risk has been detected and a list of control operations has been formed. The implementation of measures requiring a detailed inspection of the consignment or vehicle is proposed
0,69 ... 0,50	Orange Zone	An average risk has been detected and a list of control operations has been formed. A documentary inspection and a check of some consignments or vehicles should be performed
0,49 ... 0,30	Yellow Zone	A low risk has been detected and a list of control operations has been formed. All forms of control should be provided for the documentary checks and other measures that do not require inspection of consignments or vehicles
0,29 ... 0,01	Green Zone	No risk has been detected; no checks of consignments are required

On the basis of the described model of risk analysis at BTS, a software program written in the Delphi language has been developed. The program user interface has text fields for inputting the main factors for the risk calculations and label fields for returning the calculated values of correlation coefficients, and the fields to display the risk assessment results.

With reference to Fig. 4a, when a consignment enters the red zone of risk, it is necessary to conduct a detailed check of the consignment or the train (Table 3); with reference to the yellow risk zone shown in Fig. 4b, the document checks and other measures that do not require the inspection of cargo or vehicles should be performed.

The set of indicators of the risk management system provides a precise algorithm for the processing of each consignment that, according to conducted forecasts, will reduce downtime at Ukrainian BTS by a factor of around 3.5. Further research and calculations have shown that the processing time of transit trains with a full cycle of border operations may be reduced by a minimum of 45 minutes to a maximum of 170 minutes, the duration of operations for transit trains may be reduced by a minimum of 35 minutes to a maximum of 120 minutes, and the duration of train maintenance – from 75 to 180 minutes.

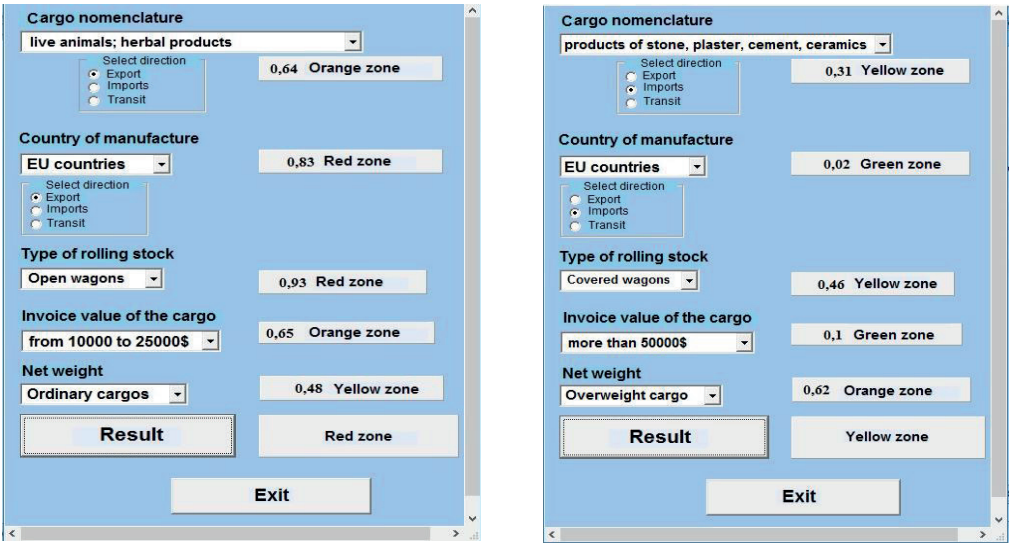

Fig. 4. Interface of software for assessing the level of risk at BTS: a) red zone, b) yellow zone

4. Conclusions

The conducted analysis of the Ukrainian BTS operation allowed us to determine the main reasons for the delaying of rail freight wagons. The performed literature analysis has shown that in many works, no attention has been paid to the problem of optimising the border and customs operations in order to reduce downtime at BTS. To optimise the transmission system of freight traffic at BTS, a simulation model of the interaction process at stations has been developed and the use of a risk management system has been proposed. The approach for the risk assessment of rail freight wagon delays that takes into account the key factors influencing the passage of trains through BTS has been developed; on this basis, an algorithm for developing customs procedures for BTS based on an operation risk module has been proposed.

To determine the level of the transport system reliability for goods admission with regard to international traffic, simulation models based on the Petri nets have been built. The integration of a correlation and regression analysis method into the decision support system in the risk management system has been introduced. The list of appropriate specific measures for processing the consignments at BTS has been provided.

The implementation of the analysis and risk management systems would help Ukrainian border stations create suitable conditions for transport operators, improve the efficiency of technological procedures, reduce the downtime of rail freight wagons at BTS; together, these would facilitate the further integration of Ukrainian railway transport into the European transport system.

References

[1] Mironenko, K.P., *Study the operation conditions of border transfer points in processing of wide nomenclature of import cargoes,* Kharkiv 1975.

[2] European Agreement on Important International Combined Transport Lines and Related Installations, United Nations Economic Commissions for Europe Inland Transport Committee, Geneva, 1991.

[3] The concept and the program of restructuring of railway transport of Ukraine, Ministry of transport, 1998.

[4] Kirpa G.N., *A new level of economic cooperation in the field of international transport business,* Railway transport of Ukraine, vol. 3, 2002, pp. 2-8.

[5] Kirpa G.N., *Integration of railway transport of Ukraine into the European transport system*, Dnepropetrovsk National University of Railway Transport, 2004.

[6] Droździel P., Buková B., Brumerčíková E., *Prospects of international freight transport in the East-West direction,* Transport Problems, vol. 10(4), 2015, pp. 5-13.

[7] Abramović B., Zitricky V., Biškup V., *Organisation of railway freight transport: case study CIM/SMGS between Slovakia and Ukraine,* European Transport Research Review, vol. 8(4), art. no. 27, 2016.

[8] Cauty M., *Utilisation d'une liaison telematique pour gerer la circulation entre deux gares frontier*, Revue Generale des Chemins de Fer, vol. 106(1), 1987, pp. 25-29.

[9] Ferreira L., Sigut J., *Measuring the performance of intermodal freight terminals*, Transportation Planning and Technology, vol. 17, 1993, pp. 269-280.

[10] Li X., Xie R., *Analyses of freight forward-time in railway transportation*, Proceedings of the Conference on Traffic and Transportation Studies, ICTTS, 2000, pp. 198-201.

[11] Jarašūnienė A., *The solution of customs posts management problems at railway border stations,* Transport, vol. 18(3), 2003, pp. 108-113.

[12] Alyoshinskiy E.S., *Basis for the formation of the international rail freight transport,* Thesis, Ukrainian State Academy of Railway Transport, 2009.

[13] Kihteva J.V., *Improvement functioning of the information subsystem for border transfer stations*, Thesis, Ukrainian State Academy of Railway Transport, 2010.

[14] Wan L., Guo Y.C., Wei Y.Y., *Shanghai west railway station's design based on communication space and ecological integration,* Applied Mechanics and Materials, vol. 584-586, 2014, pp. 439-442.

[15] Zitrický V., Černá L., Abramovič B., *The proposal for the allocation of capacity for international railway transport,* Procedia Engineering, vol. 192, 2017, pp. 994-999.

[16] Aleshinskiy E., Naumov V., Prymachenko G., *Using the Petri nets to form technological lines of the passenger trains in Ukraine*, Archives of Transport, vol. 38(2), 2016, pp. 7-15.

[17] Zhang Y., Zhang H., Wang H., *Security analysis on railway network time protocol based on colored Petri nets*, Journal of the China Railway Society, vol. 39(10), 2017, pp. 82-88.

[18] Lan L., Zhang Y., *Vulnerability analysis of railway time synchronization network protocol based on stochastic Petri net,* Journal of the China Railway Society, vol. 39(8), 2017, pp. 85-92.

[19] Yianni P.C., Rama D., Neves L.C., Andrews J.D., Castlo D., *A Petri-Net-based modelling approach to railway bridge asset management*, Structure and Infrastructure Engineering, vol. 13(2), 2017, pp. 287-297.
[20] Menéndez M., Martínez C., Sanz G., Benitez J.M., *Development of a Smart Framework Based on Knowledge to Support Infrastructure Maintenance Decisions in Railway Corridors,* Transportation Research Procedia, vol. 14, 2016, pp. 1987-1995.
[21] Zhang J., *Analysis on line capacity usage for China high speed railway with optimization approach,* Transportation Research Part A: Policy and Practice, vol. 77, 2015, pp. 336-349.
[22] Pattanaik L.N., Yadav G., *Decision support model for automated railway level crossing system using fuzzy logic control*, Procedia Computer Science, vol. 48(C), 2015, pp. 73-76.
[23] Guidance document on customs formalities on entry and import into the European Union, Brussels 2016, 40.
[24] Stengel D., *From full stop on the border to selective customs control,* First Seminar on Multimodal Transport and Logistics. Kyiv, 4-5 June 2013.

If you want to quote this article, its proper bibliographic entry is as follow: Evgen Aleshinskiy, Vitalii Naumov, Oksana Pestremenko-Skripka, *The modelling of technological processes at border transfer stations in Ukraine*, Technical Transactions, Vol. 6/2018, pp. 55-66.

TECHNICAL TRANSACTIONS 6/2018
CIVIL ENGINEERING
DOI: 10.4467/2353737XCT.18.087.8692
SUBMISSION OF THE FINAL VERSION: 22/05/2018

Krystian Birr (krystian.birr@pg.edu.pl)
Highway and Transportation Engineering Departament, Gdańsk University of Technology

Mode choice modelling for urban areas

Modelowanie wyboru środka transportu dla obszarów zurbanizowanych

Abstract

This article addresses the issue of mode choice modelling using a four-stage travel modelling process. The article indicates limitations of the currently used simplified methods of mode choice modelling and proposes the use of a more detailed approach that accounts for additional, statistically significant factors with the use of advanced mathematical tools and discrete choice models. A need has also been identified to include qualitative factors in forecasting the modal split and in the scenario analyses.

Keywords: travel modelling, modal split, mode choice modelling

Streszczenie

W artykule przedstawiono problematykę modelowania wyboru środka transportu w czterostopniowym procesie modelowania podróży. W artykule wskazano ograniczenia obecnie stosowanych uproszczonych metod modelowania wyboru środka transportu oraz przedstawiono możliwości zastosowania bardziej szczegółowego podejścia uwzględniającego dodatkowe, statystycznie istotne czynniki z wykorzystaniem zaawansowanych narzędzie matematycznych, w szczególności modeli wyboru dyskretnego. Wskazano również potrzebę uwzględnienia czynników jakościowych w prognozowaniu podziału zadań przewozowych i analizach scenariuszy.

Słowa kluczowe: modelowanie podróży, wybór środka transportu

1. Introduction

Travel modelling is a mathematical reflection of the behaviour and decisions of transport users and the condition of the transport network. In general, traffic modelling entails identifying and describing the relationship between the volume and structure of traffic, the spatial distribution of traffic, specific explanatory variables and mapping reality or its on the basis of the collected data in order to replace the analysed object in the planned research.

The results obtained from the conducted simulation analyses have a significant impact on decisions regarding transport policy in cities and allow the assessment of the efficiency of the transport system management, including the modal split, which may contribute to a reduction in the total transport costs of up to 30% [13].

The modal split model is one of the most important elements in the development of a transport system model. This kind of model provides a mathematical reflection of the decisions of the transport network users about which modes of transportation they will choose, accounting for the various factors affecting these decisions. The factors include distance, travel time, and also factors that are hard to measure, such as: safety, perceived reliability, punctuality and efficiency, comfort, aesthetics, or a sense of freedom during the journey. The values assigned to each of the factors depend not only on the actual statistics, but also on the mentality and individual attitude of users to modes of transportation, especially collective transport services.

The results of the research presented in this article constitute a synthesis of selected issues contained in the author's doctoral thesis on the issue of travel mode choice modelling in urban areas.

2. The present situation

The current approach to modal split modelling is, in the clear majority of cases, limited to considering the changes of behaviour in relation to the attractiveness of individual forms of transport (individual and collective) expressed by the ratio of the average travel time on said modes of transport. The share of a given mode is greater, when travel time compared to the alternative modes of transport is shorter. However, although previous research [6, 13] shows that time is an important factor influencing the choice of the particular travel mode, there are other factors that influence the decision [2, 5, 9, 12]. One such basic factor may be car ownership. The current general approach does not enable accurate mapping of the transport behaviour of residents, and does not factor in their mobility, preferences and other external factors.

The problem of an approach to mode choice modelling that is too general is particularly noticeable when conducting analyses on the development of the transport system for forecasting purposes when the journey time value for travellers and the level of propensity to choose a given mode of transport in relation to travel time are unknown.

When forecasting transport behaviour this way, the factors that change habits and mentality, as a result of, for example, education or changes in economic status are omitted. Because of such an approach, traffic forecasts are not sufficiently precise, and at the same time,

there is a limited possibility to analyse scenarios that account for the impact of other factors on the share of individual modes of transport (e.g. transport policy).

Meanwhile, forecasting the travel mode choice is the basic stage required to conduct a cost-benefit analysis for planned investment projects in the transport sector in Poland for which beneficiaries apply for financial assistance from European Union funds. Therefore, it is particularly important that the traffic forecasts (including modal split) are as precise as possible, since their results, among other things, determine whether a given project would be considered sound for implementation.

In recent years, a lot of studies have been conducted on factors that influence the choice of travel mode, in particular, the tendency to change the mode, preferably to public transport or bicycle. These studies have shown that the important factors influencing these decisions have socio-demographic attributes [1, 8].

3. Methods of modal split modelling

In the process of modal split modelling, as is the case with travel modelling, it is necessary to adopt assumptions regarding the scope, scale and methods of testing the analysed phenomenon. In Poland, the most commonly used approach is the approach of the two-stage journey split. In the first stage, pedestrian trips are separated from all journeys, usually with a division into trip purposes. Then, in the second stage, these trips are defined as being either car trips or trips involving collective transport.

When approaching travel modelling, an assumption should be made regarding the range of transport options that can be selected. Due to the continuous increase in the share of bicycle trips, it is recommended to extend the calculations for this mode of transport. In the case of using a two-step approach, bicycle trips should be separated in the second stage of calculations, i.e. from the pool of non-pedestrian trips, because bicycle trips are significantly longer than trips taken on foot.' However, it is possible to use alternative methods through the use of various mathematical tools (non-linear regression, discrete choice models, neural networks and others). One of the alternative methods may be the use of a multimodal logit model with the structure as in Fig. 1.

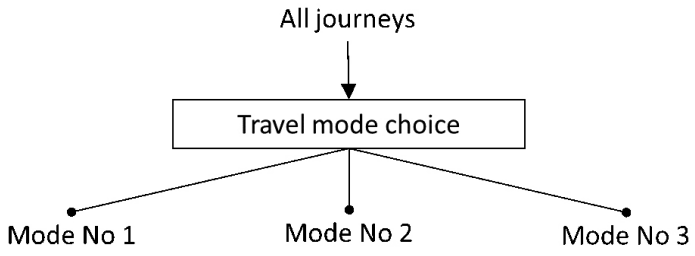

Fig. 1. Scheme of choice alternative in nested logit model approach (own study)

The disadvantage of this approach is the high sensitivity of such models to changes the attractiveness of alternatives to pedestrian modes of transport in terms of the probability of pedestrian trip choice In the case of a significant increase in the attractiveness of, for example, a car, the model would react with a significantly lower probability of choosing walking for short distance travel (up to 1 km) causing a significant deviation from values obtained by means of empirical research. Another method to limit this problem is the use of a nested logit model with the structure shown in Fig. 2. In addition to the discrete choice models, other tools can also be successfully applied, such as neural networks, which have also been analysed by the author.

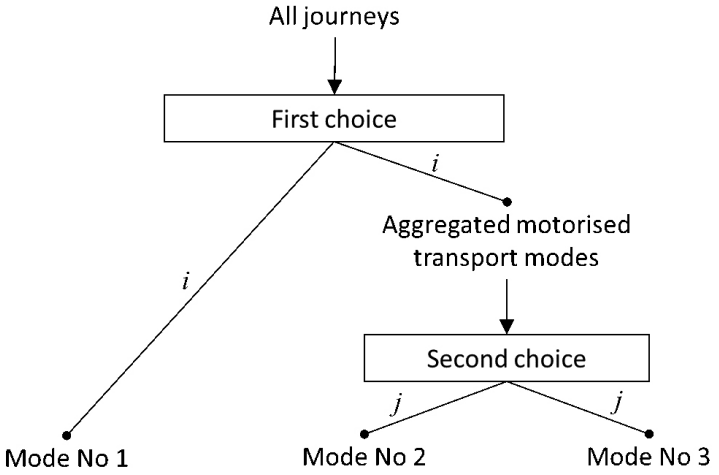

Fig. 2. Scheme of choice alternative using a nested logit model approach (own study)

4. Selection of variables

The selection of explanatory variables depends on their statistical significance and is limited by the availability of data. Factors affecting the mode choice can be divided into two basic groups [2, 4, 7]:

- easy-to-measure, which can also be quantified as they describe the elements of the analysis numerically (e.g. time, travel distance, number of vehicles in the household),
- difficult to measure, the quantification of which requires additional testing.

One of the basic factors that probably influences the travel mode choice is the income per household member. Unfortunately, this data is difficult to obtain; therefore, it is necessary to find alternative factors describing the status of the trip maker and the situation describing the conditions that affect the decision on choice of travel. When analysing comprehensive traffic research conducted in Polish cities, it is possible to include many factors characterising the user, the performed journey and the journey origin and destination points in the mode choice modelling. Such factors include:

- factors describing a user:
  - car availabilty,
  - mobility,
  - age,
  - education,
  - number of children,
- factors describing the jouney:
  - distance,
  - travel time by bicycle,
  - travel time by car,
  - perceived journey time by collective transport,
  - waiting time for public transport at the first stop of the journey,
  - number of transfers in public transport,
  - share of rail transport trips in total time of a single journey,
- factors describing journey origin or destination:
  - direct rail transport availability,
  - paid parking zones,
  - density of population.

5. Model examples

The research conducted by the author has shown that it is possible to include additional variables in mode choice modelling and most of the above-mentioned variables show statistical significance in selected trip purposes. The research was carried out using discrete choice models. These were nested logit models including four modes of transport: pedestrian, bicycle, individual transport, collective transport. The basis of the research were the latest comprehensive traffic researches for selected large cities: Gdansk, Cracow and Warsaw [10, 11, 14].

The example factors that may influence the mode choice which were presented in the previous section can be used to more accurately calculate the modal split in the four-stage travel modelling process. For this purpose, it is necessary to formulate multifactor models, in which for each of the analysed modes of transport *m* should be defined the utility function U_s^m, depending on the situation s, described by selected factors and accounting for the random variable ε_s^m which allows to include the individual user's preferences and subjective perception of utility in the model.

$$U_s^m = V_s^m + \varepsilon_s^m \tag{1}$$

where:

U_s^m – the general utility of the travel mode *m* in situation *s,*

V_s^m – the measurable utility of the travel mode *m* in situation *s*, factoring in the variables applied in the model, selected by an analyst,

ε_s^m – a random variable with a logistic distribution, mapping values not included in the utility and individual factors characterising a particular user.

A typical utility function (measurable) used in logit models takes a linear form (2); however, it is possible that some variables are functions of a non-linear form in cases when it is justified and significantly affects the result of the model.

$$V_s^m = \beta_0 + \beta_1 x_1 + \beta_2 x_2 + \cdots + \beta_n x_n \tag{2}$$

where:
β_n – function parameters,
x_n – function variables.

Based on the utility of each of the travel modes *m* thus determined, it is possible to calculate the probability of its selection for the journey in the situation *s*. The following equation is used for this purpose in standard bimodal and multimodal models:

$$P_s^m = \frac{e^{\mu U_s^m}}{\sum_m e^{\mu U_s^m}} \tag{3}$$

where:
P_s^m – the probability of choosing a travel mode *m* in situation *s,*
U_s^m – the utility of a mode *m* in situation *s*,
μ – the model scale parameter.

In the case of more complex models which include nested logit models, it is necessary to use the product of probabilities to calculate the probability of selecting one of the alternatives:

$$P_{ij} = P_i \times P_{j/i} \tag{4}$$

where:
P_{ij} – the probability of choosing a travel mode 'j' from the group of transport modes 'i',
P_i – the probability of choosing an alternative 'i',
$P_{j/i}$ – conditional probability of choosing an alternative 'j' from a branch 'i'.

The application of the above relationship in the analysed case requires defining the general utility of non-pedestrian travel modes , which depends on the particular utility of these non-pedestrian travel modes (bicycle, individual transport, collective transport):

$$U_{NP} = \frac{1}{\mu_j} \log\left(\sum_{i \in j} e^{\mu_j U_{ij}}\right) \tag{5}$$

Therefore, the above relationship defining the probability of the mode choice in the nested model takes the form:

$$P_{ij} = \frac{e^{\mu_j U_{ij}}}{\sum_{i \in j} e^{\mu_j U_{ij}}} \cdot \frac{e^{\mu_i \left[\frac{1}{\mu_j} \log\left(\sum_{i \in j} e^{\mu_j U_{ij}} \right) \right]}}{\sum_{j=1}^{m} e^{\mu_i \left[\frac{1}{\mu_j} \log\left(\sum_{i \in j} e^{\mu_j U_{ij}} \right) \right]}} \tag{6}$$

where:

U_{ij} – the utility of the mode 'j' from the group of transport modes 'i',

μ_i, μ_j – the model scale parameter.

One of the model examples accounting for additional factors is a model using variables: travel distance (DIS), travel time by bicycle (TT0r), travel time by individual transport (TTC), perceived journey time by collective transport (PJT), car availability (CAR), paid parking zones at the origin or destination (PARK) and direct availability of rail transport (RA). Based on statistical analyses, the following utility functions have been formulated for this model:

$$V_P = \beta_{10} + \beta_{11} \cdot DIS \tag{6}$$

$$V_R = \beta_{20} + \beta_{21} \cdot TT0r$$

$$V_{TI} = \beta_{30} + \beta_{31} \cdot \frac{TTC}{PJT} + \beta_{32} \cdot CAR + \beta_{33} \cdot PARK$$

$$V_{TZ} = \beta_{40} + \beta_{41} \cdot RA$$

The parameter values of the above functions were determined for each of the analysed cities for each of the seven basic trip purposes. Examples of parameter values for the 'from home to work' purpose are presented in Table 1.

Table 1. Parameters of the utility functions of the model example

Data from:	σ2	μ1	μ2	β_{10}	β_{11}	β_{20}	β_{21}	β_{30}	β_{31}	β_{32}	β_{33}	β_{40}	β_{41}
Gdansk	0.428	1.000	2.380	1.790	-0.920	0.218	-0.036	-0.402	-0.287	2.150	-0.241	0.000	0.196
Cracow	0.408	1.000	9.540	-0.270	-0.424	-0.202	-0.005	-0.133	-0.048	0.439	-0.036	0.000	0.029
Warsaw	0.436	1.000	1.710	0.418	-0.605	-0.943	-0.022	-1.590	-0.398	2.670	-0.315	0.000	0.319

Statistical analysis of the above model example, accounting for all trip purposes, indicates good and very good fit between the results and empirical values. The coefficient σ2, depending on the purpose of the trip, takes values in the range 0.32-0.48 for each of the analysed cities, which is a significant increase in the quality of the model in comparison to the model using only variables of distance and travel time, where σ2 is 0.22-0 35.

To the example presented above, similar studies have been conducted for various combinations of factors for each of the trip purposes using the results of comprehensive traffic studies from the above three cities. Based on the studies conducted in this manner, it has been found that the most important variables affecting the mode choice decision are the

distance (particularly in the case of short journeys up to 1 km) and car availability. In the case of very short trips (up to 1 km), there is an increased probability of the choice of walking (Fig. 3). With the increase in travel distance, the probability of alternative mode choices (bicycle, car and public transport) increases. For long journeys (over 20 km), there is an increased probability of choosing a car.

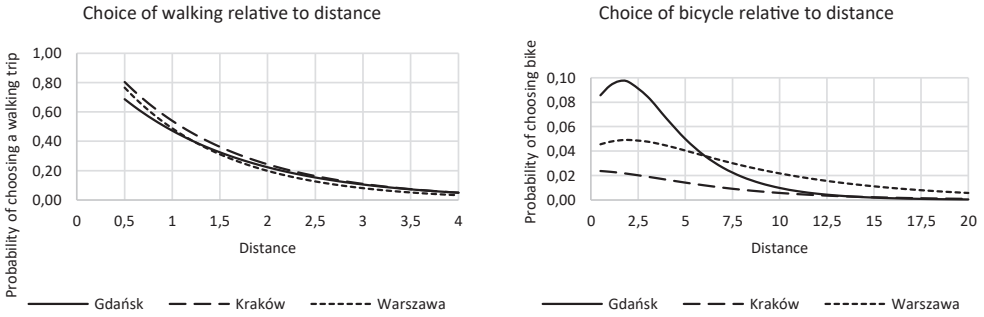

Fig. 3. Distribution of the probability of choosing walking and bicycle trips (own study)

With an increase in the availability of a car in a household, the probability of choosing this mode significantly increases. In addition, in regions with direct access to rail transport, there is an increased probability of choosing public transport (Fig. 4).

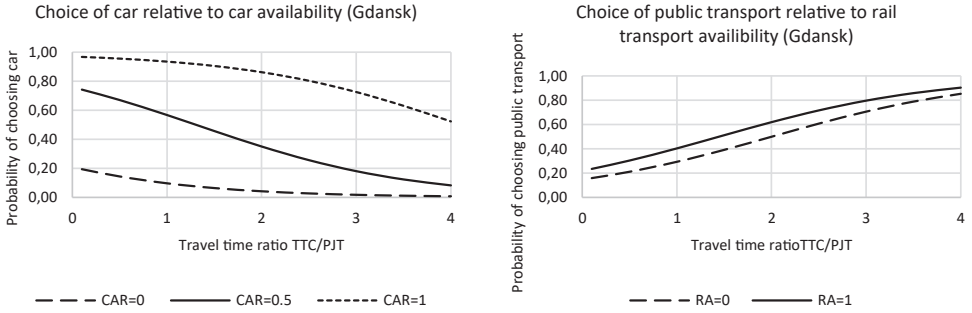

Fig. 4. Distribution of the probability of choosing a car and public transport (own study)

The other factors mentioned in the previous section also have a significant impact on the mode choice, but to a much lesser extent than the availability of a car. With the increase of mobility, age, and the number of children in the household, the probability of choosing a car trip increases. At the same time, with the increase in population density, as well as in the case of paid parking zones or the possibility of using rail transport, the probability of choosing collective transport increases.

6. Qualitative variables

In addition to the above-mentioned easy-to-measure factors, the travel mode choice is also influenced by difficult to measure factors related to the quality of travel and transport policy. The significance of the impact of factors related to the soft actions of transport policy on the mode choice has been emphasised in many foreign publications [4, 7]. Soft factors are factors that are related to the user's individual perception of travel and the standard of the transport system. It is believed that the importance of quality factors in the travel mode choice will grow over time due to changes in social standards and income [3]. In Poland, the importance of factors related to transport policy is also becoming more and more significant due to the introduction of ever-increasing restrictions on road transport by cities, while at the same time, striving to increase the attractiveness of the public transport offer.

Accounting for the qualitative factors in travel mode choice modelling is a complex issue. To investigate the potential impact of selected soft actions, the author conducted heuristic studies with the participation of national scientific experts specialising in travel modelling and transport policy. The results obtained showed that such activities as: a) an increase in comfort of public transport travel (new vehicles, more seats, etc.); b) tariff and ticketing integration; c) extended access to information on the functioning of public transport (travel planners, real dynamic timetable, etc.), d) educational campaigns promoting ecological modes of transport and active mobility; may reduce the probability of choosing a car trip by approximately 4% (in the scale of all four modes of transport).

The obtained results of the study can be used as a starting point for further research into the impact of qualitative factors on the travel mode choice. These factors can be used at the stage of travel forecasting to produce various development scenarios related to the transport policy of cities. Additional factors can be included in the mode choice model by extending the utility functions of selected modes by additional qualitative variables with the calibrated parameters of the model.

7. Summary

The modal split model is an important stage in travel modelling and knowledge in this field is important for examining the impact of various activities and investments on changes in traffic within the transport network of cities and for implementing an efficient transport policy in cities. The conducted research has shown that the most important factors influencing the mode choice are travel distance and car availability. However, other factors (listed on the fourth page of this article) also significantly influence the probability of choosing particular modes of transport.

The method of modal split modelling presented in this paper with factors showing a different degree of dependence on the probability of choosing a given mode of transport may be used in travel modelling. Taking into account these and the additional ones listed in

chapter 2 and other factors may have a positive effect on the quality of the model. In addition, it allows to:

- the opportunity to develop and analyse scenarios for the development of the city and its transport system;
- improvement to the calibration process of the travel model due to a greater diversification of transport regions in terms of the modal split;
- conducting analyses and forecasts taking into account factors significantly affecting the mode choice;
- the taking into account changes in transport behavior of travelers, resulting from various external factors, including transport policy for forecasting states;
- the opportunity to develop scenarios in order to predict the effects of transport policy.

References

[1] Banister D., *The influence of habit formation on modal choice – a Heuristic model*, Transportation, Amsterdam 1978.

[2] Birr K., *Możliwości uwzględnienia czynników jakościowych związanych z polityką transportową miast w modelowaniu podziału zadań przewozowych*, [in:] *Problemy komunikacyjne miast w warunkach zatłoczenia motoryzacyjnego*, X Poznańska Konferencja Naukowo-Techniczna. SITK Poznań, Poznań-Rosnówko 2017.

[3] Goodwin P., Hallett S., Kenny F., Stokes G., *Transport: The new realism*, University of Oxford, 1991.

[4] Jakobsson C., *Motivational and Behavioral Effects of Economic Disincentives on private Car Use*, Department of Psychology, Göteborg 2001.

[5] Jovic PJJ Modal Split Modelling - Some Experience. 1–9.

[6] Kucharski R., Szarata A., Bauer M., Kulpa T., *Modelowanie Wyboru Środka Transportu – Porównanie regresji logistycznej i logitowego modelu wyboru dyskretnego*, [in:] *Problemy Komunikacyjne miast w warunkach zatłoczenia motoryzacyjnego*, X Poznańska Konferencja Naukowo-Techniczna, Poznań-Rosnówko 2015.

[7] Loncar-Lucassi V.M., *Spårtrafik kontra buss? Mjuka faktorers inverkan på resenärers färdmedelsval*, KFB-Meddelande 1, 1998.

[8] Olsson A-LL., *Factors That Influence Choice of Travel Mode in Major Urban Areas*. The Attractiveness of Park & Ride, 2003

[9] Ortúzar JDD, Willumsen LG: Modelling Transport, 2011.

[10] PBS Sp. z o.o., Politechnika Krakowska, Politechnika Warszawska, Warszawskie Badania Ruchu, 2016.

[11] Politechnika Krakowska, PBS Sp. z o.o., Kompleksowe Badania Ruchu, Kraków 2013.

[12] Santos G., Maoh H., Potoglou D., von Brunn T., *Factors influencing modal split of commuting journeys in medium-size European cities*, Journal of Transportation Geografy 30, 2013, 127–137

[13] Szarata A., *Ocena efektywności funkcjonalnej parkingów przesiadkowych* (P+R), rozprawa doktorska, Kraków 2005.
[14] Via Vistula, Biuro Rozwoju Gdańska (2016), Gdańskie Badania Ruchu, 2016.

If you want to quote this article, its proper bibliographic entry is as follow: Krystian Birr, *Mode choice modelling for urban areas*, Technical Transactions, Vol. 6/2018, pp. 67-78.

TECHNICAL TRANSACTIONS 6/2018
CIVIL ENGINEERING
DOI: 10.4467/2353737XCT.18.088.8693
SUBMISSION OF THE FINAL VERSION: 15/05/2018

Mariusz Dudek
Katarzyna Solecka (ksolecka@pk.edu.pl)
Institute of Road, Railroad and Transportation Engineering, Faculty of Civil Engineering, Cracow University of Technology

Matthias Richter
Faculty of Business Sciences, University of Applied Sciences, Zwickau

A multi-criteria appraisal of the selection of means of urban passenger transport using the Electre and AHP methods

Wielokryterialna ocena wyboru środków miejskiego transportu pasażerskiego z wykorzystaniem metod Electre i AHP

Abstract

This article presents the main components of the multi-criteria decision making (MCDM) methodology and their application in the assessment of several public transportation solutions in a specific traffic corridor. The corridor in question is 15 km long and runs through the centre of Wrocław, Poland. The analysis focused on six alternative scenarios. The following elements were taken into consideration in their design: alternative means of land transport; different types of vehicles and priorities for public transportation; location of bus and tram stops. The individual solutions were assessed based on six criteria designed to measure different aspects of the problem with the use of two alternative MCDM methods: Electre III/IV and AHP. Computational experiments established the final ranking of transport solutions in the corridor from best to worst in terms of the analysed criteria.

Keywords: transportation corridor, public transportation, multi-criteria decision making

Streszczenie

W artykule przedstawiono elementy metodologii wielokryterialnego wspomagania decyzji (MCDM), a następnie możliwość zastosowania metod MCDM do oceny rozwiązań obsługi pasma zabudowy komunikacją zbiorową. Rozważany korytarz transportowy zlokalizowany jest w centrum miasta Wrocławia (korytarz o długości 15 km). Ocenie poddano 6 wariantów rozwiązań, przy konstruowaniu których uwzględniono następujące elementy: alternatywne środki transportu (środki transportu naziemnego), różne typy pojazdów, priorytety dla transportu publicznego, lokalizację przystanków. Do oceny rozwiązań przyjęto zestaw 6 kryteriów uwzględniających różne aspekty rozważanego problemu. Zbiór wariantów oceniono dwiema metodami wielokryterialnego wspomagania decyzji (MCDM): metodą Electre III/IV oraz AHP. W wyniku przeprowadzonych eksperymentów obliczeniowych uzyskano uszeregowanie końcowe wariantów od najlepszego do najgorszego względem rozważanych kryteriów.

Słowa kluczowe: korytarz transportowy, komunikacja zbiorowa, wielokryterialne wspomaganie decyzji

1. Introduction

A public transport system is a complex operational system that is available to the general public and carries fare-paying passengers by means of a variety of transportation modes (underground/metro, buses, trams, light-rail) from their origins to their destinations on fixed routes and according to a predetermined timetable [2, 3, 28]. Public transport systems are usually operated in large cities and in densely populated areas. Large cities maintain public transport systems because they often have more traffic congestion and less parking space than smaller towns. Urban transportation helps reduce the number of vehicles on the road and it is a convenient option for people travelling over relatively short distances.

The main objective of a public transport system is to provide the passengers with a high quality service. Public transport systems encompass organised forms of passenger transport that are regulated by law and utilise publicly available space and infrastructure. Public transport systems should be characterised by the following features:

- integration (between modes) and coordination,
- safety, security and reliability for passengers,
- economic efficiency and providing good value for money,
- easy access and support for economic growth,
- health and environmental sensitivity.

Public transport systems are usually managed, organised and operated by companies called public transportation operators. These companies can be classified into two main types: common carriers and contract carriers. Common carriers are usually operated by city or regional government agencies and are open to all members of the public who are willing to pay the stated fare. Common carrier systems include transport services that are run along established routes within a city or metropolitan area, allowing people to travel without using cars or other private modes of personal transport. Contract carriers are privately-run companies that provide customised transportation services, e.g. door-to-door transportation services or a specifically designed single trip to a given destination. Contract carriers are usually more expensive than common carriers but can offer a higher level of transportation service, including transporting passengers to places which are not accessible by bus or metro and/or operating at times when a common carrier service may not be scheduled.

Similar to other complex operational systems, public transport systems face a variety of different, complicated and challenging problems. The most important problems in public transport planning are: designing the most suitable transport network which meets to the needs and expectations of passengers; defining rational timetables that guarantee matching between supply, demand and sufficient fleet utilisation; assuring appropriate funding for transport infrastructure maintenance and development; fleet composition and replacement; satisfying the interests of different stakeholders, including passengers that demand high transportation standards; providing environmentally friendly solutions; assuring coordination and integration between different transportation modes; improvement of the transportation infrastructure such that it guarantees better travel conditions for disabled and elderly persons.

Different transportation projects and solutions are focused on the elimination of and/or the allaying of the above-mentioned public transport problems. Different public transportation projects and solutions require thorough and comprehensive appraisal. In many cases, the analysed projects must be ranked and prioritised due to limited availability of financial resources. Thus, proper appraisal of public transportation projects is highly important. In this appraisal, different aspects of technical, economic, social and environmental needed to be taken into account. Interests of different stakeholders are also analysed. The authors of different publications [7, 12, 20, 22, 23] prove that appraisal of public transportation projects should involve the analysis of between eight and twenty-one parameters. The most commonly used characteristics include [11–16, 25]: punctuality, frequency, safety, comfort, accessibility, journey time and cost, regularity, waiting time, investment profitability (e.g. passenger 's time savings, lower operating costs), financial efficiency.

Many of the above-mentioned criteria are in conflict with each other and a compromise solution [27] must be found to at least partially satisfy them. In such circumstances, the methodology of MCDM constitutes a valuable methodological framework for the appraisal of alternative public transportation projects. This methodology enables the decision maker (DM) to carry out a comprehensive appraisal of the public transportation projects in which several, often conflicting points of view must be taken into account [11].

This paper presents the application of multi-criteria decision making (MCDM) methodology to the appraisal of alternative transport solutions designed for a specific traffic corridor in a medium-sized metropolitan area. The corridor is situated in the central part of the city and has a length of 15 km. The scenarios are designed heuristically, using common sense and expert knowledge. Two alternative MCDM methods – Electre III/IV and AHP – are applied in the appraisal process.

The paper is composed of five sections. In the introduction, the background to the research is presented. Section 2 focuses on the description of the MCDM methodology which is the major methodological framework applied in the article; in this section, the applied MCDM methods are characterised. Section 3 presents the construction of scenarios. In section 4, the appraisal of scenarios is carried out; this section includes definitions of the consistent family of criteria, modelling of the decision maker's (DM) preferences and results of computational experiments. The last section is comprised of the final conclusions followed by a list of references.

2. Multiple criteria decision making methodology

2.1. Definition of multiple criteria decision making

Multi-criteria decision making is a dynamically developing field which aims at giving the decision maker some tools in order to enable him/her to advance in solving complex decision problems, where several – often contradictory – points of view must be taken into account [27]. In contrast to the classical techniques of operations research, multi-criteria methods do not yield the 'objectively best' solutions, because it is impossible to generate such solutions which are simultaneously the best from all points of view [29].

The multi-objective decision problem is a situation in which having defined a set of actions/scenarios/solutions *A* and a consistent family of criteria *F*, the DM tends to [27]:

- define a subset of *A* which is the best with respect to *F* (choice problem),
- divide a set of *A* according to certain norms (sorting problem),
- rank actions/scenarios/solutions/variants in *A* from best to worst, according to *F* (ranking problem).

The main attributes of multi-criteria decision problems are the set of action/scenarios/solutions/variants *A* and a consistent family of criteria *F*. The set of action *A* is a set of decision objectives, candidates, scenarios or actions which is analysed and appraised as part of the decision making procedure. The set of *A* can be defined directly in the form of a complete list or indirectly in the form of certain rules and formulas that determine feasible actions/scenarios/solutions/variants, e.g. in the form of constraints. The consistent family criteria *F* should be characterised by the following features [19]: it should provide a comprehensive and complete appraisal of *A*; each criterion in *A* should have a specific direction of preferences (minimized – min or maximized – max) and should not be related to other criteria in *F*. The domain of each criterion in *F* should be disjoint with the domains of other criteria.

The MCDM methodology clearly identifies the major participants of the decision making process, such as the DM and the analyst, and describes their roles in this process. The DM (an individual or a group of individuals) defines the objectives of the decision process, expresses preferences and then evaluates the generated results. Finally, s/he selects the best solution, which is the most desirable scenario. The analyst, who is an external person in the decision making process. Their role is to construct a decision model and select the most appropriate tool to solve the decision problem. The analyst explains the consequences of certain actions to the DM and then recommends the most desirable action.

In accordance with [19, 27], MCDM methods are usually classified as:

- methods of American inspiration, based on the utility function (e.g. AHP [21], UTA [9]) that aggregate different criteria (points of view) into one global criterion called the utility function – these methods eliminate incomparability between scenarios,
- methods of the European (France) inspiration based on the outranking relation (e.g. ELECTRE III/IV methods [1, 18], Promethee I and II [1]), Oreste ([17]) that take into account the incomparability between scenarios,
- interactive methods (e.g. GDF [6], SWT ([8]), Steuer ([26]) that are based on the 'trial and error' approach in each iteration of the solution search procedure and characterised by phases of computation alternating with phases of decision making.

Multi-criteria decision making is characterised by methods that support planning and decision processes through collecting, storing and processing different kinds of information and constructing a viable idea of how to solve a multi-criteria decision problem.

The decision process for a multiple criteria problem is described by the following distinct phases:

- definition and construction of the problem (scenarios),
- definition of a set of consistent family of criteria,

- identification of the preference system of the decision maker,
- selection of the multi-criteria method appraisal,
- computational experiment,
- analysis and comparison of results,
- choice of the best solution and conclusion.

In this paper, two multiple objective ranking methods of MCDM (ELECTRE III/IV and AHP) are applied to evaluate alternative transportation solutions (scenarios) for a specific transportation corridor. The corridor is located in a medium sized metropolitan area, in the city of Wroclaw, Poland. It stretches from the north-western to the south-eastern boundary of the city and connects the housing estates of Kozanów and Jagodno. The corridor is 15 km long and 1 km wide – it passes through the Popowice housing estate, the central railway station in Wrocław and the Krzyki residential area. Different transportation modes, including trams and buses, operate along this corridor. For the purposes of calculation, it was assumed that the average journey distance for public transport in Wrocław is 5 km and the average mobility in a working day is around 0.7 journeys per resident per day (this assumption is based on [5]). The maximum passenger flow was assumed at 20,000 passengers for an average 5 km journey.

2.2. Electre III/IV method

The ELECTRE III/IV method belongs to the family of ELECTRE methods proposed by Roy [18] and it is based on the binary outranking relation [24, 28]. In this method, the basic set of data is comprised of the following elements: a finite set of scenarios A; a family of criteria F; preferential information submitted by the DM. The preferential information is defined in the form of criteria weights – w, indifference – q, preference – p and veto – v thresholds [24]. Scenarios a and b are considered to be indifferent if the difference between their appraisals $f(a)$ and $f(b)$ on a specific criterion is so small (smaller than q) that the DM cannot make any distinction between scenarios. Scenario a is only slightly preferable to scenario b if the difference between their appraisals $f(a)$ and $f(b)$ on a specific criterion is noticeable to the DM (between q and p) but s/he is reluctant to prefer one scenario over the other. Scenario a is strongly preferred over scenario b if the difference between their appraisals $f(a)$ and $f(b)$ on a specific criterion is substantial to the DM (between p and v) and s/he is convinced that a is preferable to b. Scenarios a and b are incomparable if the difference between their appraisals $f(a)$ and $f(b)$ on a specific criterion is so large (larger than v) that the DM cannot consider them as comparable objects.

The outranking relation in the ELECTRE III/IV method is built on the basis of the so-called concordance and discordance tests. In the concordance test, a concordance matrix is constructed composed of the global concordance indicators $C(a, b)$. In the discordance test, a discordance index $Dj(a, b)$ is calculated for each criterion j. The outranking relation indicates the extent to which a outranks b overall. This relation is expressed by the degree of credibility $d(a, b)$, which is equivalent to the global concordance indicator $C(a, b)$ weakened by the discordance indexes $Dj(a, b)$. The values of $d(a, b)$ are from the interval $[0,1]$. Credibility $d(a, b) = 1$ if, and only if, the assertion $a\ S\ b$ (a outranks b) is well founded, $d(a, b) = 0$ if there

is no argument in favour of $a\ S\ b$ (not $a\ S\ b$ – a does not outrank b). The definition of $d(a, b)$ results in the construction of a credibility matrix based on which the method establishes two preliminary rankings (complete pre-orders) using a classification algorithm (distillation procedure). During this procedure, one can obtain a descending and an ascending pre-order. In the descending distillation, the ranking process starts with the selection of the best scenario, which is placed at the top of the ranking. In the ascending distillation, the scenarios are ranked in the inverse order. The final ranking is generated as an intersection of the above-mentioned complete pre-orders – this can be presented either in the form of the ranking matrix or in the form of the outranking graph. The following situations in terms of the relation between variants can be distinguished there: indifference (I), preference (P), lack of preference (P-) and incomparability (R). The method details, described using algorithm flowcharts, formal formulae with equation numbering, were presented in the literature by Vincke, P. [27].

2.3. AHP method – Analytic Hierarchy Process

The AHP (Analytic Hierarchy Process) method is a multiple objective ranking procedure proposed by T. Saaty [21] which is focused on the hierarchical analysis of the decision problem. The method is based on the multi-attribute utility theory [10] and allows the ranking of a finite set of scenarios A. Through the definition of the overall objective, appraisal criteria, sub-criteria and scenarios, the method constructs the hierarchy of the decision problem. On each level of the hierarchy, the DM's preferential information is defined in the form of relative weights w_a based on the pair-wise comparisons of criteria, sub-criteria and scenarios [21]. Each weight represents the relative strength of the compared element against another and is expressed as a number from 1 to 9. All weights have a compensatory character, i.e. the value characterising the less important element (1/2, 1/5, 1/9) is the inverse of the value characterising the more important element in the compared pair (2, 5, 9).

The algorithm of the AHP method focuses on finding a solution for a the so-called eigenvalue problem [21] on each level of the hierarchy. As a result, a set of vectors containing normalised, absolute values of weights w_a for criteria, sub-criteria and scenarios is generated. The sum of the elements of the vector is 1 (100%). The absolute weights w_a are aggregated by an additive utility function. The utility of each scenario i – U_i is calculated as a sum of the products of absolute weights w_a on the path in the hierarchy tree (from the overall goal, through criteria and sub-criteria) the scenario is associated with. The utility U_i represents the contribution of scenario i in reaching an overall goal and constitutes its aggregated appraisal that defines its position in the final ranking.

The important element of the AHP algorithm is the investigation of the consistency level of matrices of relative weights w_a on each level of the hierarchy. Through the calculation of a, the so-called consistency index CI one can measure how consistent the preferential information provided by the DM is. If the value of CI is close to 0, the preferential information provided by the DM is considered to be almost perfect. The acceptable level of CI is below 0.1. The method details described using algorithm flowcharts, formal formulae and equation numbering are presented in the literature by Saaty, T. [21].

3. Construction of scenarios

Six scenarios (V1, V2, V3, V4, V5, V6) have been constructed as alternative transport solutions for the above-described traffic corridor located in Wroclaw, Poland. The following elements have been taken into consideration in the construction of the scenarios:

- alternative modes of transportation (buses and/or trams),
- different types of vehicles considered (standard or articulated buses, different models of trams and buses),
- various approaches to handling transportation priorities for public transport, such as separate bus lanes or tram tracks, traffic lights controlled by bus or tram drivers, no priorities for public transport – buses and trams moving together with the general traffic (private cars, commercial vehicles),
- location and distribution of bus and tram stops along the traffic corridor; different distances between stops,
- alternative technical solutions applied in the construction of bus lanes and tram tracks (different pavements, alternative types of tramways).

In the public transportation modes analysis, only surface transportation modes have been considered. Metro (underground) has been eliminated from considerations due to the fact that it is not a feasible transportation solution for a metropolitan area inhabited by a smaller number of people than 1 million. Metro construction is very expensive and the generated investment costs are very high. Relatively small passenger flows do not guarantee that the investment costs will be paid back. The analysed scenarios are described below [4].

Scenario 1 – standard city-bus

In this scenario, a standard city-bus with a maximum capacity of 100 passengers (for example, Solaris Urbino 12 or Mercedes Citaro O530) is introduced as a means of transportation. The optimal capacity in a standard city-bus is 80. The bus stops are uniformly distributed along the traffic corridor. The average distance between stops is 500 m (the typical distance beyond the city centre area). The average distance pedestrians walk to the bus stop is 389 m and it takes them an average of 5.403 minutes. The bus operational speed is 12 km/h. For a standard city-bus, renewal of the road (width 7 m), investment cost (vehicles) and the cost of maintenance are taken into account.

Scenario 2 – articulated bus

In this scenario, the means of transportation is an articulated bus with a maximum capacity of 176 passengers (for example, Solaris Urbino 18 or Mercedes Citaro O530G). The optimal capacity in an articulated bus is 140. The bus stops are uniformly distributed along the traffic corridor. The average distance between stops is 500 m (the typical distance beyond the city centre area). The average distance pedestrians walk to the bus stop is 389 m and it takes them on average of 5.403 minutes. The bus operational speed is 12 km/h. For articulated buses, renewal of the road (width 7 m), investment cost (vehicles) and cost of maintenance are taken into account.

Scenario 3 – standard city-bus using separate bus lane

In this scenario, a standard city-bus using a separate bus lane with a maximum capacity of 100 passengers (for example, Solaris Urbino 12 or Mercedes Citaro O530) is introduced as a means of transportation. The optimal capacity in this scenario is the same as scenario 1 and is 80. The bus stops are uniformly distributed along the traffic corridor. The average distance between stops is 500 m (the typical distance beyond the city centre area). The average distance pedestrians walk to the bus stop is 389 m and it takes them on average of 5.403 minutes. The bus operational speed is 18 km/h (higher speed applies due to lack of disturbance from traffic and other vehicles). For standard city-buses using a separate bus lane, the building of two bus lanes (width 3.5 m), renewal of the road (width 7 m), investment cost (vehicles) and the cost of maintenance are taken into account.

Scenario 4 – articulated city-bus using separate bus lane

In this scenario, an articulated city-bus using a separate bus lane with a maximum capacity of 176 seats (for example, Solaris Urbino 18 or Mercedes Citaro O530G) is introduced as a means of transportation. The optimal capacity in this scenario is the same as scenario 2 and is 140. The bus stops are uniformly distributed along the traffic corridor. The average distance between stops is 500 m (the typical distance beyond city centre area). The average distance pedestrians walk to the bus stop is 389 m and it takes them on average of 5.403 minutes. The bus operational speed is 18 km/h. For articulated buses using a separate bus lane, the building of two bus lanes (width 3.5 m), renewal of the road (width 7 m), investment cost (vehicles) and cost of maintenance were taken into account.

Scenario 5 – traditional tram

In this scenario, a traditional tram with a maximum capacity of 250 seats (for example, Moderus Beta tramway in Wroclaw or Poznan) is introduced as a means of transportation. The optimal capacity in a traditional tram is 200. The tramway stops are uniformly distributed along the traffic corridor. The average distance between stops is 500 m (typical distance beyond city centre area). The average distance pedestrians walk to the tram stop is 389 m and it takes them on average of 5.403 minutes. The tramway operational speed is 18 km/h. The tram uses a track set into the road for half the route, while for the second half, the tram uses a separate track. For a traditional tram, which uses the road for half the route with the rest on a separate track, the building of a separate tram track, renewal of the separate tram track, building of the tram track into road, renewal of the tram track into road, investment cost (vehicles), maintenance of the tram track in the road and maintenance of the road (width 7 m) are taken into account.

Scenario 6 – fast tram

In this scenario, a fast tram with a maximum capacity of 250 seats (for example – Pesa Twist 32 m long tram in Wroclaw and Silesia or Solaris Tramino tram in Poznan, Olsztyn and planned for Krakow) is introduced as a means of transportation. The optimal capacity in this scenario is the same as scenario 5 and is 200. The tram stops are uniformly distributed along the traffic

corridor. The average distance between stops is 700 m (this has an influence on high speed operation). The average distance pedestrians walk to the fast tram stop is 473 m and it takes them on average of 6.569 minutes. The tram operational speed is 24 km/h. The tram uses a separated tramway line over the entire track, with signal lights assuring tram priorities. For a fast tram whose entire journey is on a separate track away from the influence of car traffic, the building of a separate tram track, the renewal of the separate tram track, the building of the tram track into the road, the renewal of tram track into the road, investment cost (vehicles), maintenance of the tram track into the road and maintenance of the road (width 7 m) are taken into account.

4. Appraisal of scenarios

The scenarios are evaluated by a consistent family of criteria with the application of ELECTRE III/IV and AHP methods. Two different models of decision-maker preferences were created, which is characteristic for these methods. The problem was solved taking into account the passengers' point of view. The results of computational experiments lead to the final rankings of scenarios. The final stage is the comparison of the obtained results – this shows how different solutions can be obtained.

4.1. Family of criteria

In order to rate the alternatives, a set of a coherent family of six criteria was proposed. These criteria are as follows:

- Waiting time [minutes] – average time spent by a passenger at a stop; this criterion is determined as a 0.5 interval; minimised criterion,
- Riding time [minutes] – time required to cover the distance of an average trip; this criterion considers the journey distance – 5km and operational speed (this depends on the means of transport); minimised criterion,
- Accessibility to the stop [minutes] – time the passenger needs to reach the bus/tram stop; it is the quotient of walking distance to bus/tram stop and walking speed; walking speed was assumed as 1.2 m/s; minimised criterion,
- Comfort of travel [%] – share of seated passengers in maximum number of flow; maximised criterion,
- Cost of rolling stock purchase [zł/km/year] – converted cost of rolling stock purchase per one passenger; the cost is dependent on length of corridor and journey distance, accepted discount rate, cost of rolling stock purchase; minimised criterion,
- Cost of building, maintenance and renewal of route [zł/km/year] – converted cost of building, maintenance and renewal of route per one passenger; the criterion depends on the length of corridor, journey distance, passenger flow, unit cost of building and maintenance of routes and accepted discount rate; cost of building, maintenance and renewal is calculated taking into account a discount rate of 6% for 20 years; the cost was accepted according to actual market values (Table 1.); minimised criterion.

Table 1. Unit cost (market value) of building, renewal, maintenance and investment (vehicles)

Objects	Unit	Standard bus	Articulated bus	Traditional tramway	Fast tramway
Building of separate tram track	[zł/ km]			12,000,000	18,000,000
Reconstruction of the separate tram track	[zł/ km]			8,000,000	12,000,000
Building of tram track into road	[zł/ km]			14,000,000	21,000,000
Reconstruction of the tram track into road	[zł/ km]			10,000,000	15,000,000
Building of two bus lanes (width 3.5 m)	[zł/ km]	4,000,000	4,000,000		
Reconstruction of the road (width 7 m)	[zł/ km]	2,000,000	2,000,000		
Investment cost (vehicle)	[zł/ piece]	1,150,000	1,550,000	4,300,000	8,970,000
Cost of maintenance separate track of tram	[zł/km/year]			52,000	62,000
Cost of maintenance of tram track into road	[zł/km/year]			72,000	86,000
Cost of maintenance of road (width 7 m)	[zł/km/year]	24,000	24,000		

The calculations exclude the running costs of vehicles, assuming that this cost will on the whole be covered by revenue from sales of tickets. The main characteristic value for each criterion and direction of preferences are described in Table 2.

Table 2. Characteristic parameters of scenarios

Criterion		Direction of preferences	Average journey distance 5 km Max. number of flow 20,000					
			V1	V2	V3	V4	V5	V6
C1	Waiting time	Min	1.2	2.1	1.2	2.1	3	3
C2	Riding time	Min	25	25	16.66	16.66	16.66	12.5
C3	Accessibility of stop	Min	5.403	5.403	5.403	5.403	5.403	6.569
C4	Comfort of travel	Max	0.155	0.22	0.155	0.155	0.1	0.345
C5	Cost of vehicles purchase	Min	0.302	0.216	0.201	0.146	0.256	0.317
C6	Cost of building, maintenance and renewal of route	Min	0.013	0.013	0.255	0.255	0.323	0.354

4.2. Modelling of the decision-making preferences

The ELECTRE III/ IV and AHP methods, which were described in section two, were applied for assessment. The problem was solved by experts taking into account preferences of the passenger and operator. The ELECTRE III/IV method utilises a preference model based on weights of criteria – w and thresholds q, p and v. These thresholds represent the sensitivity of the DM to the changes in criteria values. All four values – w, q, p and v are defined separately for each criterion. The model of the DM's preference characteristic for the ELECTRE III/IV method is presented in Table 3.

Table 3. The DM's preference characteristic model for the ELECTRE III/IV method

Criterion			Direction of preferences	Passenger				Operator			
				w	*q*	*p*	*v*	*w*	*q*	*p*	*v*
C1	Waiting time	[min]	Min	10	0.5	1	2	3	1	3	5
C2	Riding time	[min]	Min	6	2.5	3	5	8	3	15	20
C3	Accessibility of stop	[min]	Min	8	2.5	3	4.5	4	0.5	2	6
C4	Comfort of travel	[%]	Max	5	0.05	0.1	0.3	6	0.05	0.1	2
C5	Cost of purchase	[zł/pas]	Min	1	0.05	0.2	0.8	10	0.05	0.3	4
C6	Cost of building, maintenance and renewal route	[zł/pas]	Min	1	0.01	0.1	0.25	2	0.15	0.25	0.1

As a result of the computational experiments, two different models of the DM's preferences were obtained – a graphical (final graph) and a numerical form (ranking matrix) – which take into consideration the relations: I – indifference, P – preference, P* – lack of preference and incomparability – R. The results of the experiments carried out by the ELECTRE III/IV method are presented in Figs 1 & 2.

The results obtained from the ELECTRE III/IV method show that the best solution from the passenger viewpoint is scenario V3 (standard city-bus using a separate bus lane) and from the operator viewpoint, it is scenario V4 (articulated city-bus using a separate bus lane).

In the AHP method, the model of the DM's preferences is based on the relative weights representing the strengths of particular elements in the pair-wise comparison of criteria and scenarios described in section 2. In the AHP method, the final ranking is based on the computation of the utility function of each scenario. Tables 4 and 5 show the model of DM preferences characteristic of the AHP method for two different DM model preferences.

Ranking Matrix

	V1	V2	V3	V4	V5	V6
V1	I	P	P-	I	P	P-
V2	P-	I	P-	P-	P	P-
V3	P	P	I	P	P	P
V4	I	P	P-	I	P	P-
V5	P-	P-	P-	P-	I	P-
V6	P	P	P-	P	P	I

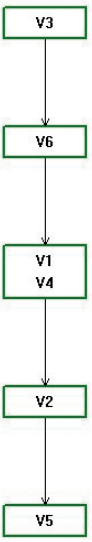

Fig. 1. Graphical results of computational experiments – passenger preference

Ranking Matrix

	V1	V2	V3	V4	V5	V6
V1	I	P-	P-	P-	P-	P-
V2	P	I	P-	P-	P-	P-
V3	P	P	I	P-	I	P-
V4	P	P	P	I	P	P
V5	P	P	I	P-	I	P-
V6	P	P	P	P-	P	I

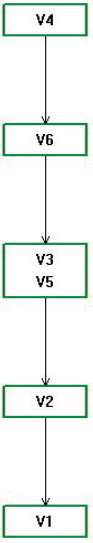

Fig. 2. Graphical results of computational experiments – operator preference

Table 4. The model of DM preferences characteristic of the AHP method, comparison of criteria – passenger preference

	C1	C2	C3	C4	C5	C6
C1	1	3	2	4	7	7
C2	1/3	1	1/2	1	4	4
C3	1/4	2	1	2	5	5
C4	1/4	1	1/2	1	3	3
C5	1/7	1 /4	1/5	1/3	1	1
C6	1/7	1/4	1/5	1/3	1	1

Table 5. The model of DM preferences characteristic of the AHP method, comparison of criteria – operator preference

	C1	C2	C3	C4	C5	C6
C1	1	1/5	1/2	1/3	1/7	2
C2	5	1	4	2	1/2	7
C3	2	1/4	1	1/2	1/5	2
C4	3	1/2	2	1	1/3	3
C5	7	2	3	3	1	7
C6	1/2	1/7	1/2	1/3	1/7	1

The graphical results of computational experiments carried out by the AHP method are presented in Figs 3 & 4.

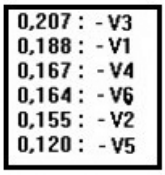

Fig. 3. Graphical results of computational experiments – passenger preference

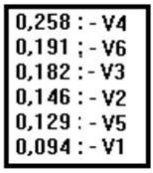

Fig. 4. Graphical results of computational experiments – operator preference

The values of the utility function for scenarios counted by the AHP method are aggregated values which show the positions of individual scenarios in the final ranking. The value enables the description of the distances between the individual scenarios – this is not possible in the ELECTRE III/IV method. The best solution, taking passengers' needs into consideration, is scenario 3 (standard city bus using a separate bus lane); however, taking into consideration the operator's view of point, the best solution is scenario 4 (articulated city bus using a separate bus lane) in both the AHP and the ELECTRE III/IV method.

5. Summary and conclusion

The paper presents the application of a multi-criteria method of appraising public transport. Various means of transport along a 15 km transportation corridor were evaluated. The experiments were carried out using computer implementations of the ELECTRE III/IV and AHP methods taking into account two models of DM preference: passenger and operator. In the first case (ELECTRE III/IV), the final generated ranking was based on the calculation of the outranking relation, while the second experiment (AHP) was based on the computation of the utility function of each scenario.

Six scenarios were created. First, some scenarios concerning the means of transport using the transportation corridor were created. Next, the consistent family of criteria that assures the comprehensive appraisal of scenarios was defined. The DM's model of preferences then was created, and in the last step, the problem was solved by special software for multi-criterion assessment (AHP, Electre III/IV). Taking into account passenger preferences, the best scenario is V3 (standard city-bus using a separate bus lane) and the worst scenario is V5 (traditional tram) according to both the AHP and the ELECTRE III/IV methods. Taking into account operator preferences, the best scenario is V4 (standard city-bus using a separate bus lane and fast tram) and the worst scenario is V1 (standard city-bus) according to both the ELECTRE III/IV and the AHP methods. Despite the use of two different MCDM methods, the results obtained are quite similar. This article shows the different functionality of the modes of transport from both the passengers and the operators perspective. The results are somewhat different for operators and passengers because they have different preferences. Some criteria are more important for the passenger (waiting time, accessibility to the bus stop) and some criteria are more important for the operator (cost of purchase). The results of the above-described analysis extend the knowledge on real cases of selection of transportation scenarios and can be used in the practice of decision making by local governments in Polish cities.

References

[1] Brans J., Mareschal B., Vincke P., *Promethee. A new family of outranking methods in multicriteria analysis*, Brans J. (ed.) Operations Research '84, North-Holland, Amsterdam1984.

[2] Cascetta N., *Transportation system engineering: theory and methods*, Kluwer Academic Publishers, London 2001.

[3] Daganzo C., *Fundamentals of transportation and traffic operations*, Pergamon Press, San Francisco 1997.

[4] Dudek M., Rudnicki A., *Optymalizacja obsługi pasma zabudowy transportem zbiorowym*, Warszawa 2007.

[5] Ernst & Young / Politechnika Krakowska, *Plan Generalny rozwoju transportu szynowego we Wrocławiu*. Część 1: *Ogólna koncepcja transportu szynowego we Wrocławiu*, 2007.

[6] Geoffrion A., Dyer J., Feinberg A., *An interactive approach for multi-criterion optimization, with an application to the operation of an academic department*, Management Science, Vol. 19, No.4, 1972.

[7] Gupta A., *Comparative study of private and public bus transport in Delhi*, Proceedings of the 8th IFAC Symposium on Transportation Systems, Chania 1997.

[8] Haimes Y. Y., Hall W. A., *Multiobjectives in water resources systems analysis: The SWT method*, Water Resources Research, Vol. 10/1975.

[9] Jacquet-Lagreze E., Siskos J., *Assessing a set of additive utility functions for multicriteria decision making: the UTA method*, European Journal of Operational Research, Vol. 10/1982.

[10] Keeney R., Raiffa H., *Decisions with multiple objectives. Preferences and value tradeoffs*, Cambridge University Press, Cambridge 1993.

[11] Kiba Janiak M., Żak J., *Multiple Criteria Evaluation of Different Redesign Scenarios of the Public Tram System*, Transportation Research Procedia, Vol. 3/2014.
[12] Kiciński M., Judt W., Kłosowiak R., *Wielokryterialna ocena wariantów dojazdu mieszkańców aglomeracji poznańskiej do Poznania*, Autobusy, Technika, Eksploatacja, Systemy Transportowe, vol. 12, 2017, 560-563.
[13] Kobryń A., *Wielokryterialne wspomaganie decyzji w gospodarowaniu przestrzenią*, Warszawa 2014.
[14] Litman, T., *Well measured-developing indicators for sustainable and livable Public transport planning*, Victoria Transport Policy Institute, Victoria, Canada, http://www.vtpi.org/wellmeas.pdf (access: 10.01.2018).
[15] Macharis C., Bernardini A., *Reviewing the use of Multi-Criteria Decision Analysis for the evaluation of transport projects: Time for a multi-actor approach*, Transport Policy Vol. 37/2015, 177-186.
[16] Owczarzak Ł., Żak J., *Design of passenger public transportation solutions based on autonomous vehicles and their multiple criteria comparison with traditional forms of passenger transportation*, 18th Euro Working Group on Transportation, EWGT 2015, 14-16 July 2015, Delft, The Netherlands, Transportation Research Procedia, Vol. 10/2015, 472-482.
[17] Pastijn H., Leysen J., *Constructing an outranking relation with ORESTE*, Mathematical and Computer Modelling, Vol. 12, No 10/11, 1989.
[18] Roy B., *The outranking approach and the foundations of Electre methods*, [in]: Bana e Costa C. (Ed.), *Readings in Multiple Criteria Decision Aid*, Springer-Verlag, Berlin 1990.
[19] Roy B., *Wielokryterialne wspomaganie decyzji*, Wydawnictwo Naukowo-Techniczne, Warszawa 1990.
[20] Rudnicki, A., *Jakość komunikacji miejskiej*, SITK, Krakow 1999.
[21] Saaty, T., *The Analytic Hierarchy Process: Planning, priority setting, resource allocation*, McGraw-Hill, New York 1980.
[22] Saaty T., *Transport planning with multiple criteria: The Analytic Hierarchy Process applications and progress review*, Journal of Advanced Transportation, Vol. 29, No. 1, 1995.
[23] Sawicki P., Kiciński M., Fierek S., *Selection of the most adequate trip-modelling tool for integrated transport planning system,* Archives of Transport, 2016, Vol. 37, Iss. 1, 2016, 55-66.
[24] Skalka, J., Bouyssou, D., Bernabeu, Y., *ELECTRE III et IV. Aspects methodologiques et guide d'utilisation*, LAMSADE, 25, Paris 1986.
[25] Solecka K., *Wielokryterialna ocena wariantów zintegrowanego miejskiego transportu publicznego w Krakowie*, praca doktorska, Kraków 2013.
[26] Steuer R., *An interactive multiple objective linear programming procedure' TIMS studies in the management sciences*, Computers & Operations Research, 1977.
[27] Vincke P., *Multicriteria decision-aid*, John Wiley&Sons, Chichester 1992.
[28] Vuchic V., *Urban transit systems and technology*, John Wiley & Sons, New York 2007.
[29] Żak J., Fierek S., *Design and evaluation of alternative solutions for integrated urban transportation system*, CD – Proceedings of the World Conference on Transport Research, Berkeley 2007.

If you want to quote this article, its proper bibliographic entry is as follow: Mariusz Dudek, Matthias Richter, Katarzyna Solecka, *A multi-criteria appraisal of the selection of means of urban passenger transport using the electre and ahp methods*, Technical Transactions, Vol. 6/2018, pp. 79-94.

TECHNICAL TRANSACTIONS 6/2018
CIVIL ENGINEERING
DOI: 10.4467/2353737XCT.18.089.8694
SUBMISSION OF THE FINAL VERSION: 14/05/2018

Bożena Hoła
Tomasz Nowobilski (tomasz.nowobilski@pwr.edu.pl)
Department of Construction Methods and Managements, Faculty of Civil Engineering, Wroclaw University of Science and Technology

Jarosław Rudy
Faculty of Electronics, Wroclaw University of Science and Technology

Krzysztof Czarnocki
Faculty of Computer Science and Management, Lublin University of Technology

An analysis of the influence of selected factors on the accident rate in the construction industry

Analiza wpływu wybranych czynników na wypadkowość w budownictwie

Abstract

This paper presents the results of research aimed at constructing a linear mathematical model that determines the influence of selected factors characterising construction production on the accident rate in the construction industry. A number of linear multi-factor mathematical models were developed, which were then compared with each other, and those that best described the analysed phenomena were selected.

Keywords: accident factor, occupational accident, construction and assembly production, linear multi-factor mathematical model

Streszczenie

W artykule zawarto rezultaty badań, których celem było zbudowanie liniowego modelu matematycznego określającego wpływ wybranych czynników charakteryzujących produkcję budowlaną, na wypadkowość w budownictwie. Opracowano kilkanaście liniowych wieloczynnikowych modeli matematycznych, które następnie porównano ze sobą i wytypowano te, które najlepiej opisują analizowane zjawisko.

Słowa kluczowe: czynnik wypadkowy, wypadek przy pracy, produkcja budowlano-montażowa, liniowy wieloczynnikowy model matematyczny

1. Introduction

The construction industry is a very diverse area of human activity. Due to the large variety of buildings and construction works related to their execution, and also the ever-changing conditions of construction, there are a number of factors that may affect the accident rate in the construction industry. These include factors directly related to the manufacturing process which directly generates causes of accidents and also many unidentified factors that indirectly influence the development of accidents. Whilst the direct factors are well recognized [1–10], knowledge about indirect factors is limited [11].

When analysing the statistical data published by the Central Statistical Office (CSO), it can be noted that the values of indicators that describe the construction industry with regards to occupational safety and also the size of construction and assembly production are changing each year. Based on this observation, the authors of the article undertook research that aimed to define the factors that describe the specificity of the construction industry and also investigate whether and how these factors affect the accident rate.

The final result of the research is a collection of mathematical models describing the phenomenon of accidents in the construction industry which takes into account the influence of the defined factors on the occurrence of accidents. These models can be used to forecast the number of people who will be injured in occupational accidents in the construction industry in relation to the changing structure of construction and assembly production.

2. Factors describing the construction industry

Table 1 summarises the factors that characterise the construction industry which were defined on the basis of statistical data published by the CSO [12, 13].

Table 1. Analysed factors with their designations

Lp.	Main factor	Component factors	Adopted designation
1	the size of construction and assembly production	size of production executed by: construction entities – in general	W
2		entities employing more than 9 people	W_{+}
3		entities employing less than 10 people	W_{-}
4		the size of production associated with: construction of buildings	W_{B}
5		construction of civil engineering objects	W_{LW}
6		specialised construction works	W_{S}

7	the size of construction and assembly production with regards to investments	size of production associated with: the construction industry – in general	I
8		construction of buildings	I_B
9		construction of residential buildings	I_{BM}
10		construction of non-residential buildings	I_{BN}
11		construction of civil engineering objects	I_{LW}
12	the size of construction and assembly production with regards to renovation works and other works	size of production associated with: the construction industry – in general	R
13		renovation of buildings	R_B
14		renovation of residential buildings	R_{BM}
15		renovation of non-residential buildings	R_{BN}
16		renovation of civil engineering objects	R_{LW}
17	occupational safety	total number of people injured in occupational accidents	P

Each of the factors defined in Table 1 is described numerically by adding the corresponding value of the construction works to it. The occupational safety aspect (factor 17) is described by the number of people injured in occupational accidents. By knowing the numerical values of the above factors, it is possible to determine the degree of dependence between a given factor and the number of occupational accidents. Statistical data [12, 13] for 16 voivodships in Poland from 2005 to 2015 was used in the calculations. Some of the data concerning the voivodship of Lower Silesia which was adopted for the calculations is presented in Table 2.

Table 2. Fragment of statistical data for the voivodship of Lower Silesia that was adopted for the calculations

No.	**Factor - according to the adopted designations**		**Year**				
			2005	**…**	**2010**	**…**	**2015**
1 17	W	PLN mln	6888.7	…	13036.9	…	14656.7
	I		1976.1	…	3766.4	…	4208.7
	R		999.4	…	2565.7	…	2518.7
	P	people	593	…	776	…	443

3. General mathematical model of the analysed phenomenon

A multiple linear regression model was adopted for the description of the impact of the defined factors on occupational safety [14]. In this model, a response variable is the number of victims, and explanatory variables are the values of appropriately selected factors. The choice of such a model is dictated by the fact that it is the simplest and most correct method of determining the impact of factors on the accident rate when the functional form of this dependence is unknown. In addition, as has been demonstrated in previous studies [15], all analysed factors show relationships that are close to being linear. The analysis was performed using the MATLAB package, and the general form of a model for i explanatory variables is as follows:

$$P = b_0 + b_1 x_1 + b_2 x_2 + ... + b_i x_i + ... + b_I x_I + \varepsilon \quad (1)$$

where:

P – the response variable – the number of people injured in occupational accidents in the construction industry,

x_i – the independent explanatory variables – the numerical values of factors defined in Table 1, $(i=1,\ldots,I)$,

b_0 – the absolute term,

b_i – the parameters of the model, $(i=1,\ldots,I)$,

ε – a random component – the rest of the model.

The least squares method was used to estimate the parameters. This method applies such an adjustment to the model's b_i parameters so that the mean square error of the difference between the individual $\hat{P}$ values generated by the model and the empirical values P corresponding to them was as small as possible. As quality meters for the assessment of the adjustment of the model to empirical values, the following were used [14, 16]: the multiple correlation coefficient R_p; coefficient of determination R^2; Mean Squared Error (MSE) and Root Mean Squared Error (RMSE).

4. Mathematical model of the dependence between the number of occupational accidents on the value of construction and assembly production

Due to the complexity of the phenomenon, ten different mathematical models were developed which take into account various factors. The selection of explanatory variables for each model was made on the basis of the analysis of the structure and also the correlation matrix of factors. In the analysed case, the structure of factors is strongly hierarchical. For example, factor W can be decomposed into factors W_+ and W_-, while the sum of the values of these factors is equal to the value of production described by factor W. The choice of explanatory variables was based on the desired level of detail. Table 3 summarises the obtained mathematical models.

Table 3. Summary of mathematical models

No.	Mathematical models
1	$P = 132.335 + 0.041W$
2	$P = 129.042 + 0.039W_{+} + 0.044W_{-}$
3	$P = 119.080 + 0.028W_{B} - 0.022W_{LW} + 0.183W_{S} + 0.036W_{-}$
4	$P = 152.551 + 0.008I + 0.211R$
5	$P = 133.290 + 0.003I + 0.194R + 0.014W_{-}$
6	$P = 127.237 + 0.031I_{B} + 0.00465I_{LW} + 0.048R_{B} + 0.278R_{LW}$
7	$P = 91.487 + 0.035I_{B} - 0.013I_{LW} + 0.004R_{B} + 0.270R_{LW} + 0.023W_{-}$
8	$P = 119.388 - 0.014I_{BM} + 0.048I_{BN} - 0.001I_{LW} + 0.518R_{BM} - 0.147R_{BN} + 0.294R_{LW}$
9	$P = 89.386 - 0.027I_{BM} + 0.057I_{BN} - 0.017I_{LW} + 0.419R_{BM} - 0.165R_{BN} + 0.286R_{LW} + 0.022W_{-}$
10	$P = 80.032 - 0.368W_{B} - 0.334W_{LW} - 0.289W_{S} + 0.015W_{-} + 0.368I_{BM} + 0.364I_{BN} + 0.335I_{LW} + 0.742R_{BM} + 0.187R_{BN} + 0.618R_{LW}$

In the next stage, the models were compared. For this purpose, the above-mentioned factors were used: R_P, R^2, R_S^2, *MSE* and *RMSE*. The values of these coefficients for all the models are given in Table 4. The best adjustment of the model to the actual values is obtained when R_P, R^2, and R_S^2 are close to unity, and *MSE* and *RMSE* have low values.

Table 4. Summary of parameters characterising the obtained mathematical models

No.	R_P	R^2	R_S^2	*MSE*	*RMSE*
1	0.82	0.68	0.68	45283	212
2	0.82	0.68	0.67	45526	213
3	0.82	0.69	0.68	44465	210
4	0.87	0.77	0.77	34314	185
5	0.87	0.77	0.77	34128	184
6	0.91	0.84	0.84	20751	144
7	0.92	0.85	0.85	19841	140
8	0.92	0.85	0.84	20188	142
9	0.92	0.78	0.76	19419	139
10	0.93	0.87	0.85	18806	137

Based on analysis of Table 4, it can be seen that the "best" models:

- due to the value of the R_P coefficient, are models 10, 9, 8 and 7;
- due to the value of the R^2 coefficient, are models 10, 8, 7 and 6;
- due to the value of the R_S^2 coefficient, are models 10, 7, 8 and 6;
- due to the value of the measure of variability *MSE* and *RMSE*, are models 10, 9, 7 and 8.

Although model 10 has the best values of the analysed indicators, it will not be considered in further analysis due to the large number of parameters included in it; practical use of this model is more laborious. Out of the remaining 4 models, model 9 was also eliminated due to the lower value of the R_S^2 coefficient when compared to the other models.

Finally, it should be stated that the best and most consistent models are models 8, 7 and 6. They show similar values of coefficients R_p, R^2 and R_S^2, and small differences in values of *RMSE*. These models will be used in further studies to predict the number of victims of occupational accidents in the construction industry.

5. Summary

On the basis of statistical data published by the CSO, 16 factors were identified that describe construction and assembly production, and these characterise: business entities performing construction works, the size of construction production related to investments and renovations, and also the type of executed building objects.

A linear multiple regression model was used to describe the impact of the defined factors on occupational safety. In this model, the response variable is the number of victims injured in occupational accidents and the explanatory variables are the analysed factors. As a result of the conducted analyses, ten mathematical models that describe the studied phenomenon were obtained, each of which differed in the number and type of explanatory variables.

Based on the analysis of the values of the evaluation measures, models 8, 7 and 6 were selected as the best models. These models will be used to assess the risk of the occurrence of construction disasters, accidents and hazardous events at workplaces that involve construction scaffolding in order to predict the number of people injured in occupational accidents in the construction industry.

The article is the result of the implementation by the authors of research project No. 244388 "Model of the assessment of risk of the occurrence of building catastrophes, accidents and dangerous events at workplaces with the use of scaffolding", financed by NCBiR within the framework of the Programme for Applied Research on the basis of contract No. PBS3/A2/19/2015.

References

[1] Hoła B., *Methodology of hazards identification in construction work course*, Journal of Civil Engineering and Management, Volume 16, Issue 4, 2010, pp. 577-585.

[2] Stępień T., *Identification of factors determining accident rate in construction industry*, Technical Transactions, vol. 1-B, 2014, pp. 265-281.

[3] Rahim A., Hamid A., Maimi Abd Majid M., Singh B., *Causes of Accidents at Construction Sites*, Malaysian Journal of Civil Engineering, No. 20(2), 2008, pp. 242-259.

[4] Hale A., Walker D., Walters N., Bolt H., *Developing the understanding of underlying causes of construction fatal accidents*, Safety Science, No. 50, 2012, pp. 2020-2027.

[5] Hoła, B., Szostak, M., *Analysis of the Development of Accident Situations in the Construction Industry,* XXIII R-S-P SEMINAR, Theoretical Foundation of Civil Engineering

(23RSP) (TFOCE 2014), Book Series: Procedia Engineering, Volume 91, 2014, pp. 429-434.
[6] Radziszewska-Zielina E., *The Application of Multi-Criteria Analysis in the Evaluation of Partering Relations and the Selection of a Construction Company for the Purposes of Cooperation*, Archives of Civil Engineering, Volume 62, Issue 2, 2016, pp. 167-182.
[7] Hoła B., *Identification and evaluation of processes in a construction enterprise", Archives of Civil and Mechanical Engineering*, Volume 15, Issue 2, 2015, pp. 419-426.
[8] Hoła, B., Szostak, M., *Analysis of the state of the accident rate in the construction industry in european union countries*, Archives of Civil Engineering, Volume 61, Issue 4, 2015, pp. 19-34.
[9] Hoła B., Nowobilski T., Rudy J., Borowa-Błazik E., *Dangerous events related to the use of scaffolding*, Technical Transactions, Vol. 7/2017, pp. 31-39.
[10] Klempous, R., Kluwak, K., Idzikowski, R., Nowobilski, T., Zamojski, T., *Possibility analysis of danger factors visualization in the construction environment based on Virtual Reality Model*, 8th IEEE International Conference on Cognitive Infocommunications, CogInfoCom 2017: proceedings, Debrecen, Hungary Danvers, September 11-14, 2017, MA:IEEE, cop. 2017. pp. 363-367.
[11] Nawrot T., *About failures and catastrophes in the construction industry*, Inżynieria i Budownictwo, y.62, No. 12, 2006, pp. 656-657.
[12] Central Statistical Office. Statistical yearbook 2005-2015. Warsaw 2006-2016.
[13] Central Statistical Office. Occupational accidents 2005-2015. Warsaw 2006-2016.
[14] Stanisz A., *Przystępny kurs statystki z zastosowaniem STATISTICA PL na przykładach z medycyny*, Tom 2: *Modele liniowe i nieliniowe*, Kraków 2007.
[15] Hoła B., Nowobilski T., Szer I., Szer J., *Identification of factors affecting the accident rate in the construction industry*, Procedia Engineering, Vol. 11, 2017.
[16] Stanisz A., *Przystępny kurs statystki z zastosowaniem STATISTICA PL na przykładach z medycyny*, Tom 1: *Statystyki podstawowe*, Kraków 2006.

If you want to quote this article, its proper bibliographic entry is as follow: Bożena Hoła, Tomasz Nowobilski , Jarosław Rudy, Krzysztof Czarnocki, *An analysis of the influence of selected factors on the accident rate in the construction industry*, Technical Transactions, Vol. 6/2018, pp. 95-102.

TECHNICAL TRANSACTIONS 6/2018
CIVIL ENGINEERING
DOI: 10.4467/2353737XCT.18.090.8695
SUBMISSION OF THE FINAL VERSION: 08/06/2018

Piotr Sawicki (piotr.sawicki@put.poznan.pl)
Szymon Fierek
Division of Transport Systems, Poznan University of Technology

The impact of long-term travel demand changes on mixed decision problems of mass transit lines construction and vehicles' depots location

Wpływ długoterminowych zmian popytu na problem jednoczesnego wyznaczania przebiegu linii i lokalizacji zajezdni w systemie transportu zbiorowego

Abstract

The paper is concentrated on solving a mixed decision problem of mass transit line construction and vehicles' depots location (MTLC&VDL). The authors have iteratively solved this problem as a function of scenario-based, long-term travel demand changes, and finally have analysed the generated results. As a product of the computations, it has been proved that the solution of the mixed MTLC&VDL decision problem depends on changes in travel demand, both in terms of the line construction and the location of the depot. 5 and 10% increase of travel demand leads to changes in the optimal mass transit line's configuration, while the change of the optimal depot location takes place with 10% of the travel demand change. The results have implied a conclusion that to make strategic decisions on transport systems and solving mixed decision problems, forecasting travel demand changes (its volume and structure) over the long-term horizon has to be performed.

Keywords: mass transit lines construction, vehicles' depots location, travel demand, exact optimisation, traffic modelling

Streszczenie

Artykuł dotyczy łącznego rozwiązania dwóch problemów decyzyjnych związanych z systemem publicznego transportu zbiorowego, tj. wyznaczania przebiegu linii transportowych (MTLC) oraz ustalania lokalizacji zajezdni transportowych (VDL). Autorzy zastosowali iteracyjne rozwiązanie obu problemów, zakładając różne scenariusze długoterminowych zmian popytu oraz przeanalizowali uzyskane wyniki. Jak dowiodły obliczenia, rozwiązanie połączonego problemu MTLC i VDL zależy od zmian popytu. Wzrost popytu o 5 i 10% skutkuje zmianą optymalnego układu linii transportu zbiorowego, podczas gdy do zmiany optymalnej lokalizacji zajezdni dochodzi przy zmianie popytu na poziomie 10%. Wyniki prac pozwoliły wnioskować, że do podejmowania strategicznych decyzji dotyczących systemów transportowych i rozwiązywania mieszanych problemów decyzyjnych należy prognozować zmiany popytu (jego wielkość i strukturę) w długim horyzoncie czasowym.

Słowa kluczowe: publiczny transport zbiorowy, przebieg linii transportowych, lokalizacja zajezdni, modelowanie podróży

1. Introduction

1.1. Travel demand

Travel demand changes derivate from both, external phenomena such as: transport behaviours, demographics, etc., and strategic development of the region, including spatial development, investments and macroeconomics, etc. The land use characteristic is the main issue influencing trip generation rates. This is because factors like the number and size of households, automobile ownership, types of activities (residential, commercial, industrial, etc.), and density of development all drive how much travel flows from or to a specific area within the region. Changes to these factors can affect travel activity and therefore costs and problems such as congestion, accidents and pollution emissions.

The wide range of factors that influence travel activity is especially important for transportation demand management (TDM). The Federal Highway Administration [8] defines TDM as providing travellers with travel choices, such as work location, route, time of travel and mode. In the broadest sense, demand management is defined as providing travellers with effective choices to improve travel reliability. Therefore, a reduced demand for motor vehicle travel (or at least, growth in demand) and an increased demand for alternative modes are crucial.

1.2. Mass transit line construction and vehicles' depots location

A strategic decision considered in the paper is related to mixed decision problems of the mass transit line construction – MTLC and vehicles' depots location – VDL. The essence of combining these two strategic problems (MTLC&VDL) is to find a solution that guarantee the required standards for passengers (maximised availability) offered at the lowest operating costs for the operator (minimised deadhead). In fact, the nature of each separate decision problems is contradictory while considered together. The problem of MTLC is strongly dependent on travel demand. The lines' routing is highly related to the areas characterised by significant volumes of traffic production and attraction, and thus related to a high density of population. On the other hand, the VDL problem refers to setting all technical facilities related to the operation of the operated fleet. In order to minimise empty runs between transport lines and depots, they should be located as close as possible to each other. Due to the amount of space demanded for the proper depots' operation and market value of parcels, however, a less urbanised location (with less cost of acquisition at the same time) is usually searched for. Thus, a contradiction of those decisions means that a reduction of investment costs is directly translated into an increase of operating costs of empty runs (depot-line) at the same time, and vice versa.

The result of the research on joint consideration and solution of the mixed MTLC&VDL decision problem has been presented by the authors [13, 14] before. The principle of this methodology is a combination of the construction of four-stage traffic modelling with the construction and application of a single-criterion mathematical model solved with the use of

exact optimisation algorithm. Each individual step of the methodology is iteratively repeated until a globally satisfactory solution is obtained. The schema of its dependence is presented in Fig. 1.

In the methodology of modelling and solving mixed MTLC&VDL decision problem, the current travel demand volume is assumed, and it is unchangeable for a considered single time period. This volume is consistently applied into all consecutive computations.

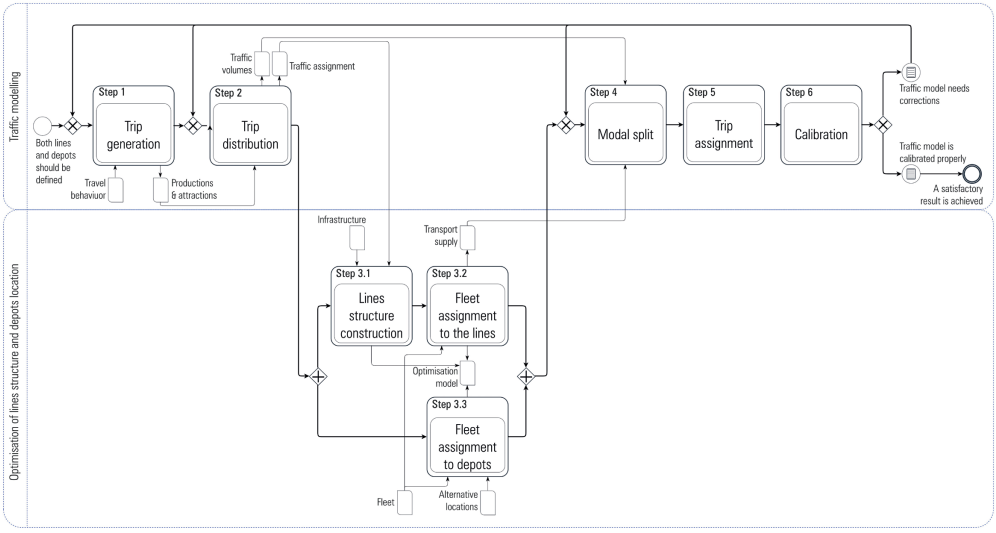

Fig. 1. Key steps of the methodology of solving mixed MTLC and VDL decision problems [14]

1.3. Current state of the decision problem

MTCL is a one of the fundamental decision problems in the mass transit research domain. It has been widely discussed in the literature, either in works on the principal concepts from the last century, e.g. Baaj & Mahmassani [2], Dial & Bunyan [6], Dubois et al. [7], or from the recent period, e.g. Ceder [5], Schöbel [15], Teodorović & Janić [17], Abdallah [1]. In this research, MTCL is concentrated on building a mass transit network with a simultaneous determination of other associated issues, including the frequency of running (e.g. [4, 16]), transferring to other lines at the stations [12] and others.

VDL, as a decision problem, has not been extensively discussed in the literature on mass transit research domain. This problem with references to the bus depots location has been analysed by Hamdouni et al., [9, 10], and with reference to the tram network by Kupka & Sawicki [11]. The main assumption in such a research is an unchangeable structure of routes. A simultaneous consideration and solution of depot location and routing problems is a very common approach in the freight transportation research domain. In the mass transit research domain, simultaneous solutions of a depot location problem with other decision problems has reference to rolling stock circulation, e.g. for railway rapid transit system [3].

Concluding, MTCL and VDL are decision problems, which are considered and solved separately, or possibly in combination with other decision problems; however, a simultaneous consideration of both of them has not been extensively discussed up to now, except the previous research of the authors of this paper [13, 14].

1.4. Objective of the research

The research presented in this paper deals with the study on the impact of long-term changes in travel demand while solving mixed the MTLC&VDL decision problem. The authors have conducted a series of computational experiments, as a function of travel demand changes in a long-term planning horizon, and the result of the MTLC&VDL decision problem has been analysed. Travel demand changes are iteratively changed and each change is characterised by a different scenario.

The concept of the research applied in this paper is schematically shown in Fig. 2. Steps 1–6 are referred to the methodology defined in the previous research [14], see Fig. 1.

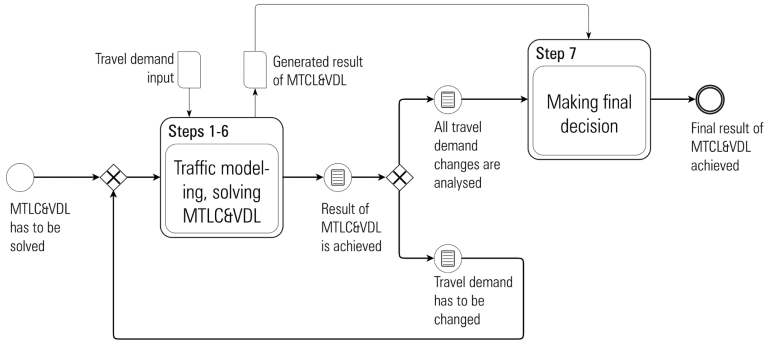

Fig. 2. The methodology of solving mixed MTLC & VDL decision problem as a function of a long-term travel demand changes

2. Computational results

2.1. Key assumptions and parameters

All the computations performed in this paper constitute a further step of the previous research [13, 14]. Thus, some methodological assumptions result from earlier findings, others are related to subsequent methodological steps. Based on the result of previous research, the key assumptions are as follows:

- the objective function, i.e. minimised cost function C, and the set of corresponding constraints are the same [13],
- the generation of a set of i-th lines on the graph of the transport network $G = <j, k>$, is conducted with the application of the ZLT1 algorithm [13], i.e. opposite nodes (located on the border of the considered area) of the transport network are joined with the i-th line,

- a fleet is homogenous, i.e. the same capacity for each vehicle in the fleet is applied; q_i = 105 [pas.],
- the passenger comfort factor is assumed and constant; λ_i= 0.75 [-],
- one out of six alternative locations for vehicle's depot (l = 1, 2, …, 6) is looked at; their alternative locations are the same and presented in Fig. 3,
- the computation is performed on the basis of a testing model of a transport network, typical for a city inhabited by around 60,000 inhabitants and covering an area of 47 km^2; the picture of the considered transport network is presented in Fig. 3.

With respect to the objective of this paper, the authors have defined the following additional assumptions:

- traffic analysis zones in the considered area (its number, structure and location) are unchangeable during analysis; there are 13 zones (including 4 zones representing external traffic) and their location is presented in Fig. 3,
- travel demand changes result from two key factors, including *i*) inhabitant's migration from the city centre to the peripheries, and *ii*) increased population number in the considered area,
- different time horizon perspectives are analysed, incl. current state – 1 perspective, and long term – 2 perspectives.

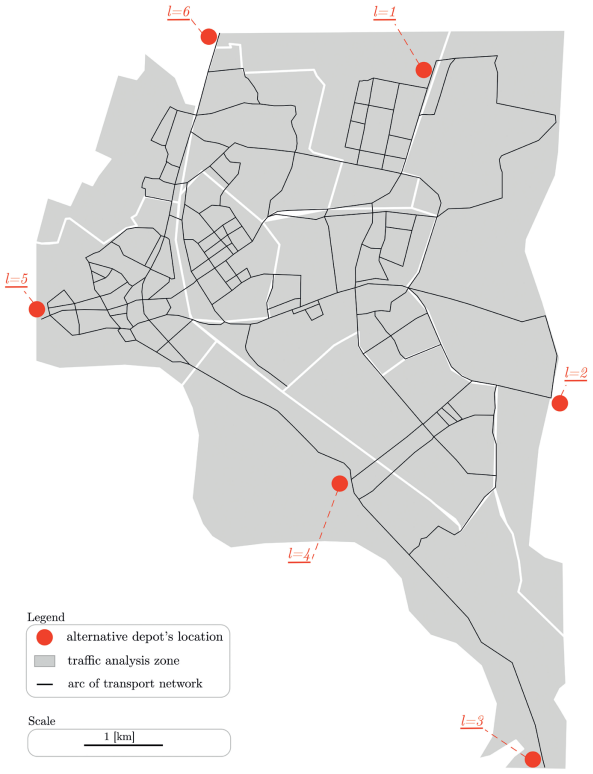

Fig. 3. A general picture of the considered area

2.2. Experiments

All computations based on a schema presented in previous sections, see Fig. 1 and Fig. 2, have been iteratively repeated 3 times for each specific scenario. Scenario 1 (S1) is a representation of the current state of travel demand, and the mixed decision problem of MTLC&VDL is solved. With a scenario 2 (S2), 5% increased explanatory variables (such as the number of inhabitants, employees, students etc.) used to calculate trip generation have been faced, and a considered mixed decision problem is solved again. The decision problem is solved again within scenario 3 (S3), where the same explanatory variables are increased by 10%, compared to S1.

A draft traffic allocation to arcs on the considered transport network is presented in Tab. 1. It consists of the results of analysis in scenario S1, S2 and S3. The representation of the final traffic assignment for a rush hour (7 am–8 am), after modal split operation, as well as the length of each link d_{jk}, are presented in Tab. 2, for scenarios S1, S2 and S3 as well.

Table 1. A draft traffic allocation to arcs of the network for 24 hours

Nodes		Traffic volumes [pas./24h]						Velocity [km/h]						d_{jk} [km]
		P_{jkt}			P_{kjt}			v_{jk}			v_{kj}			
j	k	S1	S2	S3	S1	S2	S3	S1	S2	S3	S1	S2	S3	
1	6	1769	1821	1886	1290	1326	1362	35	35	35	35	35	35	.80
1	115	1356	1404	1473	1845	1923	1995	45	45	45	45	45	45	.58
4	137	1511	1519	1532	2043	2053	2071	35	35	35	35	35	35	1.21
10	11	3840	3918	3998	3710	3811	3915	60	60	60	60	60	60	.47
11	118	3195	3248	3309	3252	3334	3414	60	60	60	60	60	60	.13
...	...	...	...	...	...	...	...	...	...	...	...	...	...	...
138	149	3801	3782	3769	5009	5024	5041	60	60	60	60	60	60	.74
143	144	1470	1449	1424	1043	1040	1053	45	45	45	45	45	45	.46
144	32	1470	1449	1424	1043	1040	1053	35	35	35	35	35	35	.61
161	162	2558	2664	2777	2147	2229	2311	35	35	35	35	35	35	.26
162	31	2965	3085	3206	2509	2603	2700	35	35	35	35	35	35	.20

Since the possibility of presenting a complete list of traffic volumes is limited in this paper, a comparison of passenger traffic volume profiles for each scenario is shown in Fig. 4a. Additionally, a comparison of passenger traffic volume differences between scenarios, i.e. S2-S1 and S3-S1, is presented in Fig. 4b.

While comparing the passenger traffic volumes at individual arcs of the transport network (see Fig. 4b), i.e. scenarios S2-S1 (red line, demand increased by 5%) and S3-S1 (green line,

demand increased by 10%), significantly higher differences are observed in the first case. The range of differences for S2-S1 is (-61, 106) [pas./h], and its profile across the transport network is noticeably concentrated around selected arcs of the network. In the case of S3-S1, the differences are in the range (-59, 66) [pas./h], and their profile is relatively equally distributed over the network.

Table 2. A traffic allocation to arcs of the network for rush hours (7am-8am), mass transit only

Nodes		Traffic volumes [pas./h]						Velocity [km/h]						d_{jk} [km]
		P_{jkt}			P_{kjt}			v_{jk}			v_{kj}			
j	k	S1	S2	S3	S1	S2	S3	S1	S2	S3	S1	S2	S3	
1	6	42	140	83	40	62	70	34	33	33	35	33	34	.80
1	115	40	62	70	42	140	83	45	44	45	45	44	44	.58
4	137	103	83	91	96	113	113	33	33	32	31	30	30	1.21
10	11	59	50	58	91	66	97	55	54	54	54	54	53	.47
11	118	58	50	58	67	66	69	59	59	59	58	58	57	.13
...	...	...	...	...	...	...	...	...	...	...	...	...	...	...
138	149	102	80	53	132	77	73	59	59	58	58	56	56	.74
143	144	156	156	160	145	133	157	45	45	45	45	45	45	.46
144	32	156	156	160	145	133	157	35	35	35	35	35	35	.61
161	162	113	171	106	99	107	87	27	27	25	30	26	28	.26
162	31	113	171	106	99	107	87	27	27	25	30	26	28	.20

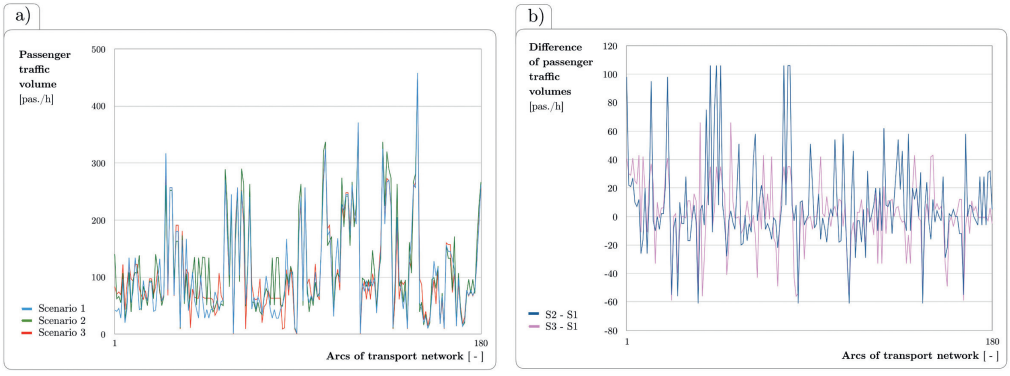

Fig. 4. The scenario-based profile of passenger traffic volume allocated to the arcs of transport network: a) the volumes, b) difference between scenarios

2.3. Discussion of the results

All the computations have been performed using the PTV Visum software (for the traffic modelling part) and Solver Premium Platform (for optimisation part), using LP simplex solver for discrete optimisation. The results obtained under individual scenarios: S1, S2 and S3, are summarised in Tab. 3. They indicate the following key observations:

- in each case, 8 transport lines are defined for the mass transit system, and the common set for all considered scenarios (S1, S2 and S3) is composed of 5 lines, i.e. {5, 7, 11, 12, 21};
- the increased number of the homogenous fleet of vehicles (from 8 vehicles at S1 and S2 to 9 vehicles at S3) results from increased travel demand;
- the total number of 12 courses during rush hour (7 am–8 am) are performed in each scenario;
- one location of the vehicle's depot is suggested for each scenario (a'priori assumed), however, the location at S1 and S2 (l = 6) is different than S3 (l = 5);
- along with the increase of traffic volume over different time horizons (S1, S2 and S3 respectively), and locations of vehicle's depot, the total transport cost is increased too; the value varies from 1,243 to 1,360 [zł/h], depending on scenarios.

Table 3. Scenario-based final results of MTLC&VDL mixed decision problem

Results		Scenarios		
Name	Unit	S1	S2	S3
Total number of lines	[items]	8	8	8
Line's numbers*	[-]	{3, *5, 7, 11, 12*, 17, 18, *21*}	{3, *5, 7*, 10, *11, 12*, 18, *21*}	{*5, 7*, 10, *11, 12*, 15, 17, *21*}
Fleet size	[veh.]	8	8	9
Courses	[items/h]	12	12	12
Depot location (l=)	[-]	6	6	5
Objective function C	[zł/h]	1,243.0	1,246.9	1,360.1

* line's numbers written by italic are common set for scenarios S1, S2 and S3

3. Conclusions

3.1. Research findings

In the paper, the mixed mass transit line construction and vehicles' depots location decision problem (MTLC&VDL) has been considered. The research presented in this paper has been carried out based on extensive research methodology that is a consecutive step of the work previously undertaken by its authors [13, 14].

The extension of the research is a scenario-based and iteratively repeated solving of the decision problem. Each considered scenario, incl., S1, S2 and S3, has been characterised by a different time horizon (S1 is a current state, S2 and S3 are long-term horizons), and diversified travel demand (S1 – current demand, S2 and S3 – demand increased by 5 and 10% with reference to S1, respectively). As a result of the performed computations, several methodological conclusions have been formulated.

Planning the structure of transport lines, together with the location of the depots for serving the fleet operated on those lines, traffic modelling with anticipated long-term travel demand changes should be performed. Thanks to this, it is possible to determine a resilient solution in the scope of: structure of the lines and corresponding frequency, fleet size, and location of the depot. It also can be stated that the performed calculations have proved a high sensitivity of the mixed MTLC&VDL decision problem of changing the decision situation.

3.2. Further research

Further research related to the mixed MTLC & VDL decision problem will be conducted bi-directionally. On the one hand, research will be carried out related to the evaluation of the simultaneously changed travel demand and supply as well (including, the redefined key parameters of transport infrastructure). On the other hand, it is planned to develop research towards linking the mixed MTLC & VDL decision problem with another separate decision problem, i.e. fleet composition. Thanks to the simultaneously solved, new mixed decision problem of this type, it will be possible to determine the degree of fleet differentiation, which will be adjusted to the changing travel demand in the considered area.

Acknowledgments

The research presented in the paper has been partly funded by the Ministry of Science and Higher Education, Republic of Poland (grant no. 05/51/DSPB/3524). The support is gratefully acknowledged.

References

[1] Abdallah T., *Sustainable mass transit. Challenges and opportunities in urban public transportation*, Elsevier, Amsterdam, Oxford, Cambridge MA, 2017.

[2] Baaj M.H., Mahmassani H.S., A*n AI-based approach for transit route system planning and design*, Journal of Advanced Transportation, 25/1992, 187-210.

[3] Canca D., Barrena E., *The integrated rolling stock circulation and depot location problem in railway rapid transit systems*, Transportation Research Part E: Logistics and Transportation Review, 109/2018, 115-138.

[4] Cancela H., Mauttone A., Urquhart M.E., *Mathematical programming formulations for transit network design*, Transportation Research Part B, 77/2015, 17-37.

[5] Ceder A., *Public transit planning and operation: Theory, modeling and practice*, Butterworth-Heinmann, Elsevier Ltd, Oxford 2007.
[6] Dial R.B., Bunyan R.E., *Public transit planning system*, Socio-Economic Planning Sciences, 1, 1968, 345-362.
[7] Dubois D., Bel G., Libre M., *A set of methods in transportation network seethes and analysis*, Operations Research, 30/1979, 797-808.
[8] FHWA, Mitigating Traffic Congestion-The Role of Demand-Side Strategies, prepared by ACT, Report No. FHWA-HOP-05-001, October 2004.
[9] Hamdouni M., Desaulniers G., Soumis F., *Parking buses in a depot using block patterns: A Benders decomposition approach for minimizing type mismatches*, Computers and Operations Research, 34 (11)/2007, 3362- 3379.
[10] Hamdouni M., Soumis F., Desaulniers G., *Parking buses in a depot with stochastic arrival times*, European Journal of Operational Research, 183 (2)/2007, 502-515.
[11] Kupka P., Sawicki P., *Optymalizacja lokalizacji zajezdni tramwajowej w systemie komunikacji miejskiej*, Logistyka, 2/2015, 462-472.
[12] Lownes N., Machemehl R.B., *Exact and heuristic methods for public transit circulator design*, Transportation Research, Part B, 44 (2)/2010, 309-318.
[13] Sawicki P., Fierek S., *Problem jednoczesnego wyznaczania przebiegu linii i lokalizacji zajezdni w systemie transportu zbiorowego*, Prace Naukowe Politechniki Warszawskiej – Transport, 119/2017, 429-444.
[14] Sawicki P., Fierek S., *Mixed public transport lines construction and vehicle's depots location problems*, [in:] Macioszek E., Sierpiński G., (eds.), *Recent Advances in Traffic Engineering and Transport Networks and Systems*, TSTP 2017, Lecture Notes in Networks and Systems, Springer, 21/2018, 213-224.
[15] Schöbel A., *Line planning in public transportation: models and methods*, OR Spectrum, 34/2012, 491-510.
[16] Szeto W.Y., Wu Y., *A simultaneous bus route design and frequency setting problem for Tin Shui Wai, Hong Kong*, European Journal of Operational Research, 209 (2)/2011, 141-155.
[17] Teodorović D., Janić M., *Transportation engineering. Theory, practice and modeling*, Elsevier Inc., Oxford, Cambridge, MA, 2017.

If you want to quote this article, its proper bibliographic entry is as follow: Piotr Sawicki, Szymon Fierek, *The impact of long-term travel demand changes on mixed problems of mass transit lines construction and vehicles' depots location*, Technical Transactions, Vol. 6/2018, pp. 103-112.

TECHNICAL TRANSACTIONS 6/2018
CIVIL ENGINEERING
DOI: 10.4467/2353737XCT.18.091.8696
SUBMISSION OF THE FINAL VERSION: 12/06/2018

Anna Sołtys (soltys@agh.edu.pl)
Józef Pyra
Michał Twardosz
AGH University of Science and Technology

Control of the vibration structure induced during works with the use of explosives

Sterowanie strukturą drgań wzbudzanych w czasie robót z użyciem MW

Abstract

This article presents the results of research on controlling the structure of vibrations induced during the firing of explosives with the use of non-electrical and electronic systems and the influence of the vibration structure during a transition from the ground to the building. The use of procedures associated with the selection of millisecond delay for firing explosive charges during blasting allows to get the excitation of favourable structure vibrations, thanks to a strong damping which is obtained at the transition from the ground to the structure. This means that optimally designed blasting works do not have to limit the mass of the explosives in the borehole as well as their number.

Keywords: Open-pit mining, blasting technique, millisecond blasting, vibration structure, impact of vibrations on buildings

Streszczenie

W artykule przedstawiono wyniki badań nad sterowaniem strukturą drgań wzbudzanych w czasie odpalania ładunków MW z zastosowaniem systemów nieelektrycznych i elektronicznych oraz wpływem struktury drgań na interakcję układu budynek–podłoże. Zastosowanie do projektowania robót strzałowych procedur związanych z doborem opóźnienia milisekundowego do odpalania ładunków MW, pozwala na wzbudzanie drgań o korzystnej strukturze, dzięki czemu uzyskuje się silne tłumienie przy przejściu z podłoża do obiektów. Oznacza to, że optymalnie zaprojektowane roboty strzałowe nie muszą ograniczać masy ładunków MW w otworze oraz ich liczby..

Słowa kluczowe: górnictwo odkrywkowe, technika strzelnicza, strzelanie milisekundowe, struktura drgań, oddziaływanie drgań na zabudowania

1. Introduction

The use of explosives in the process of mining rock deposits is a source of vibrations, especially when using explosive charges in long holes; this may have an affect on the buildings in the vicinity of an open-pit mining excavation. The aim of each mining plant is, on the one hand, to minimise this impact and, on the other hand, to use large masses of explosives for blasting as this ensures a reduction in the costs of blasting. The introduction of modern explosives, the mechanical loading of explosives for use in blast holes, and both non-electrical and electronic firing systems creates the possibility to carry out blasting works in a manner which is both appropriate and safe for the environment.

Blast-induced vibrations have an important feature, which is the ability to precisely determine the timing of events (the timing of the firing of charges is human determined) as well as their intensity (changes in mass of the applied charges) and structure (e.g. the use of various delays between successive charges). In the case of an earthquake or a shock induced by underground exploitation, it is difficult to predict the time of occurrence, and even more so its intensity and structure as it is an incident associated with the forces of nature.

The nature of research into the vibrations is related to activities aimed at minimising their impact on the environment. These actions, in the case of blasting works in open-pit mining, are aimed at controlling the source on the one hand and reducing the energy of vibrations transmitted from the ground to protected objects on the other [1, 3, 4, 9, 10, 16, 17, 20].

The minimisation of the vibration impact on the environment is achieved by activities at the stage of design. These are primarily based on knowledge of the technologies of the performed blasting works and the increasingly accurate identification of the nature of the propagated vibrations with simultaneous assessment of their impact on objects in the vicinity.

Specifically, the following points are important in the context of minimising the impact of vibrations on the environment:

1) recognition of the nature of the construction in the vicinity of the work site;
2) recognition of the vibration source, taking into account the condition of works and the path of vibration propagation from source to objects;
3) recognition of the mechanism of vibration transmission from the ground to the foundations of the object;
4) assessment of the impact of blasting works on the objects;
5) determination of conditions for the safe execution of the blasting works;
6) documentation of the impact by control measurements or vibration monitoring.

Analysis of the scope of work envisaged in the abovementioned points allows for the following division: points 1 to 4 prepare the basis for the implementation of point 5; point 6 is the control of the implementation of point 5. At the same time, it is important to be aware that all points are active and influence each other. Their dynamic relationship do not make it possible to say that everything has already been performed and will be continued in future years.

The dynamic variability of parameters determined in particular stages abovementioned is mainly generated in the source of vibrations, their propagation and their transfer mechanism from ground to objects, i.e. in the context of points 2 and 3. The reason for these dynamic

changes is, on the one hand, a change in the geological conditions at the location of the blasting works (shifting of exploitation fronts) and, on the other, technical progress in the execution of blasting works, i.e. the development of new explosives and new precision systems for initiating charges. In addition, thanks to the use of modern analytical apparatus which enables the study of the structure of vibrations, knowledge of both the propagation of vibrations and the interaction of the building-ground transition mechanism is better today and allows for more accurate conclusions.

Environmentally safe blasting works are primarily associated with the determination of permissible explosive charges and their possible use. Determination of the permissible charges is a basic activity, but must be performed with consideration to the manner in which the works are to be executed and certainly, by the determination of the implementing conditions for which the restrictions have been introduced.

As mentioned above, one of the points implemented in the preventative strategy is to identify the source of vibration. Today, we are able to go further than that – to recognise the possibility of controlling the source of vibration, i.e. how to design the presented source in order to achieve the best possible mining effect and at the same time minimise the impact of vibrations on the surrounding buildings. In blasting works, designing a source means selecting the geometric parameters of the blasting pattern and individual blast holes, and the selection of the mass and number of charges fired with a deliberately selected millisecond delay.

The impact of blasting work on buildings depends on the intensity of the induced vibrations and their frequency; both parameters can be adjusted by changing the parameters of the source. In terms of the assessment of the impact on the structure, it should also be remembered that the final effect taken into account is the vibration of the foundation, not the ground.

The aim of this article is to demonstrate the possibility of using modern blast control apparatus to control the structure of the induced vibrations and to indicate new possibilities for reducing the seismic effect of blasting.

2. Evaluation of the impact of vibrations on buildings in the vicinity of the excavation site

In order to assess the impact of vibrations induced by blasting works, the guidelines of PN-B-02170:2016-12 standard [8] are used. The approximate characteristics of the harmfulness of vibrations according to this standard can be presented using the dynamic SWD scale.

The frequency of vibrations plays an important role in assessing the impact using SWD scales. To illustrate this problem, Fig. 1 shows the SWD I scale, on which the limit values are applied, taking the B limit as the acceptable vibration velocity level. For example, the frequencies selected are 25 Hz, 10 Hz, 5 Hz and 2 Hz [19] and the allowable vibration velocity values are 0.62 mm/s, 1.6 mm/s, 3.0 mm/s and 50.0 mm/s, respectively. As can be observed, the difference in vibration velocity is very high; for extreme frequency values, this amounts to an 80-fold difference.

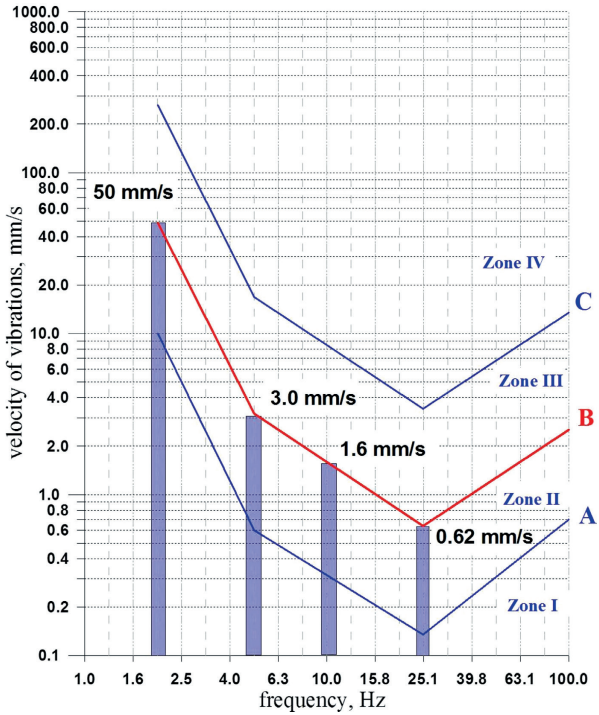

Fig. 1. SWD I scale – specific values of permissible vibration velocities for the frequencies of 25, 10, 5 and 2 Hz [19]

In many pieces of research [5, 6, 9, 17, 18], it has been proven that the applied millisecond delay has a significant influence on the structure of vibrations induced during the firing of charges. This means that by choosing a millisecond delay, it is possible to change the frequencies of propagated vibrations in the substrate and thus influence the degree of vibration transmission to the building structure.

When determining the conditions of the environmentally safe execution of blasting works, it should not be ignored that in most cases, propagation equations are determined for the ground, i.e. for vibration propagation through the ground. However, buildings on this ground are protected. This means that an important element of the procedure is to identify the interaction between the building and the groundborne vibrations. Thus, the problem of vibration frequency, i.e. the structure of vibrations induced in the substrate, again applies. It can be assumed that the vibration during the transition from the ground to the foundation of the building is more or less dampened. The frequency of vibrations is also modified and in most cases, the higher frequencies do not transfer to the foundations of the building. Frequency modification and attenuation in the lower frequency range is negligible [5, 6, 9, 17].

As a result of the factors presented above, research of the interaction between the building and the foundations should be conducted which takes into account the structure of vibrations of both the ground and the foundations of the building. Figure 2 shows the structure of the ground and foundation vibrations, recorded during the firing of a blasting pattern with a delay

of 20 ms in the limestone mine. In this case, by introducing a 20 ms delay (electronic firing), very strong vibration damping was achieved. While controlling the source, vibrations were induced in the substrate, the intensive high-frequency phase of which was dampened during the transition to the foundation and thus, without reducing the mass of charges, the impact on the buildings was minimised. The applied delay (electronic firing) induced vibrations in the ground, where the frequency of 50.12 Hz was predominant and had a value close to the frequency of the millisecond delay.

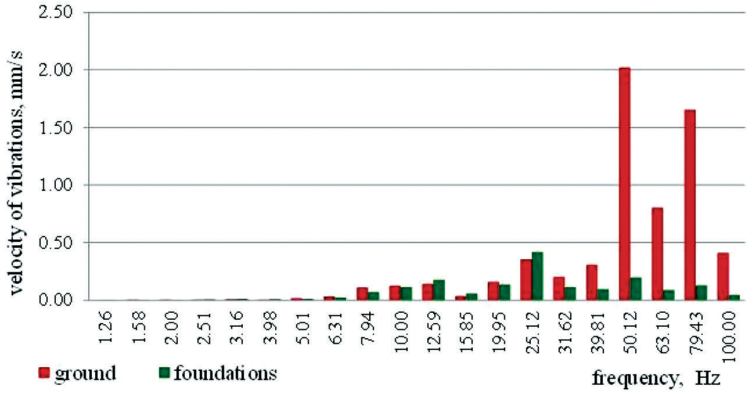

Fig. 2. Interaction of ground to foundation vibration transition system – limestone mine – delay 20 ms

Figure 3 shows the structure of ground and building vibrations recorded when firing the blasting pattern inside a dolomite mine with a delay of 67 ms (non-electric firing). As with the 20 ms delay, the applied delay induced vibrations in the ground, where the frequency of 15.85 Hz is predominant and it has a value close to the frequency of the millisecond delay (at 67 ms delay, MW charges were fired at 14.92 Hz).

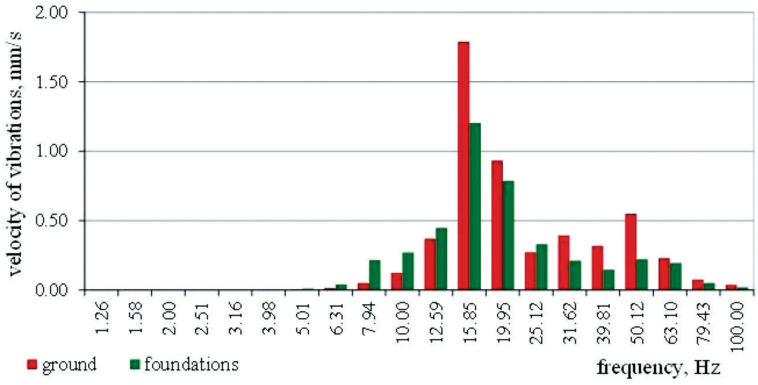

Fig. 3. Interaction of ground to foundation vibration transition system – dolomite mine – delay 67 ms

As Fig. 3 shows, during the transition to the foundation, the dominant frequency vibrations were suppressed by a small percentage, and the modification of the vibration structure was negligible. Comparing Figs. 2 and 3, it can be observed that there is a strong dependence of damping on the vibration structure propagated by the substrate. Higher frequencies, in the case of the 20 ms delay, were completely suppressed, while in the case of the 67 ms delay, the frequencies were unchanged, although the vibration intensity on the foundation was lower.

Modification of the vibration structure during the transition from the ground to the foundation must be taken into account as Polish standard [8] allows for evaluation based on the vibration recorded on the foundation. In other countries, the assessment is based on substrate vibrations and therefore, when making comparisons, conditions of the applicability of individual standards must be clearly identified.

3. Millisecond firing of charges

Since there was a possibility of changing the delay between the charges being fired in individual blast holes, the influence of the time delay between detonations of charges on the effect of blasting works was investigated. As early as 1940–1950, as a result of research conducted in the United States, millisecond firing was recognised as a technique for blasting works which reduced vibrations and allowed the obtaining of a mining product with the desired fragmentation [2, 7].

Siskind [8] writes about the criterion of 8 ms as the minimum time between charges which allows us to speak of millisecond firing. He also mentions that the genesis of this criterion is not fully known and cites the results of studies [7] for which the following delays were used: 0, 9, 17 and 34 ms.

In papers [11–13], the authors prove that the criterion of 8 ms is not always justified in all cases. In a substrate with low frequencies of approximately 10 Hz, a delay close to 8 ms increases the intensity of the recorded vibrations and the actual delay should be around 60 ms.

In [11], the authors state that the time delay should be within half of the interval of the dominant frequency, whereas Siskind in [14], who is also a co-author of the work [11], suggests that the delay should not be less than one quarter of the dominant frequency of vibrations.

Currently, three systems are used in open-pit mining for initiating charges: electric, non-electrical and electronic. The development of initiation systems is moving in the direction of increasing safety, increasing the accuracy of set delays and offering more and more options for selecting delays. It can be said that the Polish market is dominated by non-electrical systems (Euronel, Exel, Indetshock, Nitronnel, Rionel) and electronic (Ergonic, E*star, Hot Shot, i-con, Riotronic, UniTronic 600) systems offered by several foreign and domestic manufacturers.

In the case of non-electrical systems, when designing the blasting pattern and selecting millisecond delays for individual charges, it should be remembered that the delay between charges is equivalent to a connector delay only in case of charges arranged in one row series and fired with a breaking in the hole/snubber. In any other case, the actual initiation time of individual charges must be calculated and on this basis, it is possible to determine the actual millisecond delay.

For example, Fig. 4 shows a schematic connection diagram of 30 charges in three rows with 25 ms and 42 ms connectors. The actual millisecond delays achieved are significantly different from the nominal times of the applied connectors; in 80% of cases, the delay between MW charges was 8 and 9 ms (Fig. 5).

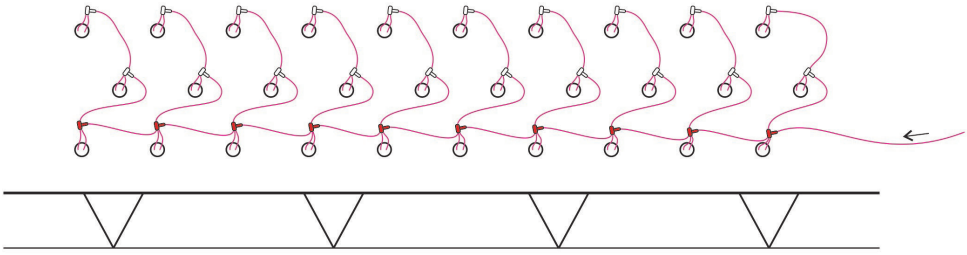

Fig. 4. Connection of the 30 MW charges arranged in three rows (25 and 42 ms connectors)

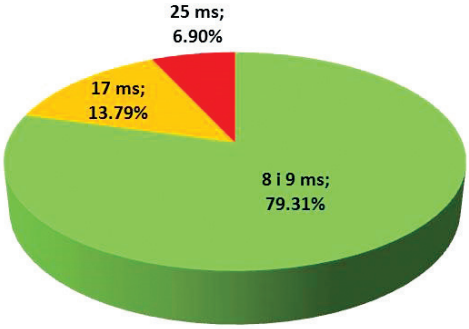

Fig. 5. Actual time of millisecond delays for the connections shown in Fig. 4

In the case of the initiation of charges with an electronic system, there are no problems with the selection of delays in multi-row blasting patterns. Each detonator can be given any delay in the range from, for example, 1–15000 ms (each manufacturer offers a slightly different range), i.e. only the blasting engineer's knowledge and connection influence the selection (Fig. 6).

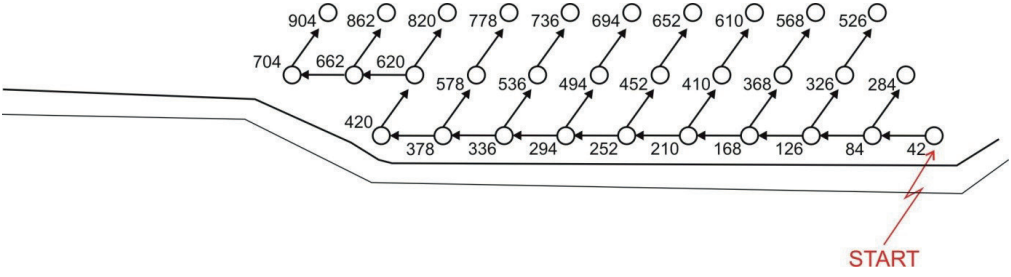

Fig. 6. Connection of the openings net using the electronic system

4. Effect of milliseconds delay time on vibration structure$_t$

As has already been mentioned, modern initiation systems, characterised by the high precision of pre-set millisecond delays, give a wide range of possibilities for selecting the duration of these delays, taking into account local geological and mining conditions. The use of an electronic system for firing the multi-row blasting patterns requires optimal design with regard to millisecond delays, which on the one hand will allow the obtaining of an appropriate granulation of the blasting product, and on the other, will ensure minimisation of the impact of the detonation of charges on the environment [15].

The selection of the optimum millisecond delay for a given set of conditions, especially in the case of multi-row patterns, requires IT support, i.e. the application of IT software for the purpose of designing. The basic information required for these programmes is:

- the location of a blast hole series and the location of protected objects;
- the parameters of the planned blasting with regard to length of the holes, their number and location, burden, distance between holes and rows, weight of explosive charge in the hole, length of stemming and rebore;
- a recording of the vibrations induced by firing a single charge at a location close to the area of the planned blasting pattern (using the Signature Hole method);
- an indication of the seismic effect of the given series at a similar location.

Based on this data, the program calculates a prediction of the seismic effect and proposes a number of solutions, from which the system operator can choose the optimal solution.

In one of the quarries (Mine A), an experimental blasting using an electronic initiation system was performed in order to minimise the impact of blasting works on the surrounding buildings.

The first blasting was prepared using experience from blasting with the use of a non-electrical system, without software support. The distribution of the achieved millisecond

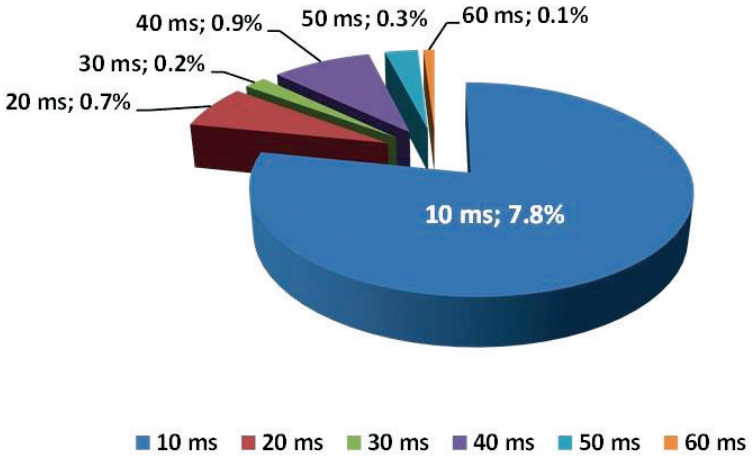

Fig. 7. Distribution of millisecond delays – testing series

delays is shown in Fig. 7 – almost 80% of the charges were detonated with a delay of 10 ms. Figures 8 and 9 show the seismogram and structure of vibrations recorded on the ground and on the building foundation (position 2 and 2'). Figures 8 and 9 show that 12.59 Hz and 15.85 Hz are the predominant frequencies in the ground and on the foundation of the building. Vibration damping is also observed when vibrations pass from the ground to the foundation at a level of 20% to 50% (within the dominant frequencies).

In the next stage of research, blasting design was introduced with the use of software in which the algorithm provides the formation of a database based on the Signature Hole method. The analysis of seismograms of vibrations obtained during the firing of individual charges indicated the possibility of shifting the frequency of vibrations propagated by the ground to the range of higher values (50 Hz to 100 Hz). The performed seismic simulations confirmed this observation; this allowed the design and execution of dozens of experimental and production blasts within a period of three years.

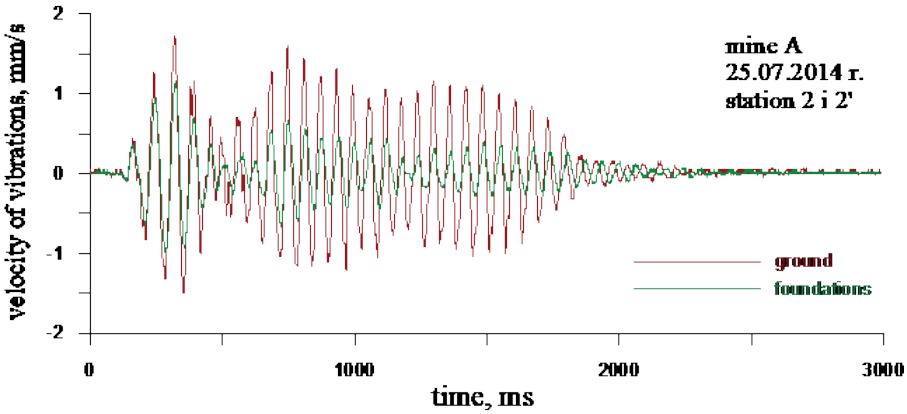

Fig. 8. Seismogram of ground and foundation vibration – component *x* – testing series

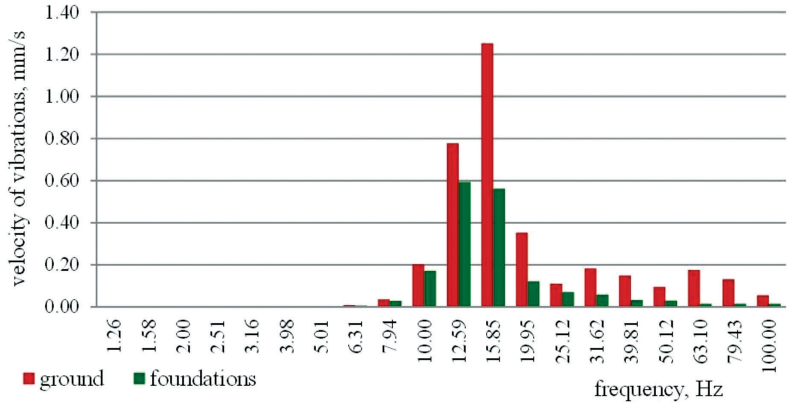

Fig. 9. The structure of ground and foundation vibration – component *x* – testing series

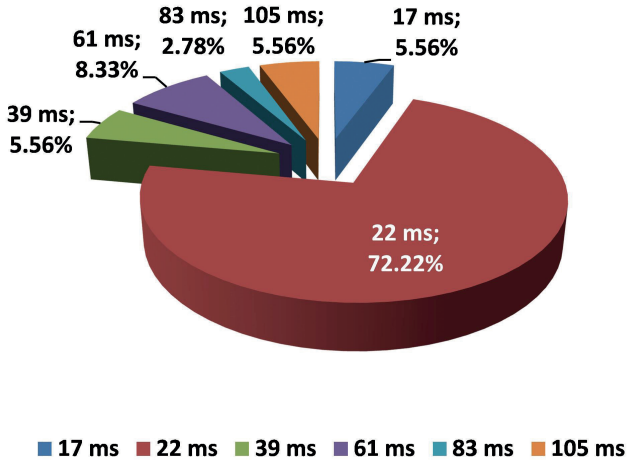

Fig. 10. Distribution of millisecond delays – production series

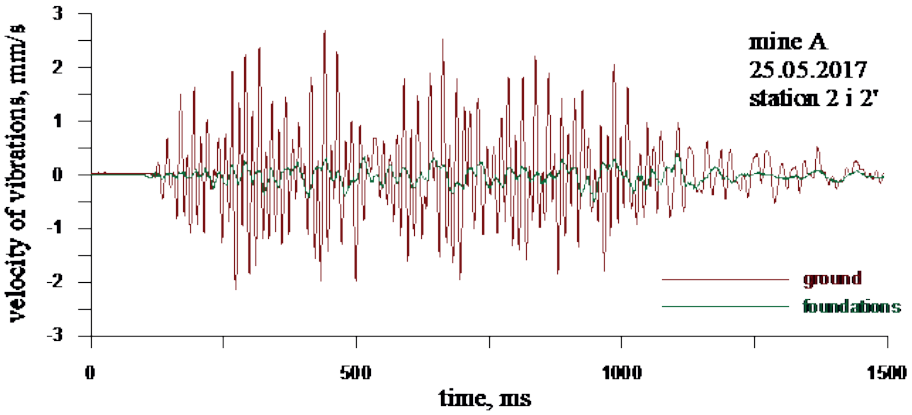

Fig. 11. Seismogram of ground and foundation vibration – component *x* – production series

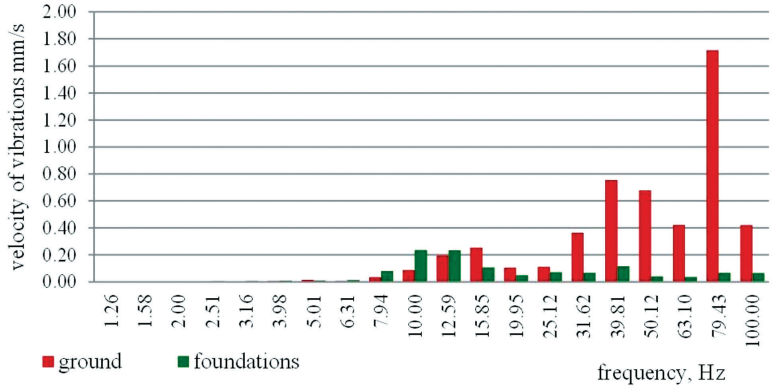

Fig. 12. Structure of ground and foundation vibration – component *x* – production series

Figures 10, 11 and 12 show the results of a seismic analysis for a production series located close to the first testing series. The measurements were taken on the ground and on the foundations of the building and the result of the analysis was presented in the same way as in the figures above. As a result of software simulation, a delay pattern was used. This resulted in more than 70% of the actual delay time of 22 ms, which is more than double that of the experimental series.

It should be added that in the production blasts, the charge weight per millisecond was increased by 30% and the analysed design was characterised by the highest intensity of blasting in 2017 on the first level 'Ia' in mine A.

Comparing the structure of the recorded vibrations (Figs. 9, 12) it can be noted that due to the use of a proper millisecond delay time, a complete change in the structure of vibrations in the substrate was achieved. A shift of frequencies dominating in the range of higher values occurred and this contributed to a significant increase in vibration level damping during the transition to the foundations of the building. In the range of frequencies dominating in the structure of foundation vibrations, the intensity has been reduced threefold.

The assumed effect of the studies was to minimise the impact of blasting works on the environment; therefore, Fig. 13 presents a comparison of the vibration impact assessment for the analysed series with the application of the SWD-I scale from Polish standard [8]

a) test series

b) production series

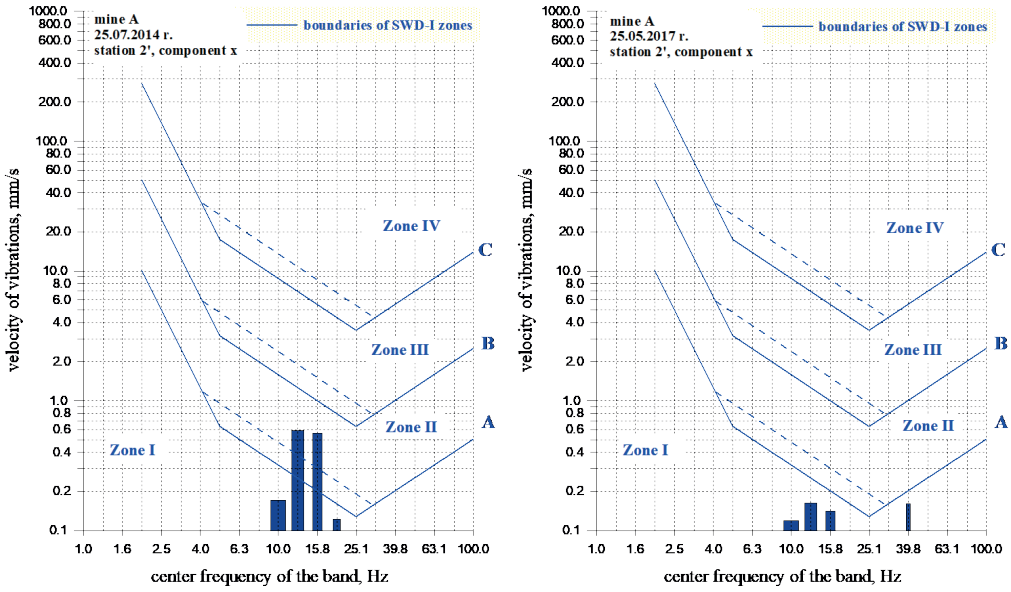

Fig. 13. Comparison of the assessment of blasting works influence on the environment – component *x* – testing series and production series

5. Summary

The impact of vibration induced by blasting works on buildings continues to be a problem that requires a prudent approach and a compromise between protecting the interests of mines and those of local communities.

The implementation of modern firing systems to blasting works in open-pit mining increases the possibility to control the undesirable seismic effects. Minimisation of the impact of blasting works on structures in the environment can be achieved not only by limiting the mass of explosives, but also by the skilful selection of millisecond delays. This allows for the modification of the frequency structure of the vibrations in the direction of increasing the attenuation when vibrations transfer from the ground to building foundations.

It should be noted that the implementation of modern firing systems does not always have the desired effect in all conditions. It is necessary to be aware that the number of factors influencing the impact of vibrations on objects requires mindfulness and knowledge based on reliable research, which is best evidenced by the effect obtained in the analysed experimental series.

References

[1] Baulovič J., Pandula B., Kondela J., *Research on the millisecond delay blasting impact in order to minimize seismic effects in Kučín quarry surrounding,* High-Energetic Materials 7/2015, p. 5-13.

[2] Duvall W.I., Johnson C. F., Mayer A. V. C., Devine J. E., *Vibrations From Instantaneous and Millisecond – Delayed Quarry Blast,* U. S. Bureau of Mines RI 6151, 1963.

[3] Kondela J., Pandula B., *Timing of quarry blasts and its impact on seismic effects,* Acta Geodyn. Geomater., Vol. 9, No. 2 (166)/2012, p. 155-163.

[4] Kuźniar K., Chudyba Ł., *Wykorzystanie sieci neuronowych do prognozowania przekazywania drgań wzbudzanych wstrząsami górniczymi z gruntu na budynek*, Technical Transactions vol. 3-B/2010, p. 109-117.

[5] Maciąg E., Winzer J., Biessikirski R., *Metodyka postępowania w ochronie otoczenia w przypadku robót strzałowych*, Bezpieczeństwo Pracy i Ochrona Środowiska w Górnictwie – Miesięcznik WUG, 9/I/2007, p. 56-60.

[6] Maciąg E., Winzer J., Biessikirski R., *Współdziałanie niskich budynków z podłożem w przypadku strzelań MW w kamieniołomach*, Warsztaty Górnicze – PAN – IGSMiE, nr 69/2007, p. 297-308.

[7] Nicholson H. R., Johnson C. F., Duvall W. I., *Blasting Vibration and Their Effects on Structures*, U. S. Bureau of Mines Bulletin 656, 1971.

[8] PN-B-02170:2016-12 Ocena szkodliwości drgań przekazywanych przez podłoże na budynki.

[9] Pyra J., *Wpływ wielkości opóźnień milisekundowych na spektrum odpowiedzi drgań wzbudzanych detonacją ładunków materiałów wybuchowych*, Wyd. AGH, Kraków 2017.

[10] Pyra J., Sołtys A., *Method for studying the structure of blast – induced vibrations in open – cast mines*, Journal of Vibroengineering, Volume 18, Issue 6, September 2016, p. 3829-3840.
[11] Siskind D. E., Crum R. E., Otterness R. E., Kopp J. W., *Comparative Study of Blasting Vibrations From Indiana Surface Coal Mines*, U. S. Bureau of Mines RI 9226, 1989.
[12] Siskind D. E., Stachura V. J., Nutting M. J., *Low-Frequency Vibrations Produced by Surface Blasting Over Abandoned Underground Mines*, U. S. Bureau of Mines RI 9078, 1987.
[13] Siskind D. E., Stagg M. S., Kopp J. W., Dowding C. H., *Structure Response and Damage Produced by Ground Vibration from Surface Mining Blasting*, U. S. Bureau of Mines RI 8507, 1989.
[14] Siskind D. E., *Vibrations from blasting*, ISEE, Cleveland 2005.
[15] Sołtys A., Gołąbek B., Żołądek T., *The application of Austin Powder Company IT systems to optimize the firing of multiple-row patterns using E*Star electronic detonators,* Inżynieria Mineralna, R. XVIII, Nr 2/2017, p. 225-235.
[16] Sołtys A., Pyra J., Winzer J., *Analysis of the blast-induced vibration structure in opencast mines,* Journal of Vibroengineering, Volume 19, Issue 1, February 2017, p. 409-418.
[17] Sołtys A., Winzer J., Dworzak M., *Dobór optymalnego opóźnienia milisekundowego – studium przypadku*, Konferencja: Technika Strzelnicza w Górnictwie i Budownictwie, Ustroń 2015, p. 225-236.
[18] Sołtys A., Winzer J. Pyra J., *Badania efektu sejsmicznego a nowoczesne systemy odpalania ładunków MW*, Przegląd Górniczy, t. 71, nr 9/2015, 69-77.
[19] Winzer J., *Przyczynek do dyskusji o sposobach minimalizacji oddziaływania robót strzałowych na zabudowania w otoczeniu*, Materiały Konferencyjne: Technika Strzelnicza w Górnictwie i Budownictwie, Ustroń 2013, ART.-TEKST, Kraków 2013, p. 347-361.
[20] Winzer J, Sołtys A., Pyra J., *Oddziaływanie na otoczenie robót z użyciem materiałów wybuchowych*, Wydawnictwa AGH, Kraków 2016.

TECHNICAL TRANSACTIONS 6/2018
ELECTRICAL ENGINEERING
DOI: 10.4467/2353737XCT.18.092.8697
SUBMISSION OF THE FINAL VERSION: 27/05/2018

Andrzej Bień
Faculty of Electrical Engineering Automatics Computer Science and Biomedical Engineering, AGH University of Science and Technology

Edward Layer (elay@pk.edu.pl)
Faculty of Electrical and Computer Engineering, Cracow University of Technology

Active power measurement based on digital processing of voltage and current signals

Wykorzystanie cyfrowego przetwarzania sygnałów do pomiaru mocy czynnej

Abstract

The concept of active power measurement based on real-time digital processing of voltage and current signals is best' introduced with a digital approximation definition . In this paper, the authors propose an integral calculation method based on Gregory's expression, correction of integration period estimation and integration result correction taking values related to the ends of the integration period into account. In the described method, the integral is calculated between two consecutive maximums of the voltage and current product.. Digital dependencies that are easy to implement are used for the evaluation of the active power value. To measure the voltage and current signals, the authors used a system with a digital signal processor and an A/D converter with a multiplexer followed by dedicated digital filters. The active power measurement method was checked by building an instrument simulation model.
Keywords: active power, digital filtering FIR

Streszczenie

Pomiar mocy czynnej za pomocą systemu pomiarowego realizującego przetwarzanie sygnałów napięcia i prądu w sposób cyfrowy wymaga przybliżenia zależności definicyjnych. W artykule zaproponowano wykorzystanie wzoru Gregoriego dla celów obliczenia całki w zależności definicyjnej mocy czynnej. Dodatkowo proponowana jest poprawka związana z wyznaczaniem przedziału całkowania i dotyczy wyznaczania maksimów sygnałów. Drugim proponowanym rozwiązaniem jest użycie jednego przetwornika A/C z multiplekserem, a następnie użycie filtrów cyfrowych w celu wyrównania opóźnień pomiędzy próbkowanymi sygnałami. Proponowane rozwiązania umożliwiają zbudowanie prostego systemu pomiarowego pracującego w czasie rzeczywistym.
Słowa kluczowe: moc czynna, filtr cyfrowy FIR

1. Active power evaluation from samples of voltage and current signals

Active power is one of the most frequently measured electrical values. The value of this power is especially helpful in the measurement of the voltage and current values, mainly in the field of simplifying their calculations. The definition of the active power for the finite-duration of signals relating to voltage and current is as follows:

$$P = \frac{1}{t_b - t_a} \int_{t_a}^{t_b} u(t) i(t) dt \tag{1}$$

where: (t_a, t_b) – time interval of voltage $u(t)$ and current $i(t)$ observation

Digital implementations of the Eq.(1) is based on the adding up of samples of voltage u_k and current i_k signals, [3]. This means calculating the integral Eq.(1) as adding products of voltage and current samples and can be realised by means of any method of numerical integration e.g. by rectangles method. Simple algorithm is easy to implementation but the integration limits with resolution referred to the sampling period leads to relatively large calculation errors. These errors are limited by reducing the sampling period which leads to a demand for greater computing power provided in aquisition card and fast A/D converters. It is also possible to determine the integral Eq.(1) applying more complex algorithms e.g. the trapezoidal algorithm [1, 2]. However, it is worth to nothing here that method based on many nodes is leading to an equally simple algorithm as the method of rectangles [4, 7]. Based on [4, 5, 7] an even more accurate method of setting the integral from the relation Eq.(1) was suggested using Gregory's interpolation formula:

$$K = \Delta t \cdot \left[\frac{9}{24} u_0 i_0 + \frac{28}{24} u_1 i_1 + \frac{23}{24} u_2 i_2 + u_3 i_3 + \cdots + u_{N-3} i_{N-3} + \frac{23}{24} u_{N-2} i_{N-2} + \frac{28}{24} u_{N-1} i_{N-1} + \frac{9}{24} u_N i_N \right] \tag{2}$$

where: Δt – sampling period of voltage and current signals.

The method significantly improves the accuracy of the calculation of the integral, for example [5, 7], but for high accuracy of the calculation of active power Eq. (1), it is also necessary to determine the range (t_a, t_b) more precisely. For this purpose, the choice of integration ranges between consecutive maximums of signals $u(t)$ and $i(t)$ and the correction considering the field between estimates of maximum and sampling places are proposed. This correction is presented in Fig. 1.

Places in which the maxima appeared were fixed by appointing their estimates $\tilde{t}_{\max}$ as the values of the maxima of parabolas passing through the three nearest registered points Eq. (3):

$$\tilde{t}_{\max} = \frac{\Delta t}{2} \cdot \frac{p(n_{\max} - 1) - p(n_{\max} + 1)}{p(n_{\max} + 1) - 2p(n_{\max}) + p(n_{\max} - 1)} \tag{3}$$

where: $n_{\max}$ – place where the maximum appears $p(n_{\max}) = u_{\max} \cdot i_{\max}$.

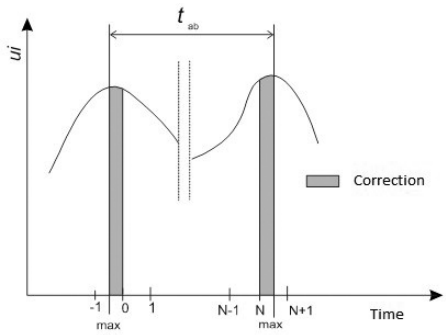

Fig. 1. Method of active power measurement (1) with correction

Correction including the displacement of the maximum with regard to sampling moments is received from the following relation (4):

$$k = \frac{p(n_{\max})}{2} \cdot \frac{p(n_{\max}-1) - p(n_{\max}+1)}{p(n_{\max}+1) - 2p(n_{\max}) + p(n_{\max}-)} \tag{4}$$

Using Eqs. (2), (3), (4) we receive the following active power formula:

$$P = \frac{1}{\tilde{t}_{mx2} - \tilde{t}_{\max 1}} \left(k_1 + k_2 + K\right) \tag{5}$$

The algorithm that determines the active power from formula (5) is as follows:

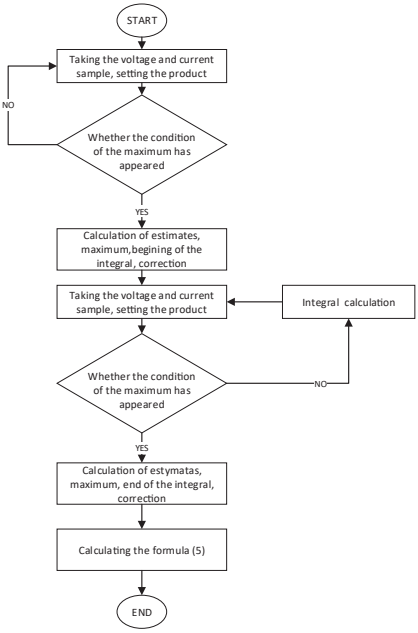

Fig. 2. Active power measurement algorithm according to Eq. (5)

The loop is used to set the integral for the sample indicator from 3 to N-3; however, the beginning and the end of formula Eq. (3) is determined in the part in which correction, associated with the estimation of the maxima, is calculated.

2. Execution of active power measurement

Measurement of the active power according to Eq. (5) requires obtaining the sequence of the voltage and the current samples that are taken at the same time. This is possible with some measuring instruments which simultaneously samples two signals. A/D converter and a multiplexer present construction of such an equipment.

Unfortunately, there is a problem referring to the time delay between samples of voltage and current. In order to avoid this problem the measurement of voltage and current signals in identical time intervals Δt was proposed.

It is worth noting here that measurement is simple for hardware implementation and, in addition, it does not impose a large dynamic requirements on the multiplexer. The synchronisation of samples is achieved by using digital filters with finite and symmetrical impulse responses [6]. A flowchart of the active power measurement with the used filters is presented in Fig. 3.

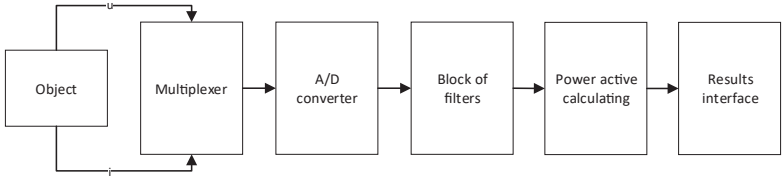

Fig. 3. Active power measurement with a single A/D converter with a multiplexer

3. Model testing

Prior to the construction of the device, the presented algorithm for active power measurement was tested by performing a sequence of experiments on the simulation model. The Matlab environment was used for testing of the model. After checking the correctness of the model, the device was able to measure the active power. In the second step, research was conducted in order to determine both the measurement accuracy and the influence on the accuracy of structural parameters.

Researches were carrying out for one sampling rate of 1 kHz signals. Depending on the chosen method of power calculation 1 kHz signal requires 2 kHz A/D converter which is critical condition of the program as the measurement should be made in time smaller than 500 μs. A sinusoidal signal was used as a test signal. The defined error during testing was calculated from the following relation:

$$\delta = \left| \frac{P_d - P_w}{P_z} \right| \tag{6}$$

where:
P_d – active power determined on the basis of the definition (1),
P_w – active power determined during simulation,
P_z – active power value corresponding to the range of tested model.

It can be observed that the measurement error decreases as the number of bits of the converter increases; however, this decline becomes insignificant as the number of bits gets to twelve or more. A small value of error of less than 0. 5%, even for small number of bits, is the result of averaging properties of integration arising from definition Eq. (1), see Fig. 4.

This curve suggests the possibility of limiting the number of bits in the A/D converter to obtain a sufficiently small expected error. Fig.5. shows the relationship between the measurement error and the frequency of voltage and current signals for an A/D converter with the resolution of 12 bits. The big change of the error above 100 Hz indicates that the integrating algorithm already introduces a significant error. Above 250 Hz, the algorithm may not perform correctly. This is due to an insufficient number of samples being processed at the range for which the measurement is implemented.

Examining the error size which is dependent upon the angle of the phase shift between the voltage and current signals did not show noticeable changes in the value of the error from the angle of phase shift.

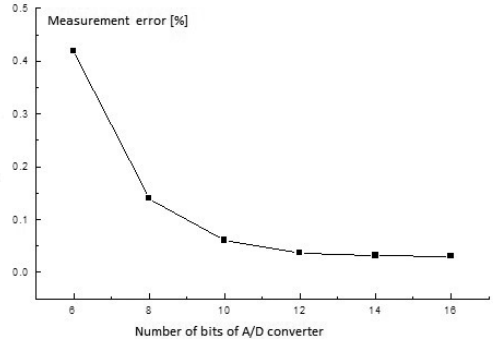

Fig. 4. Relationship between the measurement error and the number of bits of A/D converter

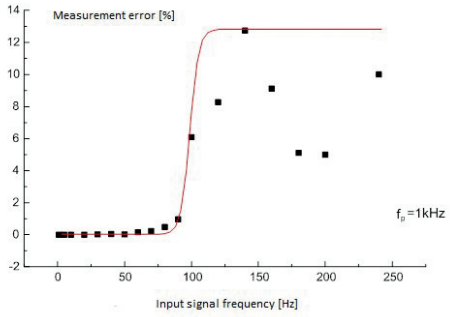

Fig. 5. Relationship between the measurement error and the frequency of voltage and current signals

4. Summary

The presented results of the model testing confirm the accuracy of the solution of the active power measurement by using an A/D converter with a multiplexer. These formed the basis for the construction of the instrument based on a real-time digital signal processor.

References

[1] Bień A., Czajkowski J., Morończyk A., *Determining the RMS Current Components During the Synchronous Machine Starting to Answer a Diagnostic Purpose,* 9th International Symposium on Electrical Instruments in Industry (IMECO TC-4) Glasgow, Scotland, September 8-9, 1997, pp. 161-163.

[2] Bień A., *Modern measurement of electrical energy quality indices*, Electrical Power Quality and Utilisation, Vol. 9-2, December 2003, pp. 63-71.

[3] Czarnecki L., *Harmonics and power phenomena,* Wiley Encyclopedia of Electrical and Electronics Engineering, John Wiley & Sons, 2000.

[4] Booth A. D., *Numerical methods*, London 1955.

[5] Kryłow W. I., *Pribliżennoje wyczislenije integrałow*, Moskwa 1967.

[6] Oppenheim A.V. Schafer R.W., *Discrete - Time Signal Processing*, 2014-EDN-3.

[7] Ralston A., Rabinowitz P., *A First Course in Numerical Analysis*, Courier Corporation, pp. 2001-606.

If you want to quote this article, its proper bibliographic entry is as follow: Andrzej Bień, Edward Layer, *Active power measurement based on digital processing of voltage and current signals*, Technical Transactions, Vol. 6/2018, pp. 127-132.

TECHNICAL TRANSACTIONS 6/2018
ELECTRICAL ENGINEERING
DOI: 10.4467/2353737XCT.18.093.8698
SUBMISSION OF THE FINAL VERSION: 08/06/2018

Krzysztof Tomczyk
Marek Sieja (msieja@pk.edu.pl)
Department of Automatic Control and Information Technology, Faculty of Electrical and Computer Engineering, Cracow University of Technology

Relationship between the absolute error and parameter values of voltage output accelerometer

Zależność błędu bezwzględnego od wartości parametrów akcelerometru z wyjściem napięciowym

Abstract

The functional relationship between the absolute error and the parameter values of a voltage output accelerometer is presented in this paper. The theoretical basis for the mathematical model of the accelerometer and its standard, which is a reference for the error determination, is discussed. The polynomial function is applied for error approximation. Optimal orders of the polynomial along with their parameters and associated uncertainties are determined. The results presented in this paper concern the maximum errors obtained by exciting the accelerometer by the signal of constrained magnitude.

Keywords: absolute error, approximation function, voltage output accelerometer

Streszczenie

W artykule przedstawiono funkcyjną zależność błędu bezwzględnego od wartości parametrów akcelerometru z wyjściem napięciowym. Omówiono podstawy teoretyczne dotyczące matematycznych modeli akcelerometru i jego wzorca, który stanowi odniesienie do wyznaczenia błędu. Do aproksymacji błędów zastosowano funkcję wielomianową. Wyznaczono optymalne rzędy wielomianów wraz z ich parametrami i towarzyszącymi niepewnościami. Przedstawione w artykule wyniki dotyczą maksymalnych błędów uzyskanych w wyniku pobudzania akcelerometru sygnałem ograniczonym w amplitudzie.

Słowa kluczowe: błąd bezwzględny, funkcja aproksymująca, akcelerometr z wyjściem napięciowym

1. Introduction

The theoretical basis of calibrating instruments intended for dynamic measurements based on the criterion of absolute error is discussed in the papers [1–3]. The procedures for determining such errors are also presented here. These procedures are designed to determine the input signals that maximise the error at the output of the instrument. Only one constraint, referring to the magnitude, or two constraints relating simultaneously to the magnitude and the rate of change, are imposed on these signals.

In the above procedures, the basic task is to determine the relationship between the error and the time of instrument testing. This error has such a property that, for a specified time, its value stops increasing. This time depends on the operating bandwidth of the instrument and corresponds to the steady state of its impulse response. Examples of the examination of selected vibration sensors based on the solutions above are presented in [4, 5]. The maximising signals are determined along with the absolute error values. The study was conducted for chosen values of time with the assumed calculation step. However, these results do not provide information about error for other testing times and are only valid for the specific sensors.

Taking into account the above limitations, this paper proposes solutions based on polynomial functions that approximate the relationship between error and time and also the relationship between error and selected parameters of the instrument model. This approach is based on theoretical solutions presented in [6, 7]. The calculations refer to the voltage output accelerometer [8, 9], whose mathematical model contains three main parameters: the voltage sensitivity, damping ratio, and non-damped natural frequency. The studies of the relationship between error and model parameters are presented for the times corresponding to the steady state of error.

2. Model of Accelerometer and Its Standard

The mechanical construction of the voltage output accelerometer is shown in Fig. 1.

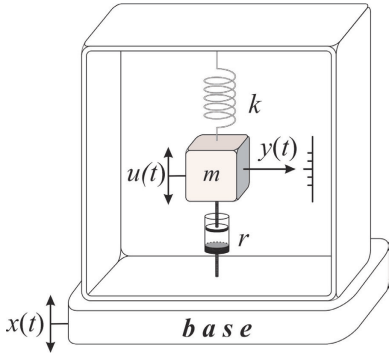

Fig. 1. Mechanical construction of the voltage output accelerometer

The construction of the voltage output accelerometer is represented by a differential equation, as follows:

$$m\ddot{u}(t)+r\dot{y}(t)+ky(t)=0, \tag{1}$$

where $u(t)$, $y(t)$, $x(t)$, m[kg], r[kg/s], k[N/m], $my(t)$, $ru(t)$ and $ku(t)$ are the absolute mass displacement, relative mass displacement, vibration (excitation), seismic mass, dumping coefficient, spring constant, moment of inertia, moment of dumping, and moment of elasticity, respectively.

Considering the absolute mass displacement in (1) as follows:

$$u(t)=x(t)+y(t), \tag{2}$$

we finally obtain

$$m\ddot{y}(t)+r\dot{y}(t)+ky(t)=-m\ddot{x}(t). \tag{3}$$

Presenting (3) in the domain s, we have:

$$K_a(s)=\frac{-S\omega_0^2}{s^2+2\beta\omega_0 s+\omega_0^2}, \tag{4}$$

where S is the voltage sensitivity, while:

$$\omega_0=2\pi f_0=\sqrt{\frac{k}{m}} \tag{5}$$

and:

$$\beta=\frac{r}{2\sqrt{km}} \tag{6}$$

are the non-damped natural frequency and the damping ratio.

The state-space representation of (4) is:

$$K_a(s)=\mathbf{C}_a(s\mathbf{I}-\mathbf{A}_a)^{-1}\mathbf{B}_a, \tag{7}$$

where:

$$\mathbf{A}_a=\begin{bmatrix}0 & 1\\ -\omega_0^2 & -2\beta\omega_0\end{bmatrix}, \mathbf{B}_a=[0 \quad -S\omega_0^2]^T, \mathbf{C}_a=[1 \quad 0], \mathbf{I}=\begin{bmatrix}1 & 0\\ 0 & 1\end{bmatrix} \tag{8}$$

are the state matrix, input vector, output vector, and identity matrix, respectively.

The model of the standard should meet the assumptions of non-distortion transformation. This means that in the range of the accelerometer work, the amplitude characteristic should be constant, while the phase characteristic should decrease linearly. These conditions fulfill the model of the Butterworth filter described by:

$$K_s(s)=\frac{n_M}{s^M+d_1s^{M-1}+d_2s^{M-2}+\ldots+d_{M-1}s+d_M}=\frac{S}{\prod_{m=1}^{M}\left(\frac{s}{2\pi f_c}-p_m\right)}, \tag{9}$$

where the m-th pole is calculated by:

$$p_m = e^{\frac{j(2m+M-1)\pi}{2M}} \tag{10}$$

while f_c is the filter's cut-off frequency, which is equal to the accelerometer bandwidth, and M, n, and d_1, d_1, ... , d_M are the order of the standard model, coefficient of the numerator, and coefficients of the denominator, respectively.

The transfer function (9) can be presented by:

$$K_s(s) = \mathbf{C}_s(s\mathbf{I} - \mathbf{A}_s)^{-1}\mathbf{B}_s, \tag{11}$$

where:

$$\mathbf{A}_s = \begin{bmatrix} 0 & 1 & 0 & \dots & 0 & 0 \\ 0 & 0 & 1 & \dots & 0 & 0 \\ \vdots & \vdots & \vdots & \ddots & \vdots & \vdots \\ 0 & 0 & 0 & \dots & 1 & 0 \\ 0 & 0 & 0 & \dots & 0 & 1 \\ -d_M & -d_{M-1} & -d_{M-2} & \dots & -d_2 & -d_1 \end{bmatrix}, \tag{12}$$

$$\mathbf{B}_s = [0 \quad 0 \quad \dots \quad 0 \quad 0 \quad n_M]^T, \mathbf{C}_s = [1 \quad 0 \quad \dots \quad 0 \quad 0 \quad 0].$$

Let us introduce a new state-space representation based on (7)–(12), as below [2]:

$$K(s) = K_a(s) - K_s(s) = \mathbf{C}(s\mathbf{I} - \mathbf{A})^{-1}\mathbf{B}, \tag{13}$$

where:

$$\mathbf{A} = \begin{bmatrix} A_a & 0 \\ 0 & A_s \end{bmatrix}, \mathbf{B} = \begin{bmatrix} B_a & B_s \end{bmatrix}^T \mathbf{C} = \begin{bmatrix} C_a & -C_s \end{bmatrix}. \tag{14}$$

This space is a combination of the accelerometer and standard models.

The cut-off frequency f_c is calculated based on the parameters β, S and f_0, by solving the equation which results from the amplitude characteristic of the accelerometer, as follows:

$$\lambda = \frac{S}{\sqrt{[1-(f_c/f_0)^2]^2 + 4\beta^2(f_c/f_0)^2}} \tag{15}$$

where:

$$\lambda = S + \frac{S}{100\%} \cdot \delta \tag{16}$$

and δ is the tolerance of the amplitude characteristic.

3. Determining the Absolute Error

If the input signal is constrained in magnitude,

$$|x(t)| \le a \tag{17}$$

the absolute error can be calculated using a continuous formula:

$$D_t = a\int_0^T |k(t)|dt \tag{18}$$

or a discrete one:

$$D_n = a\Delta\sum_{n=0}^{N-1} |k[n]| \tag{19}$$

where:

$$k(t) = \mathbf{C}e^{\mathbf{A}t}\mathbf{B} \tag{20}$$

and:

$$k[n] = \mathbf{C}e^{\mathbf{A}\Delta n}\mathbf{B} \tag{21}$$

are the continuous and discrete impulse responses and Δ denotes the sampling interval of the state-space equations over the interval $[0,T]$.

The maximising signal with one constraint is determined by:

$$x_0(t) = a\,sign\{k(T-t)\} \tag{22}$$

and:

$$x_0[n] = a\,sign\{k[N-n]\},\ n = 0,1,\ldots,N-1 \tag{23}$$

based on (20) and (21), where N denotes the number of samples [1–3].

4. Determining the Approximate Polynomial

Let the vector:

$$\mathbf{Z} = [z_0, z_{1,\ldots,} z_{J-1}]^T \tag{24}$$

be represented below by the assumed values of T, β, S, or f_0. The vector of absolute errors that corresponds to **Z** is:

$$\mathbf{D} = [D(x_0)_0, D(x_0)_1, \ldots, D(x_0)_{J-1}]^T, \tag{25}$$

The polynomial of order α that approximates the error has the form:

$$d_i(z) = g_0 + g_1 z_i + g_2 z_i^2 + \ldots + g_\alpha z_i^\alpha + \varepsilon_{1i},\ i = 0,1,\ldots,J-1, \tag{26}$$

where $g_0, g_1, \ldots, g_{J-1}$ denote the coefficients of the polynomial and ε_1 is the approximation error [6].

In matrix form, we have:

$$\mathbf{D}=\mathbf{\Phi G}+\mathbf{E}_1 \tag{27}$$

where:

$$\mathbf{\Phi}=\begin{bmatrix} 1 & z_0 & z_0^2 & \dots & z_0^\alpha \\ 1 & z_1 & z_1^2 & \dots & z_1^\alpha \\ \vdots & \vdots & \vdots & \dots & \vdots \\ 1 & z_{J-1} & z_{J-1}^2 & \dots & z_{J-1}^\alpha \end{bmatrix}. \tag{28}$$

and:

$$\mathbf{G}=[g_0, g_{1,\dots,} g_{J-1}]^T \tag{29}$$

$$\mathbf{E}_1=[\varepsilon_0, \varepsilon_{1,\dots,} \varepsilon_{J-1}]^T \tag{30}$$

We want to estimate the value **G** that minimise $\mathbf{E}_1^T\mathbf{E}_1$. Hence:

$$min\,\mathbf{E}_1{}^T\mathbf{E}_1=(\mathbf{D}-\mathbf{\Phi G})^T(\mathbf{D}-\mathbf{\Phi G}) \tag{31}$$

Simplification of the matrices gives:

$$\mathbf{E}_1{}^T\mathbf{E}_1=(\mathbf{D}^T-\mathbf{G}^T\mathbf{\Phi}^T)(\mathbf{D}-\mathbf{\Phi G})=\mathbf{D}^T\mathbf{D}-2\mathbf{G}^T\mathbf{\Phi}^T\mathbf{D}+\mathbf{G}^T\mathbf{\Phi}^T\mathbf{\Phi G} \tag{32}$$

Taking the first derivative with respect to **G** and equating to zero, we have:

$$-2\mathbf{\Phi}^T\mathbf{D}+2\mathbf{\Phi}^T\mathbf{\Phi G}=0 \tag{33}$$

Based on the first-order condition and after simplification, we have:

$$\mathbf{\Phi}^T\mathbf{\Phi}\tilde{\mathbf{G}}=\mathbf{\Phi}^T\mathbf{D} \tag{34}$$

where $\tilde{\mathbf{G}}$ denotes the estimate of **G** that minimises the error $\mathbf{E}_1$.

Multiplying both sides of (34) by $(\mathbf{\Phi}^T\mathbf{\Phi})^{-1}$, we finally have:

$$\tilde{\mathbf{G}}=(\mathbf{\Phi}^T\mathbf{\Phi})^{-1}\mathbf{\Phi}^T\mathbf{D} \tag{35}$$

which is the least-squares estimator for the polynomial approximation in matrix form.

The uncertainty of approximation [7] is given by:

$$u_A[d(z)]=\sqrt{\frac{(\mathbf{\Phi}\tilde{\mathbf{G}}-\mathbf{D})^T(\mathbf{\Phi}\tilde{\mathbf{G}}-\mathbf{D})}{J-\alpha}}=\sqrt{\frac{\sum_{j=0}^{J-1}(d[g_0,g_1,\dots,g_\alpha,z_j)-D(x_0)_j]^2}{J-\alpha}}. \tag{36}$$

The standard uncertainty for particular coefficients $g_0, g_1, \dots, g_\alpha$ is:

$$u_A(g_i)=u_A[d(z)]\cdot\sqrt{\Theta_{i,i}},\ i=0,1,\dots\alpha, \tag{37}$$

where:

$$\mathbf{\Theta} = (\mathbf{\Phi}^T \mathbf{\Phi})^{-1}. \tag{38}$$

The relative uncertainty for the coefficients $g_0, g_1, \ldots, g_\alpha$ is:

$$\delta(g_i) = \frac{u_A(g_i)}{|g_i|}, \quad i = 0,1,\ldots\alpha. \tag{39}$$

The order of the polynomial (26) is determined by checking the chi-square test:

$$\chi = \frac{\sum_{j=0}^{J-1} (\Xi_j)^2}{\sigma^2(\Xi)}, \tag{40}$$

where:

$$\Xi = \sum_{j=0}^{J-1} (d(g_0, g_1, \ldots, g_\alpha, z_j) - D(x_0)_j). \tag{41}$$

5. Example of Calculation

Below, based on Eqs. (1)–(23) and for the values of parameters β, S, and f_0 assumed in advance, the characteristic $d(T)$ was determined. An approximation of this characteristic was made based on Eqs. (24)–(41). For the assumed ranges of β and S with the steps Δ_β and Δ_S, the values of error D for constant values of T=100ms and f_0=1kHz were determined. The value of the amplitude characteristic tolerance was assumed to be equal to 10%.

Then, based on Eqs. (24)–(41), the functions $d(\beta)$ and $d(S)$, which approximate the error D, were determined. The orders of approximating polynomials were determined by checking the chi-square test.

5.1. Determining the Error *D*

The values of error D for T=0,0.01,…,0.1s as well as β=0.015, S=0.15V/(ms^{-2}), and f_0=1kHz are reported in Table 1. For such a coefficient of the accelerometer model, the value of the cut-off frequency f_c determined by (15) is equal to 931Hz.

Table 1. Values of error D

T[ms]	0	10	20	30	40	50
D[Vs]	0	0.580	0.808	0.896	0.931	0.944
T[ms]	60	70	80	90	100	
D[Vs]	0.949	0.951	0.952	0.953	0.953	

Figure 1 shows the approximation of the values of error D, while the coefficients and associated uncertainties for the sixth-order polynomial are reported in Table 2. This order is optimal because it ensures that the result of the chi-squares test will be less than 1.

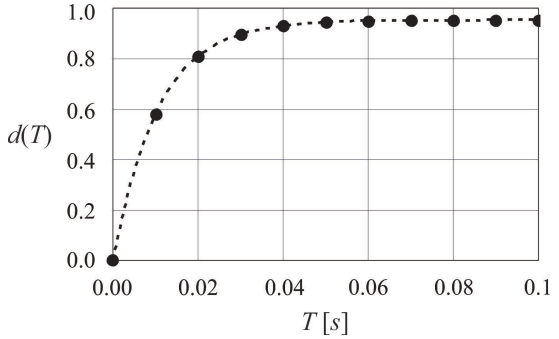

Fig. 2. Approximation of the error by the sixth-order polynomial

Table 2. Determined parameters and associated uncertainties for polynomial $d(T)$

g_0	g_1	g_2	g_3	g_4
$3.51 \cdot 10^{-4}$	85.5	$-3.44 \cdot 10^{3}$	$7.65 \cdot 10^{4}$	$-9.59 \cdot 10^{5}$
g_5	g_6	$u_A[d(T)]$[Vs]	$u_A(g_0)$	$u_A(g_1)$
$6.32 \cdot 10^{6}$	$-1.70 \cdot 10^{7}$	$2.36 \cdot 10^{-3}$	$2.35 \cdot 10^{-3}$	0.879
$u_A(g_2)$	$u_A(g_3)$	$u_A(g_4)$	$u_A(g_5)$	$u_A(g_6)$
91.7	$3.71 \cdot 10^{3}$	$6.98 \cdot 10^{4}$	$6.13 \cdot 10^{5}$	$2.04 \cdot 10^{6}$
$\delta(g_0)$[%]	$\delta(g_1)$[%]	$\delta(g_2)$[%]	$\delta(g_3)$[%]	$\delta(g_4)$[%]
$2.75 \cdot 10^{-3}$	0.0260	2.66	4.85	7.27
$\delta(g_5)$[%]	$\delta(g_6)$[%]	χ		
9.70	12.0	0.184		

From Figure 1, it follows that with the increase of time T, the error becomes constant. This corresponds to the steady state of the accelerometer impulse response, determined as the inverse Laplace transform of the transfer function (4). This impulse is presented in Fig. 2 and was obtained for $t = 0, \Delta_t, \ldots, T$, where $\Delta_t = 10^{-5}$s and T=100 ms.

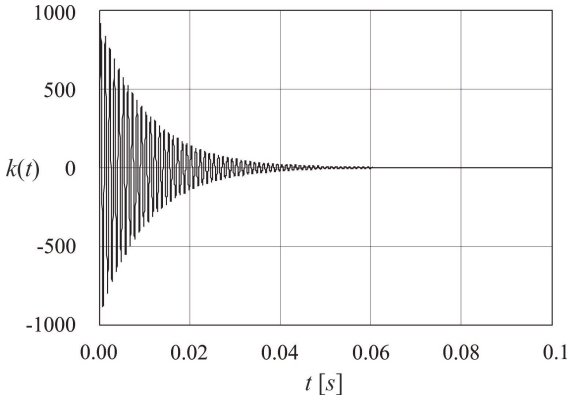

Fig. 3. Accelerometer impulse response for β=0.015, S=0.15V/(ms^{-2}), and f_0=1kHz

The values of error D determined for β=0.015, Δ_β, ...,0.015, and S=0.1, Δ_S, ..., 0.15, where Δ_β=0.0005 and Δ_S=0.005, are reported in Table 3. The error was calculated for T=100 ms.

Table 3. Matrix (44) of the errors D

		β										
		0.0100	**0.0105**	**0.0110**	**0.0115**	**0.0120**	**0.0125**	**0.0130**	**0.0135**	**0.0140**	**0.0145**	**0.0150**
S	**0.100**	0.636	0.606	0.579	0.554	0.531	0.510	0.490	0.472	0.455	0.450	0.425
	0.105	0.701	0.668	0.638	0.610	0.585	0.562	0.540	0.520	0.502	0.484	0.468
	0.110	0.769	0.733	0.700	0.669	0.642	0.616	0.592	0.571	0.550	0.531	0.514
	0.115	0.840	0.800	0.764	0.731	0.701	0.673	0.647	0.623	0.601	0.580	0.561
	0.120	0.915	0.971	0.832	0.796	0.763	0.733	0.704	0.679	0.654	0.632	0.611
	0.125	0.992	0.945	0.903	0.864	0.828	0.795	0.764	0.736	0.710	0.685	0.662
	0.130	1.07	1.02	0.976	0.934	0.895	0.859	0.826	0.796	0.767	0.741	0.716
	0.135	1.16	1.10	1.05	1.01	0.965	0.926	0.891	0.858	0.827	0.799	0.772
	0.140	1.24	1.19	1.13	1.08	1.04	0.996	0.958	0.922	0.889	0.859	0.830
	0.145	1.33	1.27	1.21	1.16	1.11	1.07	1.03	0.989	0.954	0.921	0.890
	0.15	1.43	1.36	1.30	1.24	1.19	1.14	1.10	1.06	1.02	0.986	0.953

5.2. Determining the Approximate Functions

Below, we determine the functions $d(\beta)$ and $d(S)$ approximating the error based on Table 3 as well as for S=0.15V/(ms^{-2}) and β=0.015 respectively.

Figure 4 shows the approximation functions $d(\beta)$ and $d(S)$ while Tables 4 and 5 report the polynomial coefficients and associated uncertainties. The first function was approximated by a third-order polynomial while the second one was approximated by a second-order one.

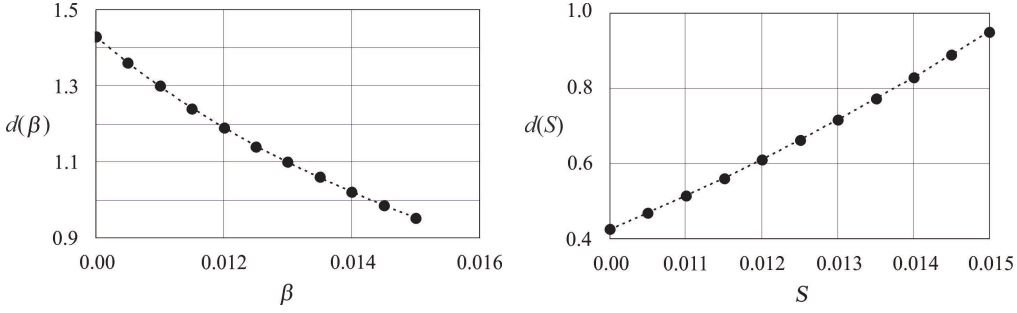

Fig. 4. Approximation functions $d(\beta)$ and $d(S)$

Table 4. Determined parameters and associated uncertainties for the polynomial $d(\beta)$

g_0	g_1	g_2	g_3	$u_A[d(T)]$[Vs]
85.5	-656	$3.74 \cdot 10^4$	$-7.86 \cdot 10^5$	$1.50 \cdot 10^{-3}$
$u_A(g_0)$	$u_A(g_1)$	$u_A(g_2)$	$u_A(g_3)$	$\delta(g_0)$[%]
0.292	71.1	$5.73 \cdot 10^3$	$1.53 \cdot 10^5$	0.0440
$\delta(g_1)$[%]	$\delta(g_2)$[%]	$\delta(g_3)$[%]	χ	
0.190	15.3	19.4	0.0420	

Table 5. Determined parameters and associated uncertainties for the polynomial $d(S)$

g_0	g_1	g_2	$u_A[d(T)]$[Vs]	$u_A(g_0)$
$7.47 \cdot 10^{-3}$	–0.0901	42.6	$3.07 \cdot 10^{-4}$	$6.50 \cdot 10^{-3}$
$u_A(g_1)$	$u_A(g_2)$	$\delta(g_0)$[%]	$\delta(g_1)$[%]	$\delta(g_2)$[%]
0.105	0.420	7.21	0.247	0.986
χ				
0.449				

From Fig. 4, it follows that as β increases, the error decreases, whereas when *S* increases, the error increases. The approximation polynomials were determined by successively increasing their order from the first order and simultaneously checking the result of the χ test. This order was assumed to be an optimal solution for which the result of this test is less than one for the first time.

It should be added that with the increase of the non-damped natural frequency, the time of steady of the absolute error decreases. The steady values of error have the same value for the different frequencies, and therefore the determination of the relationship between the error and this parameter has been omitted from this paper.

6. Conclusions

The solutions obtained in this paper can be successfully extended to a wider group of measuring instruments with more parameters and for a wider range of their variability. Based on the solutions presented in Section 4, the functions approximating the error were obtained. Such functions will allow easy determination of the maximum dynamic errors based on the results of parametric identification of measuring instruments. Analogous functions can also be successfully determined for other error criteria, for example, for the integral square criterion.

References

[1] Layer E., Gawedzki W., *Dynamika Aparatury Pomiarowej. Badania i Ocena,* PWN, Warszawa 1991.

[2] Layer E., Tomczyk K., *Determination of Non-Standard Input Signal Maximizing the Absolute Error,* Metrology and Measurement Systems, Vol. 17, 2009, pp. 199–208.

[3] Tomczyk K., *Applied Measurement Systems. Calibration of measuring systems based on maximum dynamic error,* Published by InTech, Rijeka 2012, pp. 189–210.

[4] Tomczyk K., *Impact of uncertainties in accelerometer modeling on the maximum values of absolute dynamic error,* Measurement, Vol. 80, 2016, pp. 71–78.

[5] Tomczyk K., Layer E., *Energy density for signals maximizing the integral-square error,* Measurement, Vol. 90, 2016, pp. 224–232.

[6] Foszcz D., *Estymacja Parametrów Funkcji Regresji Metodą Klasyczną oraz Metodami Bootstrapowymi,* Górnictwo i Geoinżynieria, Vol. 3(1), 2016, pp. 67–78.

[7] Dorozhovets M., *Ocena wpływu oddziaływan systematycznych na parametry niepewnosci podczas aproksymacji metoda najmniejszych kwadratow,* PAK. Vol. 12, 2006, pp. 22–25.

[8] Sun X.T., Jing X.J., Xu J., Cheng L., *A Quasi-Zero-Stiffness-Based Sensor System in Vibration Measurement,* IEEE Transactions on Industrial Electronics, Vol. 61, no. 10, 2014, pp. 5606–6114.

[9] Di Natale C., Ferrari V., Ponzoni A., Sberveglieri G., Ferrari M., *Sensors and Microsystems*, Springer, 2013.

TECHNICAL TRANSACTIONS 6/2018
MECHANICS
DOI: 10.4467/2353737XCT.18.094.8699
SUBMISSION OF THE FINAL VERSION:21/05/2018

Tomasz Dębiński (debinski@agh.edu.pl)
Faculty of Metals Engineering and Industrial Computer Science, AGH University of Science and Technology

Estimation of the localisation and geometric parameters of the semi-solid zone of steel samples

Oszacowanie lokalizacji i parametrów geometrycznych strefy półciekłej próbek stalowych

Abstract

This paper presents the use of computer graphics methods for the initial estimation of the shape, position and volume of the semi-solid zone in samples from the Gleeble 3800 physical simulator. Simulations were performed for the verification of the heating and deformation process of steel with a semi-solid zone. The numerical model consists of three separate subsystems for describing the deformation of the solid and semi-solid zones: mechanical, thermal and predictive densities. Taking into consideration the specific localisation of these zones, the initial estimation of the location of the melting zone is very helpful in understanding the process and may be the starting point for further research. This article describes the technique of selecting areas in samples that meet the thermal criteria. This allows us to approximate the location and shape of the semi-solid zone and this information can be used at a later stage to further refine its parameters.

Keywords: computer simulation, computational geometry, convex hull, visualisation of calculation results

Streszczenie

W artykule przedstawiono wykorzystanie metod grafiki komputerowej do wstępnego oszacowania kształtu, położenia i objętości strefy półciekłej w próbkach z symulatora fizycznego Gleeble 3800. W celu weryfikacji procesu nagrzewania i odkształcania stali w strefie półciekłej przeprowadzono wiele symulacji. Model numeryczny składa się z trzech odrębnych części: mechanicznej, termicznej i przewidującej zmiany gęstości opisujących odkształcenie dla strefy stałej i półciekłej. Biorąc pod uwagę specyficzną lokalizację tych stref, wstępna ocena położenia strefy przetopienia jest bardzo pomocna w zrozumieniu procesu i może być punktem wyjścia do dalszych badań. W artykule opisano technikę wybierania obszarów w próbkach, które spełniają wyznaczone kryteria, co pozwala na przybliżenie lokalizacji, kształtu i parametrów geometrycznych strefy półciekłej, co można wykorzystać w celu dalszego poprawiania jej parametrów oraz dokładności samego modelu.

Słowa kluczowe: symulacja komputerowa, geometria obliczeniowa, otoczka wypukła, wizualizacja wyników obliczeń

1. 1. Introduction

The possibility of steel deformation in its semi-solid state has recently been a topic of interest for many companies [1–3]. The integrated strip casting and rolling process is enhancement of a conventional rolling process. The new solution offers a significant reduction in cost, increased productivity and low investment costs. Temperature is a factor that largely determines the mechanical parameters of steel such as strain and stress; therefore, it is necessary to define these parameters when processing materials with a semi-solid zone. These parameters are difficult to determine especially at very high temperatures. This is why it is necessary to use advanced numerical methods. The mechanical properties of the mushy zone determine the deformation of the entire sample and therefore determine the parameters that are required. For this type of problem, the best solution is a spatial model because the calculated area has a very irregular and complex shape. A good description of the mixed zone can be used for better control of the integrated rolling process.

The position, shape and volume of the mushy zone is very important. As a result of the development of computer graphics and computation geometry, it is possible to use computer graphics methods for analysis and identification of the zones of a sample where the coexistence of both liquid and solid phases may occur. Computer graphics methods are widely used in industry and can be very helpful for the interpretation of calculation results.

One of the techniques involved in describing objects is stereology. Stereological measurements can be performed on two-dimensional images of three-dimensional structures [4, 5]. Measurements of the elements of the image allows determining the parameters that appoint the classification of objects to the appropriate class [6].

Since the computation was performed for axially symmetric samples; for their visualisation, it was necessary to build 3D solids of revolution both for the whole sample and for a chosen area of potential occurrence of a semi-solid zone.

The article describes the process of building solids and an initial estimation of the position and parameters of the semi-solid zone.

2. The simulation system

Numerical simulations were performed with the DEFFEM package, which is developed in accordance with the ONEDES (ONEDECisionSoftware) design philosophy [7]. This is based on the assumption that a set of independent modules comprising the DEFFEM package is implemented numerically in the one system. It enable to performed a virtual test of resistance heating combined with deforming in a wide range of temperatures in particular at extra-high temperatures near the solidus line, as well as in conditions of the solid and liquid phase coexistence, without the need for any commercial applications.

The developed simulation package also provides tools targeting the full identification of the selected parameters of numerical models on the basis of data coming directly from physical simulations (DEFFEM inverse module). In parallel with the design of such an

advanced simulation tool, the development of visualisation tools and the analysis of findings are being implemented. Advanced numerical algorithms have been developed for plotting the isolines of scalar fields, visualising vector fields and enabling stereoscopic data to be visualised (module DEFFEM |pre&post).

3. Prediction of the mechanical properties of steel in semi-solid state

The computer-aided procedure leading to the determination of stress-deformation dependency was developed at AGH University of Science and Technology. The physical experiment was performed at the Institute of Iron Metallurgy in Gliwice using the GLEEBLE 3800 thermomechanical simulator (Fig. 1). The material used in the study was steel of C45 and S355 types [8, 9].

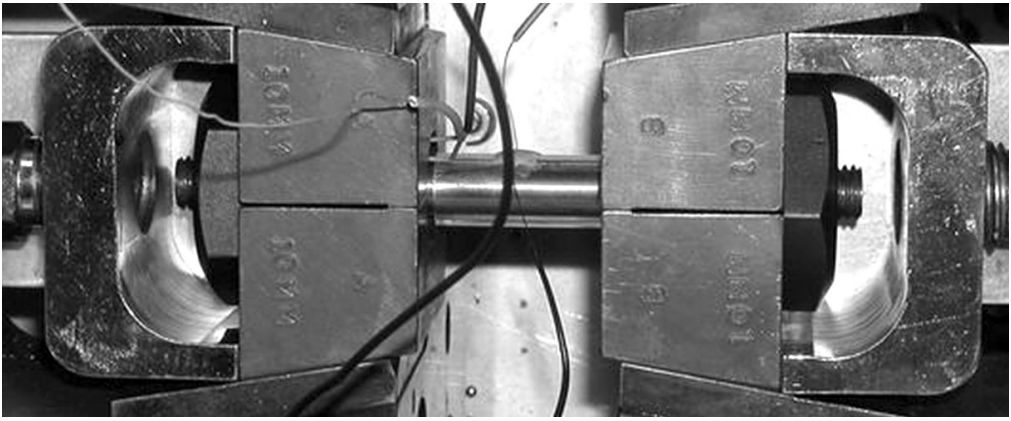

Fig. 1. Equipment before the experiment

The numerical part of the program was written in C++ and Fortran. The main objective of the program is numerical support for the measurement of the mechanical properties of steel at very high temperatures. Such an approach facilitates avoiding problems which appear while using traditional measurement methods and which are caused by strong inhomogeneity of deformations occurring in samples subjected to deformation at temperatures over 1400°C.

The solution in the form of a temperature field for the numerical model was found by solving the Fourier equation, which in the general form can be written as follows (1):

$$\nabla^T(\lambda\nabla T)+(Q-c_p\rho\frac{\partial T}{\partial\tau})=0 \tag{1}$$

where: T– absolute temperature, λ– thermal conductivity coefficient, Q – heat generation rate for volume unit, c_p – specific heat, ρ – density, τ– time

The thermo-mechanical solution was directly adapted to the boundary conditions pertaining to the Gleeble 3800 thermo-mechanical simulator system [10]. It allows the easy

and fast verification of the obtained simulation results on the basis of experimental data. The resistance heating method is applied for heating samples in the simulator system [10] and used as the input data for the simulation with a semi-solid zone.

Due to limitations concerning the computer resources which are available to technologists of metal forming processes, a very accurate computation can sometimes be impossible or the computation time can be a barrier for the practical application of complex sequential models. This is why computer programs require very long processing times and parallel computing can be used to resolve this problem [11].

Due to the very significant influence of temperature on the mechanical properties in the range of very high temperatures, it is necessary to initially estimate the range of activity of the semi-solid zone during the deformation process. For the studied axially symmetrical case, it is possible to estimate the position of the semi-solid zone and determine the parameters which describe its shape and size.

To mark the border nodes which determine the semi-solid zone, algorithms of computational geometry were used in which the temperature characteristic for the studied material was the criterion.

4. Convex hull alghoritm

There are various models allowing the determination of the coexistence of a liquid and solid zone. One of these was presented by the authors of the publication [9]. However, in this article, a different approach was used which uses one of the algorithms of computational geometry, a gift wrapping algorithm or Jarvis [12] march to be precise, which solves the problem of convex hull, which has complexity $0(kn)$, where k is the number of points on the convex hull in a given set n of points. The gift wrapping algorithm is based on observation: a line segment $\overline{pq}$ bounded by two end points from the set S is the band of the convex hull if and only if all the points from S belong to the same closed half-plane defined by the straight line, and each point on the line belongs to the segment. If the segment $\overline{pq}$ is a side of the convex hull, which is not degenerated to the segment or a point, it must have a side different from $\overline{pq}$, starting in q (an analogical condition is met for point p). Figure 2 presents a schema of determining the convex hull for Jarvis march.

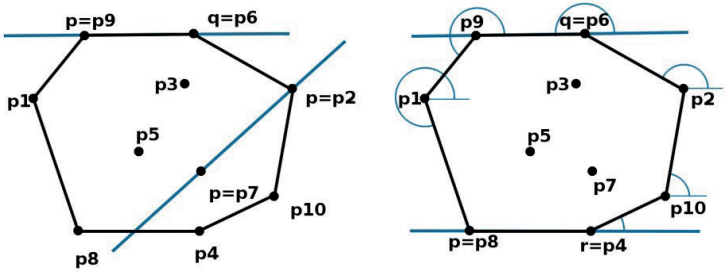

Fig. 2. Schema for determining the convex hull

This method allows separating the nodes of the mesh which met the assumed criterion of exceeding the solidus temperature for the studied material. Based on this, further analysis was performed using the chosen shape descriptors.

5. Shape descriptors

In order to describe representative sizes of the zone shape, a few shape descriptors were used [13]. The aim of the scalar measurement of the elements of the image is to reduce the element shape to a single size or a group of representative sizes for a particular element. Because the result of the simulation is a quantified and approximated representation of the real result, the determined representative sizes are a certain approximation of the real value. If the method of measurement itself is correctly chosen, the representative sizes present compact information on the shape itself.

Extensibility is the measurement of the aspect ratio, determined on the basis of equation (2).

$$k_{ar} = \frac{d_{\min}}{d_{\max}} \tag{2}$$

where:
$d_{\min}$ – the length of the smallest segment connecting two side points of the figure which crosses the centre of gravity of the element,
$d_{\max}$ –maximum length of the segment.

Circularity – is a form factor measuring the similarity of the element shape to a circle. This is determined as the ratio of the surface area of the element to the surface area of a circle the circumference of which is equal to the perimeter of the analysed element. This dependency was described with formula (3). The shape parameter takes a value close to 1 for circular-shaped elements.

$$k_{circularity} = \frac{A_i}{A_c} = \frac{A_i \cdot 4\pi}{p_i^2} \tag{3}$$

where:
A_i – surface are of the analysed element
p_i – perimeter of the element

Rectangularity is the measurement of the similarity of the object to a rectangle. This is determined as the ratio of the element's surface area to the surface area of the minimum bounding rectangle of the given element (4).

$$k_{rectangularity} = \frac{A_i}{A_p} \tag{4}$$

where:
A_p – surface area

Compactness of the object is a numerical measure of the degree of the elements' compactness described by the dependency (5T). The highest compactness takes the form of a circle for which this parameter takes the value of 1.

$$k_F = \frac{\sqrt[2]{\frac{A_i}{\pi}}}{d_{\max}} \tag{5}$$

where:
$d_{\max}$ – the length of the maximum chord of the analysed element

6. Building a solid of revolution

Since the calculations were performed for the axially symmetrical model in order to build a 3D model of samples, it was necessary to build a solid of revolution based on a 2D model with a fixed level of precision. A useful solution is determining points of the solid using the polar coordinate system. To determine the points in space which constitute the solid of the sample, it was necessary to move from the polar coordinate system to the Cartesian system. For a given radius vector where r and amplitude $\phi \in [0,2\pi)$ of point P, its Cartesian coordinates may be determined from the dependency (6), which is presented in Figure 3. The visualisation was performed using the OpenGL graphic library [14]. Creating visualisation is possible and is often performed using web technology [15] or stereoscopic techniques [16].

$$\begin{aligned} x &= r\cos(\varphi) \\ y &= r\sin(\varphi) \end{aligned} \tag{6}$$

where the Jacobian (factor) of the transformation is (7):

$$\frac{D(x,y)}{D(r,\varphi)} = \begin{bmatrix} \frac{\partial x}{\partial r} & \frac{\partial x}{\partial \varphi} \\ \frac{\partial y}{\partial r} & \frac{\partial y}{\partial \varphi} \end{bmatrix} = \begin{bmatrix} \cos\varphi & -r\sin(\varphi) \\ \sin\varphi & r\cos(\varphi) \end{bmatrix} = r\left(\cos^2\varphi + \sin^2\varphi\right) = r \tag{7}$$

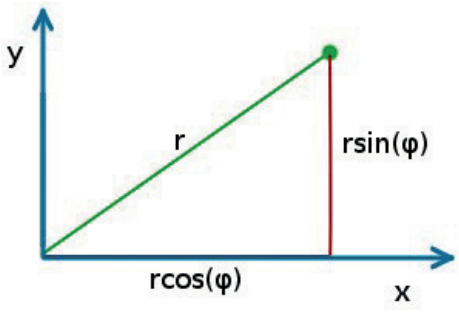

Fig. 3. Relation of Cartesian and polar coordinates

In order to build a 3D model, revolution of the 2D mesh of finite elements about the x coordinate is required. As a result, peripheral points were generated in order to create a solid of revolution with a set precision. The proposed solution allowed performing a visualisation of the samples and presenting the semi-solid zone in the form of a 3D solid for further analyses. One of these additional analyses is the determination of the volume measure of the zone in relation to the volume of the studied samples.

7. Results of analyses for exemplary samples

Four cases of samples were subjected to analysis, one before and one after deformation, and one in hot holders and one in cold holders in the Gleeble 3800 simulator. For all the samples, visualisation was performed and the chosen shape descriptors were calculated to determine the parameters of the semi-solid zone. Figure 4 shows a sample of C45 steel with the estimated position and shape of the semi-solid zone.

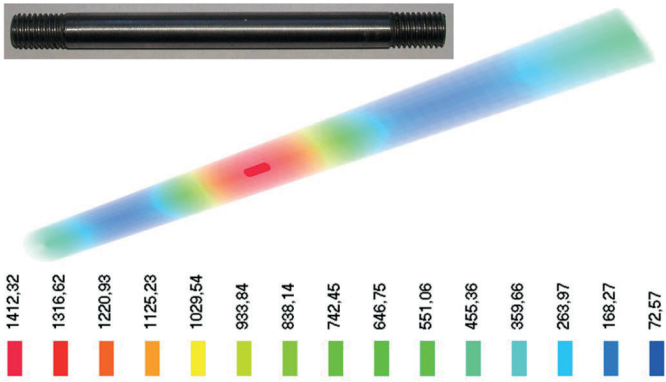

Fig. 4. Visualisation of the sample before deformation with a semi-solid zone for C45 steel with a real photo of the sample

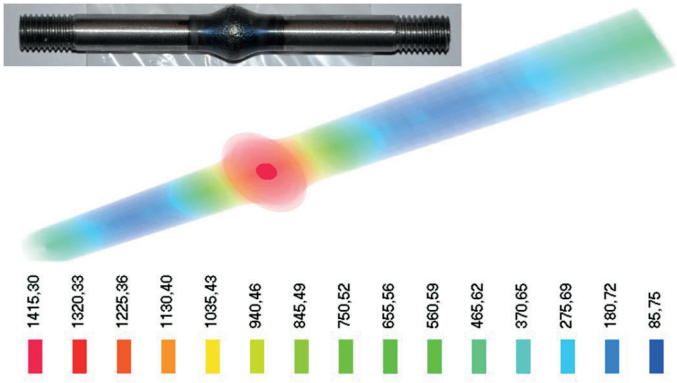

Fig. 5. Visualisation of the sample after deformation with a semi-solid zone for C45 steel with a real photo of the sample

Figure 5 presents the sample after deformation for C45 steel along with the estimated position and shape of the semi-solid zone.

In Fig. 6, a sample for S355 steel is presented along with the estimated position and shape of the semi-solid zone for cold holders of the Gleeble 3800 simulator. The semi-solid zone may border the surface of the sample because a quartz cover was used.

In Fig. 7, a sample for S355 steel is presented along with the estimated position and shape of the semi-solid zone for hot holders of the Gleeble 3800 simulator.

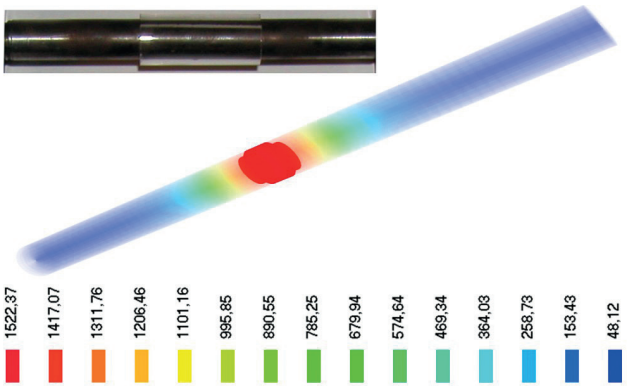

Fig. 6. Visualisation of the sample after heating with a semi-solid zone for S355 steel for cold holders with a real photo of the sample

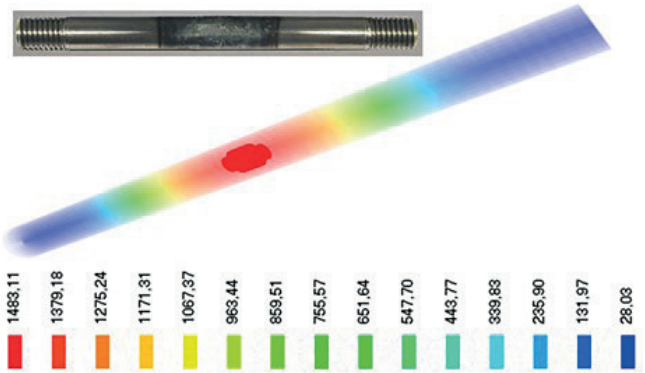

Fig. 7. Visualisation of the sample after heating with a semi-solid zone for S355 steel for hot holders

The results present the estimation of the geometrical position and shape descriptors of the remelting zone. In Figs. 4–7 the results for C45 and S355 steels are presented. Shape descriptors have been determined for each case, which are presented in Table 1. For C45 steel, it can be noted that geometrical parameters of the remelting zone worsened after deformation; the zone is more irregular, less compact, and its volume is smaller, which matters for planning further experiments and the optimisation of the process. The temperature of the holders influenced the size of the high temperature zone; it was observed that this was significantly limited in the case of cold holders. Higher temperatures caused the increase of volume of

Table 1. Overview of shape descriptors for the analysed samples

Descriptor	Material, case			
	C45 Before deformation	C45 After deformation	S355 Hot holder	S355 Cold holder
aspect ratio, extensibility	0.44	0.33	0.44	0.35
circularity, form factor	0.70	0.63	0.64	0.70
rectangularity	0.98	0.94	0.84	0.90
compactness	0.84	0.63	0.71	0.80
% of max volume	0.07	0.06	2.75	2.5

the remelting zone and its contact with the surface of the sample. In comparison to a sample heated to a lower temperature using hot holders, the remelting zone has worse geometrical parameters when heated to higher temperatures and its contact with the surface causes a lot of technical problems during the trial.

8. Summary and conclusions

Computer graphics provide many algorithms and solutions which may also be used in other areas. In the article, the use of computational geometry algorithms to determine representative points of the remelting zone for the simulation of the heating and deformation of steel samples in the Gleeble 3800 simulators has been presented. Estimation of the position and parameters of the remelting zone is very important for simulation of the process and increasing the precision of the model. Due to use of the axially symmetrical model, the polar coordinate system was used to visualise the sample. This allowed determining the points in space which constitute the zones of the sample. The remelting zone for a few samples has been described using shape descriptors, which allowed determining its shape and geometrical parameters. The obtained results may serve as a starting point for further research and to provide a more precise description of the zone, as well as to specify the input parameters of the model.

Acknowledgment

This project has been supported by the Polish National Science Centre, Decision number: DEC-2011/03/D/ST8/04041

References

[1] Park C.M., Kim W., Park G.J., *Thermal analysis of the roll in the strip casting process*, Mech Res Commun., 30, 2003, 297–310.

[2] Seo P.K., Park K., Kang C., *Semi-solid die casting process with three steps die system*, J Mater Proc Technol, 154, 2004, 442–449.

[3] Watari H., Davey K., Rasgado M.T., et al., *Semi-solid manufacturing process of magnesium alloys by twin-roll casting*, J Mater Proc Technol., 156, 2004, 1662–1667.

[4] Underwood E.E., *Quantitative Stereology*, Addison Weslay, Reading 1970.

[5] Russ J.C., *Practical Stereology*, Plenum Press, New York 1986.

[6] Stein E., Bachmann M., Heldens W., Muller A., Schmullius CH., *A Spectral feature based classification algorithm for characterization of urban surfaces in Munich*, 6th ERSeL SIG Image Spectroscopy Symposium, Tel-Aviv 2009.

[7] Hojny M., *Developing a Hybrid Model and a Multi-Scale 3D Concept of Integrated Modelling High Temperature Processes*, Computer Simulation, D. Cvetković (Ed.), InTech, 2017.

[8] Hojny M., Głowacki M., *Computer modelling of deformation of steel samples with mushy zone*, Steel Research Int., 2008, 868-874.

[9] Jędrzejczyk D., Hojny M., *Estimating of the shape and size the liquid and mixed zone in the modelling of processes with semi-solid core*, Metal, Brno, Ostrava 2016, 291–296.

[10] Hojny M., *Modeling of Steel Deformation in the Semi-Solid State*, Advanced Structured Materials, vol. 78, Springer, 2017.

[11] Dębiński T., Głowacki M., Hojny M., *Parallel computation model of semi-solid steel deformation process*, Metal Forming 2012: proceedings of the 14th international conference on Metal Forming : September 16–19, 2012, Krakow, Steel Research International, 763–766.

[12] Preparata F.P., Shamos M.I., *Computational Geometry*, An Introduction, Springer-Verlag, New York Inc., 1985.

[13] Mingqiang Y., Kidiyo K., Ronsin J., *A Survey of Shape Feature Extraction Techniques*, Pattern Recognition, PengYeng Yin (Ed.), 2008 43-90.

[14] *OpenGL*, https://www.opengl.org/, (access 2018-05-15).

[15] Dębiński T., Głowacki M., Hojny M., Gumuła A., Woźniak D., *Web system dedicated to parallel computation for modeling of mushy steel deformation*, Archives of Metallurgy and Materials, vol. 59, 2014, 865–870.

[16] Hojny M., Dębiński T., *Development advanced tools supporting simulations of steel deformation in the semi-solid state – methodology of a stereoscopic visualization*, Metal 2016, TANGER Ltd., Brno, Ostrava 392–397.

If you want to quote this article, its proper bibliographic entry is as follow: Tomasz Dębiński, *Estimation of the localisation and geometric parameters of the semi-solid zone of steel samples*, Technical Transactions, Vol. 6/2018, pp. 145-154.

TECHNICAL TRANSACTIONS 6/2018
MECHANICS
DOI: 10.4467/2353737XCT.18.095.8700
SUBMISSION OF THE FINAL VERSION: 11/06/2018

Halszka Skórska (halszkas@gmail.com)
Jerzy Sładek
Laboratory of Coordinate Metrology, Faculty of Mechanical Engineering, Cracow University of Technology

A SIMULATION STUDY OF THE GRAPHICAL USER INTERFACE OF THE HEAD-UP DISPLAY AND ITS INFLUENCE ON THE DRIVER'S PERCEPTION

SYMULACYJNE BADANIE WPŁYWU INTERFEJSU GRAFICZNEGO WYŚWIETLACZA TYPU HEAD-UP NA PERCEPCJĘ KIEROWCY

Abstract

This article presents the results of a simulation study of an augmented reality system and its influence on the user's perception and reaction time. An automotive head-up display was chosen to conduct this research. It was assumed that the configuration of the GUI influences the perception and response time of the user of the augmented reality system. The perception of the driver was tested by using an eye-tracking device with accompanying software. The optimal graphical user interface (GUI) was developed as a result of the research.

Keywords: augmented reality, head-up display, graphical user interface, simulation, perception, reaction time

Streszczenie

W artykule przedstawiono wyniki badań percepcji użytkownika systemu rzeczywistości rozszerzonej (AR) uzyskanych na podstawie przeprowadzonych symulacji. Na obiekt badań i symulacji wybrano wyświetlacz przezierny typu head-up stosowany w samochodach. Założono, że konfiguracja interfejsu graficznego systemu rzeczywistości rozszerzonej wpływa na percepcję i czas reakcji użytkownika systemu. Percepcję kierowcy zbadano, wykorzystując metodę śledzenia ruchu gałek ocznych i odpowiednie oprogramowanie. W wyniku badań opracowano optymalny interfejs graficzny systemu AR.

Słowa kluczowe: rzeczywistość rozszerzona, wyświetlacz przezierny, interfejs graficzny, symulacja, percepcja, czas reakcji

1. Introduction

Augmented reality (AR) is a system that adds virtual, interactive elements to the real world. It is used in many fields, including the automotive industry.

A visualisation method used for AR systems is the head-up display (HUD). These displays were first used in military aviation and have since become standard equipment for commercial aircraft. In 1988, they began to be used in the automotive industry. Recently, the trend has been to use them in both luxury and sports cars, as well as in mid-size cars.

There are many kinds of automotive head-up displays that are currently available on the market. The most notable are those that are an integral part of the car, portable displays, and smartphone applications. The latter enables a HUD mode for the navigation system and can work with both Android and iOS operating systems. However, the burning question of how to correctly design a graphical user interface (GUI) for HUD is still discussed in many papers, e.g. [2] and [11]. This question is a valid one, since poor design of the HUD's graphical user interface may distract the driver thus creating a potentially hazardous situation.

Motivated by the rapid growth of the automotive head-up display market and the problems that their correct design pose, it was deemed necessary to conduct a simulation study of the head-up display's GUI and its influence on driver perception and reaction time (RT).

Conducting perception and reaction time research requires several steps. First, various graphical user interfaces were designed using Photoshop Portable software. Photos were then taken in traffic from the perspective of the driver. Following this, the photos and GUI designs were then merged in order to simulate a car interior with a working HUD system. Completing those steps allowed the creation of slides that were then shown to the test subjects. The slides, created in PowerPoint, presented the road and the traffic with the GUIs added to the windscreen.

To investigate the driver's perception, eye-tracking software called GazeRecorder was used. Finally, the results of the tests were used to develop an optimal graphical user interface of an automotive head-up display.

2. Research methodology

The analysis of various sources dealing with both the designing of the GUI for head-up displays [1, 4, 6, 8] and the psycho-technical assessments [2, 3, 10, 11] was essential for the research.

Automotive HUDs present valuable information to the driver, including: vehicle speed, data from the tachometer, various alerts and warnings, navigation clues, gear position etc. Some manufacturers decide to include information about temperature, radio settings and notifications about incoming wireless calls. Data is projected on the windscreen, directly within the driver's field of view [3].

Many things have to be taken into consideration while developing the GUI for a HUD. Since the information is displayed on the windscreen, it may cause a potentially hazardous

situation for the driver. For example, data could clutter the windscreen or obscure the driver's view, or poorly designed icons could confuse the driver at a crucial moment. The ways in which a HUD affects driver perception and its influence on a driver's decision making remains a matter of study [11].

Despite the risks described above, there are undisputed merits to using head-up displays. One such merit is that head-up displays are superior to head-down displays (HDD) since the driver observes the dashboard instruments without looking down and can instead focus on the road ahead. This is especially important for young or inexperienced drivers as it reduces stress levels and improves control over the vehicle. Furthermore, using a HUD instead of a HDD can improve the reaction time of the driver. For some people, HUDs are also more intuitive to use [11].

Evidence exists that HUDs may influence the driver's perception and their ability to avoid collisions [2, 3, 10]. Thus, it is important for the data presented by the HUD to be subtle, meaningful, timely and non-distracting, and to serve its intended purpose without endangering or inconveniencing the driver.

Several sources were found in the literature that present methods for the psycho-technical assessment of drivers. Medical examinations and eye-tracking methods are used to determine perceptual functions. Medical examinations are designed to measure visual acuity, field of view and colour discrimination; however, these are not able to evaluate important elements of perception, such as accuracy and quickness [1]. Eye tracking allows for objective assessment of perceptual processes that occur through the recording of eye focus and eye movements [9].

One of the components of perception is reaction time (RT). A common method for measuring driver's reaction time is the use of test tracks and selected sections of road. Other methods include: 1) observation of the driver in actual traffic conditions, 2) tests in driving simulators, 3) stations for the psycho-technical assessment of drivers [3, 4].

The use of test tracks and observation in actual traffic conditions are the most accurate methods of driver psycho-technical assessment as they reflect the actual responses of the driver. The difficulties in performing tests are the coordination of the test, the potential lack of repeatability of conditions, the interpretation of results, and the cost of the research.

A disadvantage of driving simulators and psycho-technical stations is that the environment during testing is artificial. Furthermore, due to the difficulty of accessing such facilities and devices, it is impossible to carry out the research on a large scale. Nonetheless, these methods ensure repeatability of the research and are comfortable and practical for both the person being tested and the person conducting the test [4].

One of the testing systems that deal with the assessment of driver perception and reaction time is the Vienna Test System. It uses the Adaptive Tachistoscopic Traffic Perception Test (ATAVT) for perception assessment and the Reaction Test (RT) to determine driver reaction time. ATAVT mainly analyses the speed of perception; it assesses the speed of identifying objects and patterns. RT investigates attentional functions, and allows the study of both simple and choice reactions. With this method, the unit of measurement is milliseconds. The Vienna Test System station consists of a monitor, a computer with installed tests and external test equipment [8].

It was important to decide what is an appropriate number of participants for the study; however, the available sources don't provide a clear answer to that. Nielsen [7], while discussing graphical interfaces, claims that the best results are obtained while examining five users; he argues that this is the optimal number. Every additional person beyond the original five adds too little in the way of new information and affects the economic viability of the study. Five participants are able to provide around 75% of viable information on the usability of the interface.

Nielsen's chart presenting the proportion of the percentage of usability problems to the number of participants is shown below [7].

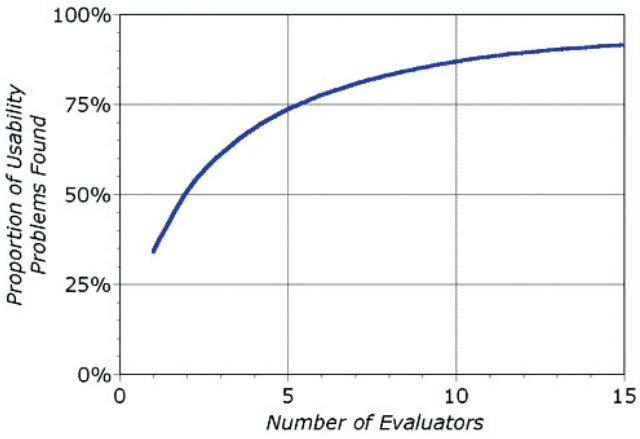

Fig. 1. Nielsen's proportion of usability problems in an interface found by heuristic evaluation using various numbers of evaluators [7]

Evaluating the usefulness of AR systems can be performed through the use of survey techniques. This is a valuable method and can be easily conducted in a chosen group of respondents to assess the general perception of the designed GUI [5].

After analysing current research methods, the following steps were taken: 1) A suitable procedure was selected, 2) the proposed GUI variants were developed, 3) the research station was created, 4) a test group was chosen.

3. The research station and the examined group of people

The simulation was conducted on a group of seven participants. This group was made up of both male and female drivers aged 23-26. All participants had a category B driving licence, some members also had A and C driving licence categories. Every participant also passed valid medical exams for drivers and their eyesight was classified as either good or corrected to normal (eyeglasses or contact lenses). Taking everything into consideration, it was decided to create a research station for both the reaction time and perception assessment.

Simulation methods were used to acquire results for both the perception and the reaction time studies. For the simulation, various slides were used; these depicted different situations on the road with the head-up display added. The proposed variants of the HUD's graphical user interface were developed using Adobe Photoshop Portable. It was important to simulate the interior of the car with a working see-through display; thus, the photos were taken from behind the wheel. It was decided to use two different cars, a Peugeot 207 and a Ford Fusion, since there are differences in the size of their windscreens and their fields of view.

Previously developed designs were added as layers to the photo, using Adobe Photoshop Portable. Complete images were then transferred to Microsoft PowerPoint. Thus, the slides designed for the simulation were finally ready to be presented to the test group at the research station. The station consisted of a 15.6" HP Pavilion notebook with a webcam and two stopwatches.

The notebook was equipped with the GazeRecorder eye-tracking software program, which could also generate the dynamic and static heat maps of the gaze. Stopwatches which were accurate to one one-hundredth of a second were used to measure the reaction time.

Fig. 2. An example of a simulated situation

4. The study of simple reaction time

The simulation study of driver reaction time consisted of ten traffic situations. Because it was important to check the driver's reaction time on an unexpected situation, the display shown either an alert or a warning information. Donders' subtractive method was used to correctly measure the time. In this case, both the person responsible for conducting the simulation and the person being tested had stopwatches. The time marked on the stopwatch of the tested person was subtracted from the time marked on the stopwatch of the researcher. Thus, the acquired result is the reaction time for the displayed stimulus.

The prepared research station enabled the presentation of twenty slides: ten different road situations without the GUI displaying an alert and ten with an alert. The slides were shown at various time intervals and the variant without the GUI and the variant with the GUI were presented alternately. The stopwatch was activated at the same time that the new situation was displayed. The driver under assessment had to stop it only after noticing and understanding an alert. At the same time, the researcher measured the actual time of displaying the alert on the second stopwatch. Both results were written down and then subtracted. The final result is the actual reaction time. The test was carried out with an accuracy of 1/100 of a second. The average reaction time of all people being tested was 0.823 s. One second is considered to be the classic value for the reaction time of a driver in ordinary conditions [1]. Taking this value into consideration, it should be noted that the average result of 0.823 s is a very good outcome.

Table 1. An example of a result of the RT study

Number of the situation	Reaction time
1	0.47
2	1.33
3	1.21
4	1.11
5	1.01
6	1.19
7	1.27
8	0.99
9	0.52
10	1.23

On the basis of the conducted reaction time study, it was observed that the configuration of the head-up display and the proper presentation of data may reduce the reaction time of respondents.

5. The study of perception

The driver's perception was examined using the eye-tracking method. This allows determining not only where the gaze focuses but also for how long.

The test was conducted using fourteen slides, designed expressly for the testing. These slides depicted different road situations with the interface of the augmented reality system added. Each slide was presented to the assessed participant for precisely seven seconds. During every testing session, various dynamic heat maps of the gaze were recorded. This was possible due to the use of the GazeRecorder software and a notebook computer equipped with a webcam. As it was important to get the most precise results of the examination, GazeRecorder was calibrated individually for each assessed participant.

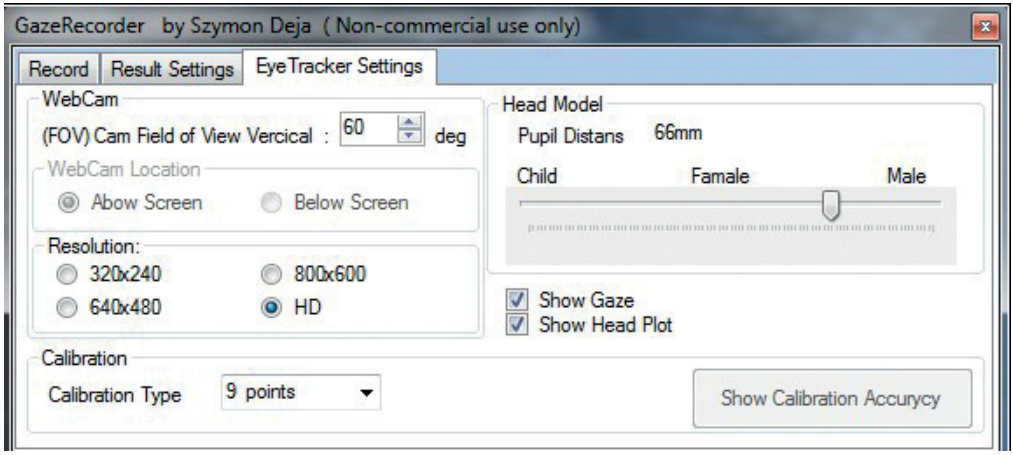

Fig. 3. Calibration settings used in the GazeRecorder software

The following settings were used: 1) the calibration was performed at nine points on the screen, and 2) the interpupillary distance was set. Individuals with refractive errors were able to state their actual interpupillary distance For those with emmetropia, it was decided to use the average interpupillary distances of 63 mm for women and 66 mm for men. The data were processed by the software at intervals of 200 ms. The video was recorded at a resolution of 1366 x 768 pixels (15.6" screen). The average time for testing each assessed participant was around two minutes. This period does not include the time needed to calibrate the GazeRecorder software.

The following step was to generate static heat maps of the gaze. These were generated on the basis of previously recorded dynamic heat maps. The testing generated ninety-eight static heat maps and seven dynamic heat maps. The map is interpreted in the following way: the warmer the colour, or the more red on the map, the longer the viewer focused their gaze on the spot in relation to the total time spent looking at the slide. Red indicates the longest time the viewer focused their gaze on the spot, green indicates the shortest. The obtained results show whether elements of the interface were spotted and for how long the viewer focused their gaze on them [9]. The Photoshop Portable's feature that allows the creation of layers was then used to obtain the general maps of the perception. It was important not to cloud the results; thus, for each slide, only the most representative three heat maps were layered. When more layers were used, the bottom layer was either completely invisible or its hues were altered. The alteration of hues was also considered to be damaging for the final results of the testing. In the end, the forty-two most representative static heat maps were used to create fourteen general heat maps.

During the interpretation of the results, it was taken into consideration that the software could interpret spots in error and that the human field of view includes more than just the point upon which the gaze is focused. The results show whether the element of the interface was noticed and for how long the assessed participant observed it. After testing, all participants completed a survey and answered eight questions regarding GUIs. The results of the survey demonstrate, amongst other things, that most participants deem HUDs to be necessary element of a car's dashboard. Moreover, the respondents' general assessment was that both

their reaction time and perception was influenced by the presented GUI. They also expressed an opinion that the design of the GUI and the presentation of data may be an essential factor influencing driver safety.

Fig. 4. An example of the general static heat map of a simulated situation

Table 2. The elements which the head-up display should contain according to the participants

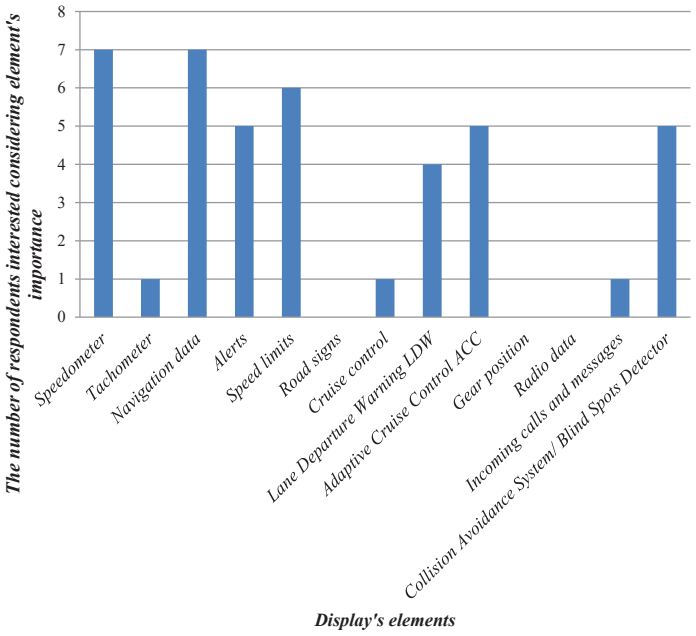

On the basis of the study and the survey, it was confirmed that driver perception is influenced by the way in which the data is presented on the display. Both colour and size of icons as well as the configuration and the position of the element are important. The positioning at the centre above the steering wheel is also important. This way, the driver always looks at the road ahead of them. It is worth noting that positioning the interface too high is undesirable. This is just one of many ways in which the GUI may be designed incorrectly. Interface elements that are positioned incorrectly can obscure the field of vision and thereby endanger the driver and their passengers.

To summarise, the perception study proved that the configuration of the AR system's graphical user interface may influence driver perception.

6. Designing an optimal graphical user interface for the display

On the basis of the results from the conducted study, the optimal graphical user interface of the AR system was developed. This was created using the GUI's designs that were created for the study. The analysis of the study results influenced the way in which the display's data is presented as well as its shape. The idea behind this project was the creation of an interface that will improve both driver safety and driving comfort.

Fig. 5. The design of an optimal graphical user interface – at twilight

It was therefore decided to reduce the number of colours used to only four: teal for the speedometer and tachometer; bright blue for navigation tips; yellow for warnings; red for alerts. In addition, the colours displayed are black and white, as the auxiliary colours for the information displayed by the navigation system and for the speed limits. It was decided to

create three modes for the GUI: standard, navigation and user's. Note that for safety reasons, it is not possible to display more than four pieces of information simultaneously.

In standard mode, the displayed pieces of information are the speed of the vehicle and speed limits on the road. In the event that the speed limit is exceeded, the colour of the speedometer changes form teal to red.

In navigation mode, the navigation cues are displayed in addition to the speedometer and the speed limits. The bright blue colour is used as it is clearly visible during both the day and at night.

The idea behind the user's mode was to allow the driver to customise the content of the display. In this mode, the only obligatory indicator is the speedometer; the remainder can be freely turned on and off.

The options available for the user to choose are the tachometer, alerts, and the following indicators: speed limit, LDW, ACC and Collision Avoidance System.

Fig. 6. Three modes of the designed GUI: a) standard, b) navigation, c) user's

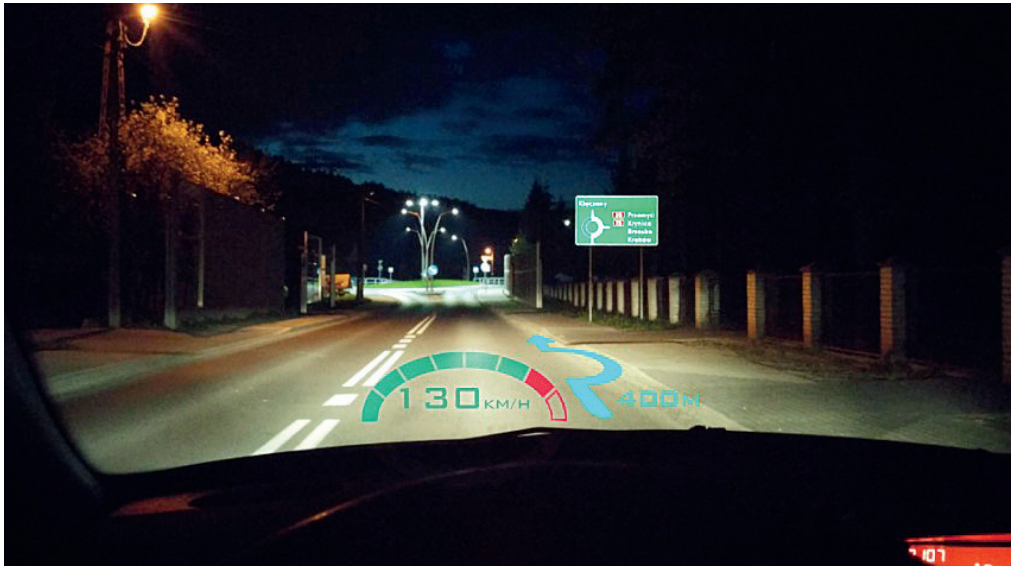

Fig. 7. The design of an optimal graphical user interface at night

Each segment on the tachometer indicates 1,000 rpm. In the event that the revolutions of the vehicle are too high, the colour of the tachometer changes to red. The range in which it changes is between 6,000 and 8,000 rpm.

It seems that the proposed design uses all the cues that resulted from the conducted simulation study as well as the survey. At the same time, it retains the requirements of readability and accessibility for the user. Thus, it could guarantee not only the retain but even the increase of safety and driving comfort.

7. Conclusions

On the basis of the conducted perception and reaction time study, the assumption was confirmed that the configuration of the head-up display's graphical user interface may influence both the reaction time and the degree of perception of the respondents.

The results were used to design the optimal graphical user interface for the head-up display. The final concept was based on the designs created for the study.

The analysis of the results influenced the way the GUI's data was presented. The final content of the display: the speedometer, tachometer, navigation system, alerts etc., was the result of the survey completed by the participants.

The aim of this project was the creation of an optimal graphical user interface of an AR system (in this case, the head-up display), one that would contribute to both safety and driving comfort.

The direction of further research will be, amongst other things, the usage of AR systems to improve the working conditions and driving safety of the TIR drivers. It is particularly important to eliminate blind spots in the truck's cabin. This can be achieved using augmented reality and see-through displays. It is possible to use information from omnidirectional cameras (also known as 360-degree cameras) for this purpose.

Acknowledgments

Presented research was carried out within the confines of the grant for science awarded by the Ministry of Science and Higher Education, No: M-10/174/2016/DS

References

[1] Bąk J., *Psychologiczne badania kierowców,* Bezpieczeństwo Pracy 6/2004, 12-15.

[2] Charissis V., Naef M., Papanastasiou S., Patera M., *Designing a Direct Manipulation HUD Interface for In-Vehicle Infotainmen,* [in:] *Human-Computer Interaction. Interaction Platforms and Techniques. HCI 2007,* Lecture Notes in Computer Science, vol. 4551., eds. J.A. Jacko, Springer, Berlin, Heidelberg 2007, 551-559.

[3] Charissis V., Naef M., Arafat S., Vlachos G., *On the Impact of User's Computer Knowledge on Driving Simulation Test Results – HUD Simulation Case Study,* Proceedings of the

European Annual Conference on Human Decision-Making and Manual Control, EAM'08/2008.
[4] Guzek M., Kobylański K., *Badanie czasu reakcji kierowców z wykorzystaniem urządzenia MCR-2001E.*, Prace Naukowe Politechniki Warszawskiej, Transport 96/2013, 191-199.
[5] Konopacki J., *The technology of augmented reality – virtual reconstructions of landscape architecture design,* Technical Transactions vol. 5-A/2014, 98-105.
[6] Merkisz J., Galant M., Orszulak B., *Badanie wpływu treningu symulatorowego na czas reakcji kierowcy,* Logistyka – Nauka 6/2014, 7293-7299.
[7] Nielsen J., Landauer T. K., *A mathematical model of the finding of usability problems,* [in:] Proceedings of the INTERCHI '93 conference on Human factors in computing systems, eds. S. Ashlund et al., ACM, New York 1993, 206-213.
[8] Niezgoda M., Kamiński T., Ucińska M., Tokarczyk E., Kruszewski M., *Komputerowe systemy wspomagania psychologicznych badań kierowców*, Logistyka – Nauka 6/2011, 3027-3034.
[9] Piotrowska I., *Okulografia w badaniach postrzegania i konstruowania wiedzy geograficznej,* Prace Komisji Edukacji Geograficznej, 3/2014, 175-189.
[10] Rusch, M. L., Schall Jr., M. C., Gavin, P., Lee, J. D., Dawson, D. J., Vecera, S., Rizzo, M., *Directing driver attention with augmented reality cues,* Transportation Research, Part F/2013, 127-137.
[11] Smith, S., Shih-Hanh F., *The relationships between automobile head-up display presentation images and drivers' Kansei*, Displays 32/2011, 58-68.

If you want to quote this article, its proper bibliographic entry is as follow: Halszka Skórska , Jerzy Sładek, *A simulation study of the graphical user interface of the head-up display and its influence on the driver's perception*, Technical Transactions, Vol. 6/2018, pp. 155-166.

TECHNICAL TRANSACTIONS 6/2018
MECHANICS
DOI: 10.4467/2353737XCT.18.096.8701
SUBMISSION OF THE FINAL VERSION: 28/05/2018

Grzegorz Kaczor
Maciej Szkoda (maciej.szkoda@mech.pk.edu.pl)
Instytut Pojazdów Szynowych, Faculty of Mechanical Engineering, Cracow University of Technology

The application of a simulation method in the evaluation of the reliability of transport systems

Zastosowanie metody symulacyjnej w ocenie niezawodności systemów transportowych

Abstract

Reliability is the one of the key features that determine the probability of the proper functioning of a transport system. It refers to the degree to which the transported load is delivered on time, according to the client's requirements. However, taking into account the complex relationships between the components of the transport system requires the application of appropriate methods of calculation. The paper presents the application of a method of reliability assessment, based on the Dynamic Fault Tree (DFT) and Monte Carlo (MC) simulation. The investigated approach may be used for the identification of weak components of the transport system and may form the basis for the improvement of reliability.

Keywords: reliability, Dynamic Fault Tree, Monte Carlo simulation

Streszczenie

Niezawodność jest jedną z najistotniejszych cech charakteryzujących funkcjonowanie systemu transportowego. Gwarantuje ona dostarczenie ładunku we właściwym czasie, zgodnie z wymaganiami klienta. Jednak, biorąc pod uwagę złożone relacje między elementami systemu transportowego, należy zastosować odpowiednią metodę obliczeń. Niniejszy artykuł dotyczy zastosowania metody Dynamicznego Drzewa Niezdatności (DFT) i metody symulacyjnej Monte Carlo do oceny niezawodności wybranego systemu transportowego. Zaproponowane rozwiązanie może być wykorzystane do identyfikacji słabych ogniw systemu transportowego, może także stać się podstawą do opracowania przyszłych działań mogących wpłynąć na poprawę niezawodności.

Słowa kluczowe: niezawodność, dynamiczne drzewo niezdatności, symulacja Monte Carlo

1. Introduction

One of the most basic aims of a transport system is the provision of the highest level of reliability in each phase of the transport process. Research results available in professional literature show that such a tendency exists irrespective of the profile of an enterprise (Fig. 1). Reliability is also one of the factors that guarantees the competitiveness of a transport system [5].

The reliability of a transport system can be evaluated by selected measurements (indexes). These present the probability level certainty level at which the given service is properly performed. The reliable realisation of transport processes depends primarily on the strategy of management and the organisation of all elements of the transport system [16]. Due to the high level of structure complexity of real transport systems, dynamic changes to the technical condition of their components occur. These are the sequence-dependent events, such as: waiting for repair, being under repair, waiting for a proper operation.

Taking into consideration failure and repair behaviours in the modelling of logic systems requires the application of adequate analytical methods. Classical methods of representing the reliability of transport processes include the Reliability Block Diagram method and Fault Tree Analysis. These techniques are successfully applied in industry; they are widely recognised as the best approaches for the evaluation of the reliability of technical systems, including transport systems [11].

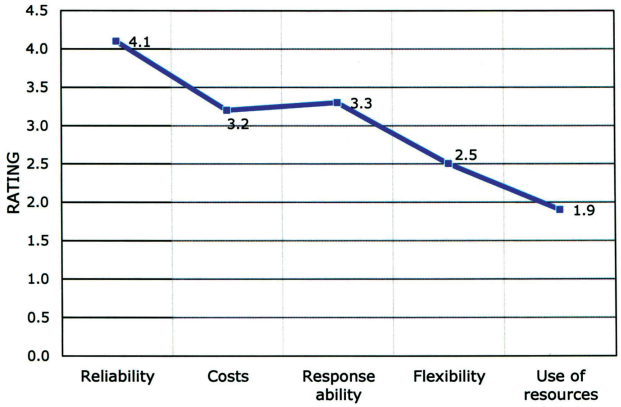

Fig. 1. The main priorities of the logistics industry [10]

FTA is a technique used for the analytical evaluation of reliability. It presents a set of independent events or processes in a graphical way. Certain combinations of these events or processes leads to undesirable events. Based on the Boolean gates 'AND', 'OR', and 'VOTING', FTA determines the probability of the top event. Since FTA is a tool for both the qualitative and the quantitative evaluation of reliability, it is possible to identify critical events and the probability of their occurrence. Like other analytical tools, FTA has one major drawback. There is no possibility to analyse the events that occur only in a specific sequence.

The dynamic fault tree analysis (DFTA) method has been was created to eliminate these limitation. It is complementary to a classical fault tree (FT) due to the inclusion of a few additional logic gates [1, 2, 4, 7].

Several methods have been proposed to solve DFT; two most frequently used are Markov models and the Monte Carlo simulation method. The first of these can only be applied when the components have a lifetime and repair time that are exponentially distributed. Moreover, in the case of a complex system with a large number of elements, the state space complicates the calculation procedure in the Markov process. Therefore, the Monte Carlo simulation method, capable of overcoming many difficulties in different scenarios, is used. This method allows the evaluation of reliability indices through a discrete simulation of the system behaviour at a specific times [3, 8].

2. Solving dft with the use of monte carlo simulation

Modelling issues and transport system reliability evaluation have been discussed in numerous academic papers since there is a need to both limit the occurrence of undesirable events and increase the efficiency of the functioning of these systems. Transport systems are complex systems; their reliability indicators change at each phase of their operation [6, 12, 18].

The analysis of a classical fault tree involves the creation of a set of Boolean equations. The equations are connected with the occurrence of undesirable events in the system. Despite many limitations of this method, e.g. the lack of the possibility of modelling dynamic scenarios for the system's components, the method is still used in a lot of cases. The quantitative and qualitative evaluation of a power system's reliability is an example of its application [17]. In paper [3], the authors carried out a case study on the reactor regulation system (RRS) of a nuclear power plant. The solving of the dynamic fault tree was accomplished with the use of the Monte Carlo simulation.

In some works, the FTA method is used for the evaluation of risk connected with the occurrence of hazards in the proper functioning of technical systems. There are examples of the application of the Monte Carlo simulation in the evaluation of accident risk in aviation. The method has been used to generate alerts for air traffic controllers about a likely collision of a taxiing aircraft on a runway with an aircraft taking off on the same runway [15].

New techniques which extend traditional fault trees are developed in order to eliminate the FTA limitations. One of these, the so-called timed fault trees (TFTs), allows the identification of faults that should be immediately eliminated. This technique also allows the determination of the time needed for maintenance activities. The example of the TFTs application in [13] refers to a case study on a simple railway transport system.

We can also use Petri nets to build transport systems. One example of the application of this method is an analysis of the reliability and efficiency of a real tram system. The performed research shows that models based on the Petri nets can also include time dependencies [13].

3. Description of the system

The scheme of the transport system under consideration in this paper is presented in Fig. 2. This is an inter-modal transport system that consists of a few subsystems in which various vehicles perform other transport tasks. The required reliability level of the transport system is achieved by calculating the number of redundant elements. It has been assumed that each subsystem consists of two identical means of transport arranged in a *cold-standby*. These are repairable objects which undergo strictly determined maintenance activities.

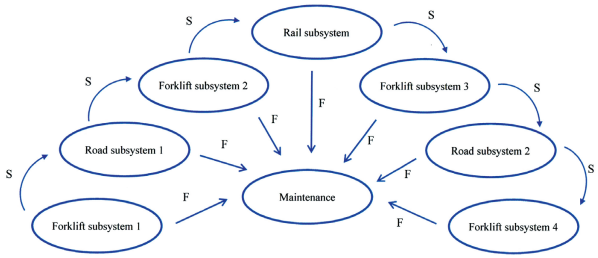

Fig. 2. Scheme of transport system functioning: S – suspended, F – failed

Analyses of transport system reliability should include not only the repair time of damaged elements but also the delay time that is connected with waiting for a standby object. The successful operation of the system requires all of its individual partial processes to be performed, these are:

a) Loading: formation of a unit load and preparation for road transport,
b) Road transport 1: transport of a unit load to the rail terminal,
c) Rail transport: transport of a unit load to the consignee's nearest terminal ,
d) Reloading: reloading of a unit load onto a means of road transport,
e) Road transport 2: transport of a unit load to the delivery point,
f) Unloading: unloading of a unit load and finishing the transport process.

If any of the elementary tasks are not performed, the transport process is assumed to be incomplete.

4. DFT of the system

In order to make a model of the presented transport system by using a fault tree and to take into consideration the described assumptions, one has to use gates with a dynamic dependency. Examples of such gates are' sequence enforcing gates (SEQ), spare gates (SPARE), priority AND (PAND) and functional dependency (FDEP); these are shown in Fig. 3. The rules for the gates are as follows [4]:

a) SEQ gate: this goes into a failure state only when all the input events occur in a specific sequence. No other combination of input events can take place.
b) SPARE gate: this includes active and spare components. If the number of active components is less than the minimum required, the gate fails.
c) FDEP gate: this is used when all the events are functionally dependent on an additional event called the trigger event.

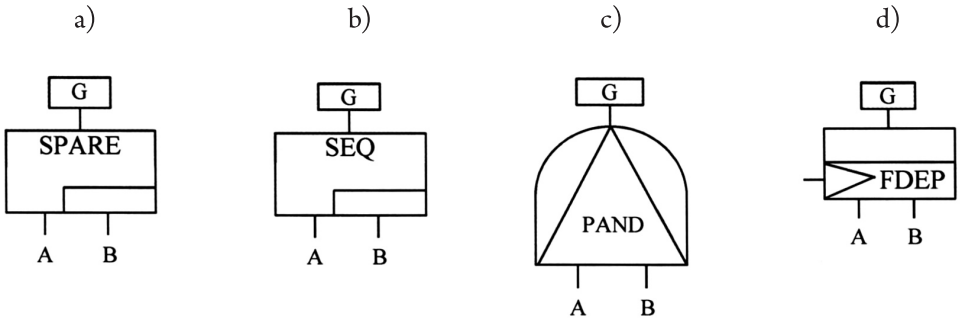

Fig. 3. Dynamic gates: a) SEQ, b) SPARE, c) FDEP, d) PAND

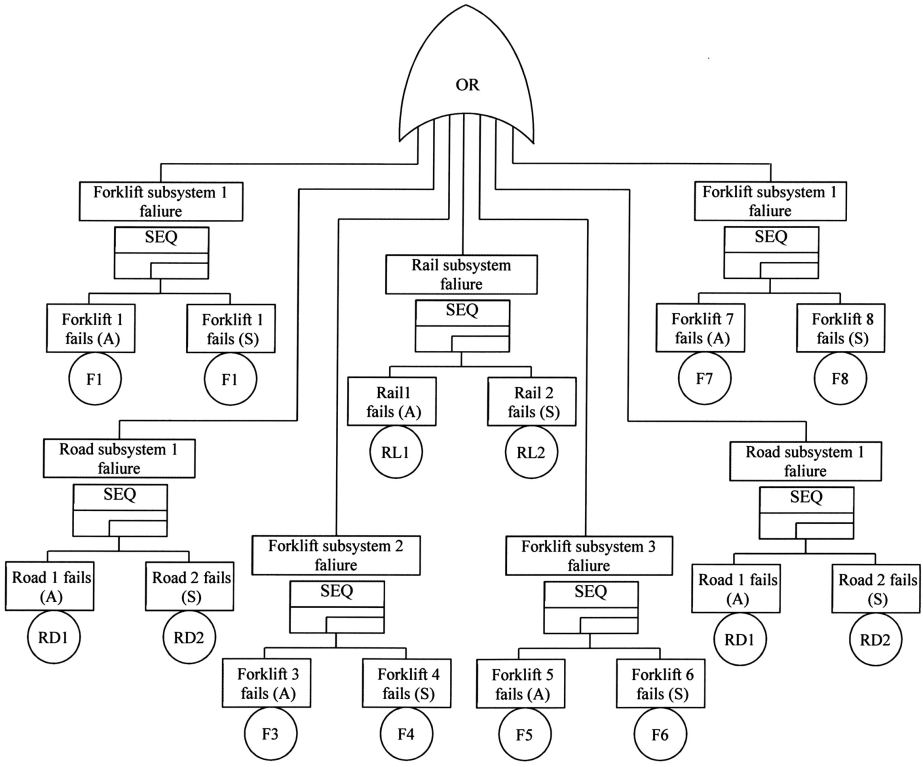

Fig. 4. Dynamic gates: a) SEQ, b) SPARE, c) FDEP, d) PAND

d) PAND gate: this gate goes into a failed state when all the inputs are in a pre-assigned order. Unlike the SEQ gate, PAND gate allows to occur the events out of the desired sequence.

A model of the fault tree of the considered transport system is presented in Fig. 4. The OR gate has been used to assign a top event. This event takes place when an optional partial transport process is. Each process uses specific means of transport. The moment the primary vehicle is damaged, the transport process is stopped and one has to wait until a substitute vehicle arrives. The damaged vehicle is under repair at that time. After the repair the vehicle goes into a standby stage. If the standby vehicle gets failed during repair activities of the primary vehicle, the whole partial process is regarded as being undone. Repair is accomplished when the vehicle is back again in as good as a new condition.

5. Case study

The study presented in the following sections aims to demonstrate the reliability and availability analysis by solving DFT with the use of the Monte Carlo simulation. The analysis was conducted based on hypothetical input data (Table 1).

5.1. Assumptions

In the analysed transport system, it was assumed that the system components have the times to failure that are normally distributed and the repair times that follow the lognormal distribution. The mean delay time (MDT), which is connected with the usage of standby elements, has also been considered. The detailed data is shown in Table 1.

Table 1. Failure and repair data used for the analysis

Component	Failure			Repair	Delay
	Distribution	Parameters		Parameter	Parameter
		Mean (days)	Std (days)	MTTR (hours)	MDT (hours)
F1, F2	NORMAL	60	5	2	2
RD1, RD2	NORMAL	95	5	4	4
F3, F4	NORMAL	70	6	2	2
RL1, RL2	NORMAL	187	11	6	6
F5, F6	NORMAL	65	5	2	2
RD3, RD4	NORMAL	100	10	4	4
F7, F8	NORMAL	55	7	2	2

5.2. Monte Carlo Simulation

The ReliaSoft software package, which provides the simulation of discrete events, was used for the Monte Carlo simulation. This software is commonly used in many industrial applications. The Monte Carlo simulation used in the calculation process is based on a random number generator with the Bays-Durham shuffle algorithm. The simulation requires the introduction of certain input parameters, such as [14]:

- Simulation End Time
- Point Results Every
- Number of Simulations

6. RESULTS

To obtain the results, one hundred thousand simulations were run over the specified period: 0 to 1,825 days. The point results every was assumed as 100,000.0. At the end of the simulation, the results were gathered in the system overview table (Table 2).

Table 2. The simulated results for the 1,825 days of operation

System Overview	
General	
mean availability (all events):	0.9996
standard deviation (mean availability):	0.000147
mean availability (w/o PM, OC & inspection):	0.9996
point availability (all events) at 1825:	0.9964
expected number of failures:	2.3691
standard deviation (number of failures):	0.5940
MTTFF (day):	1,148.7
MTBF (total time) (day):	770.3
MTBE (total time) (day):	543.3
System Uptime/Downtime	
uptime (day):	1,824.4
CM downtime (day):	0.5992
MTTFF (day):	1,148.7
MTBF (total time) (day):	770.3
MTBE (total time) (day):	543.3
System Uptime/Downtime	
uptime (day):	1,824.4
CM downtime (day):	0.5992

Mean availability A, is defined as the mean amount of the time in which the investigated vehicle remains in a state of operability. For an individual object, the availability index is defined as [16]:

$$A = \frac{\sum_{i=1}^{N} TZ_i}{\sum_{i=1}^{N} TZ_i + \sum_{i=1}^{N} TUB_i + \sum_{i=1}^{N} TUP_i}$$

where:
TZ_i – time of vehicle i in operability state,
TUB_i – time of vehicle i in unavailability state due to corrective repairs,
TUP_i – time of vehicle i in unavailability state due to preventive repairs,
N – sample size of vehicles taken for tests.

It can be stated on the basis of the obtained results that for the considered transport system, a significant decrease in the system's availability occurs at certain intervals; this is shown in Fig. 5. In order to identify the causes of the decreases in point availability, a block up/down chart may be used (Fig. 6). The timeline shows the moments at which the failures of the primary and secondary component occurs. The expected downtime periods relating to the repair activities are also shown.

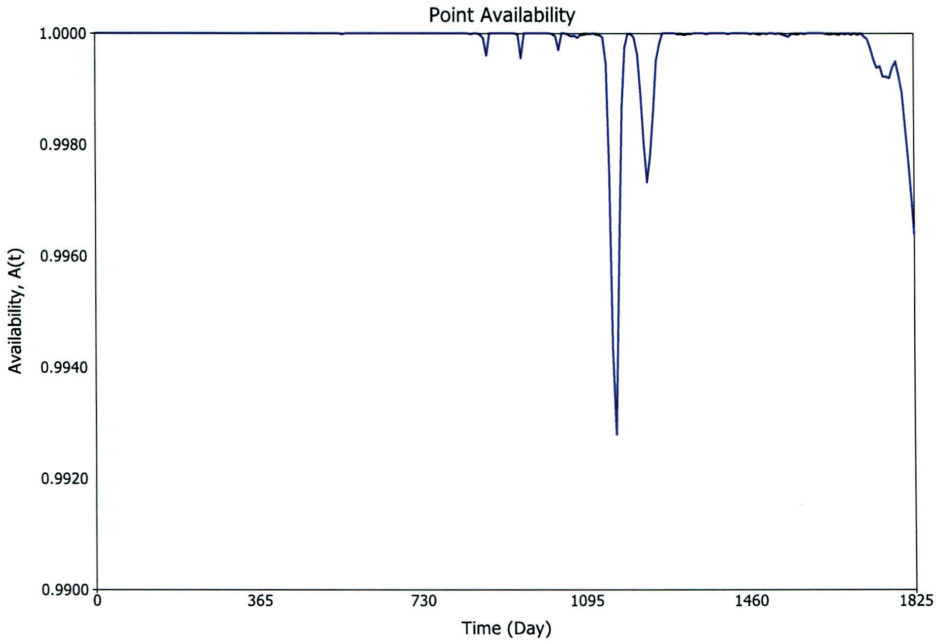

Fig. 5. Point availability vs. time plot

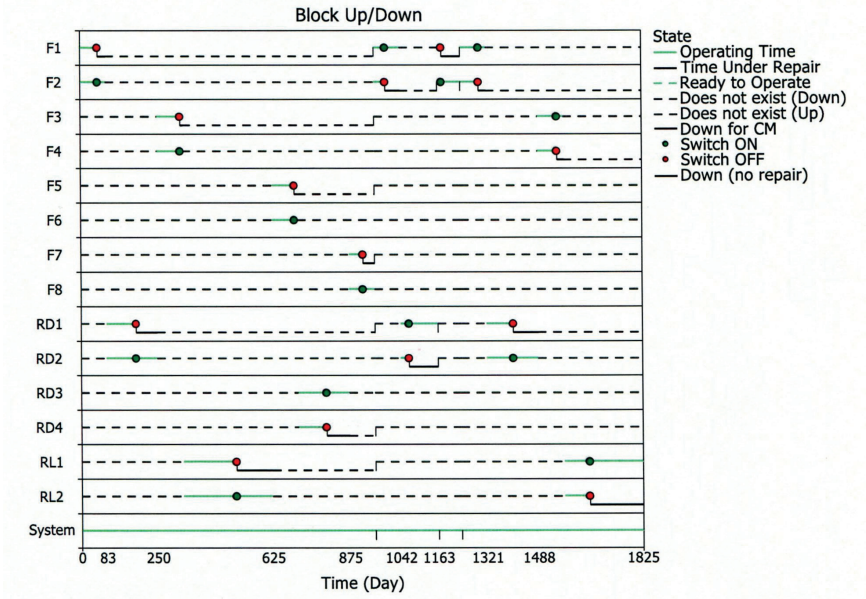

Fig. 6. The system up/down analysis

By analysing the proportion of downing events and the number of failures of the system's components, the weakest component of the system for the simulated end time can be determined. The ReliaSoft Downing Event Criticality Index (RS DECI) and ReliaSoft Failure Criticality Index (RS FCI) are used to achieve this [14].

RS DECI is a relative index which shows the percentage of times when a downing event of a given component causes the system to go down.

$$RS\ DECI = \frac{C_{NSDE}}{N_{ALLdown}}$$

where:

C_{NSDE} – the number of system downing events; this is the number of times when the given component's downing causes the system to go down,

$N_{ALLdown}$ – the number of downing events.

In the simulation results (Fig. 7), it can be observed that for the F1 component, the RS DECI = 59%. This implies that 59% of the times when the system was down were due to the F1 component being down. Furthermore, the conducted analysis enables the identification that the greatest influence on the system's downtime has two elements: F1 and F2 (forklift 1 and forklift 2). It is related to the reliability-wise configuration (standby redundancy). If the primary element gets failed, its functions are taken by the standby element.

RS FCI is a relative index that shows the percentage of times when a failure of a given component caused the system's failure. This is obtained from:

$$RS\ FCI = \frac{C_{NSDF} + F_{ZD}}{N_F}$$

where:

F_{ZD} – a special counter of the system failures not included in C_{NSDF}. This counter is not explicitly shown in the results but is maintained by the software. The reason for this counter is the fact that zero duration failures are not counted in C_{NSDF} because they do not cause the system to go down. However, these zero duration failures need to be included in computing *RS FCI*,

N_F – number of system failures.

An RS FCI chart for the selected components is shown in Fig. 8. For the RD1 component, RS FCI = 43.5%. This implies that the RD1 component failure was responsible for 43.5% of the times when the system failed. It should be noted that the combined RS FCI of RD1 and F2 is almost 80%. In other words, RD1 and F2 contributed to about 80% of the system's total downing failures.

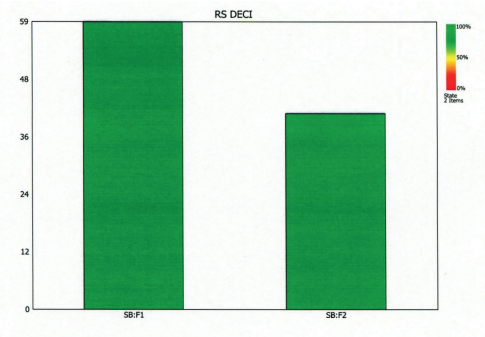

Fig. 7. RS DECI chart for the selected components

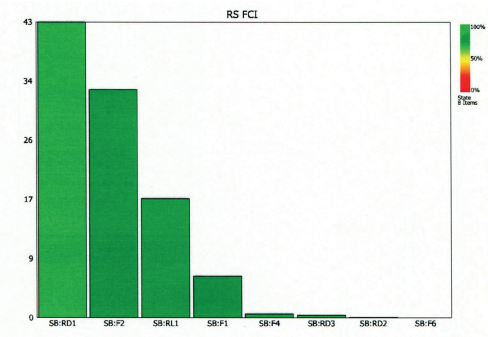

Fig. 8. RS FCI chart for the selected components

It is important to note that RS DECI relates to all the events that cause the system to go down (e. g. waiting for repair, logistic delay), whereas the RS FCI includes only the failures of the analyzed system [14].

7. Conclusion

As a result of the conducted analysis of transport system reliability with the use of a fault tree and the Monte Carlo simulation, the authors obtained the values of the selected indexes that may be used for the determination of the probability of failures of the system elements during operation. This approach allows for a qualitative and quantitative evaluation of reliability and the identification of weak components of the system. It can also constitute the basis for a preventative maintenance strategy. A model thus created of the transport system

can be further developed to achieve the required level of detail. The applied ReliaSoft software package undoubtedly makes usage of the simulation techniques easier, especially in systems with a high level of complexity.

References

[1] Amari S., Dill G., Howald E., *A new approach to solve dynamic fault trees,* Annaul IEEE reliablity and maintainability symposium, 2003, 374-389.

[2] Cepin M., Mavko B., *A dynamic fault tree,* Reliability Engineering and System Safety, 75(2002), 83-89.

[3] Durga Rao K., Gopika V., Sanyasi Rao V.V.S., Kushwaha H.S., Verma A.K., Srividya, *A Dynamic fault tree analysis using Monte Carlo simulation in probabilistic safety assessment,* Reliability Engineering and System Safety, 94(2009), 872-883.

[4] Faulin J., Juan A.A., Matrorell S., Remirez-Marquez J-E., *Simulation Methods for Reliability and Availability of Complex Systems,* Springer-Verlag London, 2010, Limited.

[5] Gajewska T., Kaczor G., *Analiza niezawodności dostaw w transporcie chłodniczym*, Logistyka, 5/2014, 453-462.

[6] Kaczor G., *Modelowanie i ocena niezawodnosci systemu transportu intermodalnego,* Logistyka, 3/2015, 2047-2054.

[7] Manno G., Chiacchio F., Compagno L., D'Urso D., Trapani N., *An integrated Monte Carlo Simulink tool for the reliability assessment of dynamic fault tree,* Expert Systems with Applications, 39(2012), 10334-10342.

[8] Marseguerra M., Zio E., *Monte Carlo estimation of differential importance measure: application to the protection system of a nuclear reactor,* Reliability Engineering and System Safety, 86(2004), 11-24.

[9] Kowalski M., Magott J., Nowakowski T., Werbinska-Wojciechowska S., *Analysis of transport system with the use of Petri nets,* Eksploatacja i Niezawodnosc – Maintenance and Reliability, vol. 13(2011), no. 1, 48-62.

[10] Nowakowski T., *Niezawodnosc Systemów Logistycznych,* Oficyna Wydawnicza Politechniki Wroclawskiej, Wroclaw 2011.

[11] Nowakowski T., *Reliability model of combined transport system. Probabilistic safety assessment and management,* Proceedings of the European Safety and Reliability Conference PSAM7-ESREL, London 2004, Springer.

[12] Nowakowski T., Zając M., *Analysis of reliability model of combined transport system,* Advances in Safety and Reliability – Proceedings of the European Safety and Reliability Conferece, ESREL 2005, 147-151.

[13] Peng A., Lu Y., Miller A., Johnson C., Zhao T., *Risk assessment of railway transportation system using timed fault tree,* Quality and Reliability Engineering International, John Wiley & Sons, 2014.

[14] ReliaSoft Corporation, *System Analysis Reference,* ReliaSoft Publishing, Tucson 2010.

[15] Stroeve S., H., Blom H.A.P., Bakker G.J., *Systematic accident risk assessment in air traffic by Monte Carlo simulation,* Safety Science, 47(2009), 238-249.
[16] Szkoda M., *Assessment of reliability, availability and maintainability of rail gauge change systems,* Eksploatacja i Niezawodnosc – Maintenance and Reliability, vol. 16(2014), no. 3, 422-432.
[17] Volkanowski A., Cepin M., Mavko B., *Application of the fault tree analysis for assessment of power system reliability*, Reliability Engineering and System Safety, 94(2009), 1116-1127.
[18] Werbińska S., *Model of logistic support for exploitation system of means of transport,* PhD Thesis, Technical University of Wroclaw, Poland, report: PRE 3/2008.

If you want to quote this article, its proper bibliographic entry is as follow: Grzegorz Kaczor, Maciej Szkoda, *The application of a simulation method in the evaluation of the reliability of transport systems* , Technical Transactions, Vol. 6/2018, pp. 167-178.